Spring 5-2018

Glacial History of the Tsagaan Gol- Potanin Glacier Valley, Altai Mountains, Mongolia

Mariah J. Radue
University of Maine, mariah.radue@maine.edu

GLACIAL HISTORY OF THE TSAGAAN GOL- POTANIN GLACIER VALLEY, ALTAI MOUNTAINS, MONGOLIA

By

Mariah Josephine Radue

B.A. Carleton College, 2014

A THESIS

Submitted in Partial Fulfillment of the

Requirements for the Degree of

Master of Science

(in Quaternary and Climate Studies)

The Graduate School

The University of Maine

May 2018

Advisory Committee:

Dr. Aaron E. Putnam, Assistant Professor of Earth and Climate Sciences, Advisor

Dr. George H. Denton, Professor of Earth and Climate Sciences

Dr. Brenda L. Hall, Professor of Earth and Climate Sciences

Dr. Karl J. Kreutz, Professor of Earth and Climate Sciences

Dr. Alice A. Doughty, Visiting Assistant Professor, Bates College

GLACIAL HISTORY OF THE TSAGAAN GOL- POTANIN GLACIER VALLEY, ALTAI MOUNTAINS, MONGOLIA

By Mariah Josephine Radue

Thesis Advisor: Dr. Aaron E. Putnam

An Abstract of the Thesis Presented
in Partial Fulfillment of the Requirements for the
Degree of Master of Science
(in Quaternary and Climate Studies)

May 2018

The last glacial termination (~19-11 ka) marks the end of the last ice age and the transition to modern interglacial conditions. The mechanisms that triggered deglaciation are unresolved. Various hypotheses for deglacial warming involve changes in Earth's orbit, an 80-ppm increase in atmospheric CO_2, a 'bipolar seesaw' in oceanic-heat redistribution, and shifting wind belts. Here, I present a ^{10}Be surface-exposure chronology for a system of glacial landforms in the Tsagaan Gol-Potanin Glacier valley in the Mongolian Altai (49°N, 88°E) to determine the nature of the termination in interior Asia. Located near the center of Earth's largest continent, the glaciers in the Mongolian Altai are well situated to test the roles of various climate mechanisms in driving the last glacial termination. My chronology is underpinned by detailed glacial-geomorphic maps made using satellite and drone imagery. The surface-exposure chronology reveals that moraine formation occurred at 23.24 ± 0.50 ka and 28.08 ± 0.58 ka during the local Last Glacial Maximum (LLGM). Glacial erratics bracketing small, discontinuous moraines are the youngest samples from the LLGM, ranging from 19.54 ± 0.36 ka to 22.11 ± 0.41 ka. The termination is documented by glacial erratics on a mid-valley bedrock mountain, Holy Mountain, and erratics next to the modern Potanin Glacier. The Holy Mountain samples record 253 m of ice-surface lowering between 18.23 ± 0.34 ka and 15.69 ± 0.34 ka. Glacial erratics outboard of the Potanin Glacier form two

populations, at 16.20 ± 0.09 ka and 17.71 ± 0.19 ka, indicating that the termination was underway by 17.71 ± 0.19 ka. I reconstructed paleo-snowlines using the accumulation-area ratio (AAR) method to translate the glacial record into a climate signal. From the LLGM to modern, snowline rose 1100 ± 90 m, equating to a temperature increase of 6.0 ± 0.5°C using a lapse rate of 0.0055°C/m. At least 640 ± 90 m of snowline rise, or 3.5 ± 0.5°C of warming, occurred by 17.71 ± 0.19 ka. Rising atmospheric CO_2 and reorganization of North Atlantic oceanic circulation lag the warming documented in this study. Possible mechanisms for deglaciation in the Mongolian Altai include rising local summer insolation, poleward heat export from the tropics, or a poleward shift of the westerly wind belts.

ACKNOWLEDGMENTS

I am entirely grateful for the mentorship from my advisor, Aaron Putnam. He has guided me through the questions of Quaternary climate science with curiosity and passion. Thank you to my committee: George Denton, Brenda Hall, Karl Kreutz, and Alice Doughty. Thank you to Brenda Hall, Peter Strand, and Gordon Bromley for their enormous help and training in laboratory work. Susan Zimmerman of the Center for Accelerated Mass Spectrometry at Lawrence Livermore National Laboratory hosted me at Livermore and taught me about Be measurements. Thank you to Nathaniel Norris, Ninjin Tsolmon, Purev-Ochir Purevdorj, Destiny Washington, Jessica Stevens, and Scott Travis for help in sample collection through hail and mosquito swarms. A special thanks to Scott Travis and Stephanie Comer for providing the drone used for mapping. I am grateful to Batbold Baatar and all the drivers of Hovsgol Travel for supporting our field expedition. Oyungerel Sambuu at the Mongolian University of Science and Technology organized sample-export permits, allowing us to transport the samples to the United States. Throughout this project, I have felt the love and unwavering support of my family and friends. Thank you for cheering, listening, and editing. This project was funded through grants from the Comer Family Foundation and the National Science Foundation, grant number EAR-1554990.

TABLE OF CONTENTS

LIST OF TABLES

LIST OF FIGURES

CHAPTER 1

THE PROBLEM

At the end of the last ice age, large Northern Hemisphere ice sheets advanced to middle latitudes and covered large tracts of North America and Europe. In both hemispheres, mountain glaciers and ice fields extended beyond their modern positions, signifying a global pattern of colder conditions. The last ice age ended abruptly in what has been dubbed the "last glacial termination" (Broecker and van Donk, 1970). Northern Hemisphere ice sheets and mountain glaciers retreated, sea level rose by about 130 m, and atmospheric CO_2 increased by about 80 parts per million by volume (p.p.m.v.) (Clark et al., 2009; Denton et al., 2010; Shakun et al., 2012). Studying transitions from glacial to interglacial periods may offer important insights into the underlying drivers of Earth's climate system.

Glacial periods, or ice ages, have long been associated with changes in Earth's orbit (Adhémar, 1842; Croll, 1867). Milankovitch (1941) suggested that Northern Hemisphere ice volume is linked with changes in summer insolation at 65°N because ice sheets are centered at this latitude. Milankovitch's (1941) hypothesis lacked robust geological evidence until Hays et al. (1976) presented a record of global ice volume from oxygen isotopes ($\delta^{18}O$) measured on deep-sea foraminifera. Hays et al. (1976) identified a correlation between periodic fluctuations in deep-ocean records of $\delta^{18}O$, Northern Hemisphere summer insolation, and Southern Hemisphere winter insolation. They concluded that periodic changes in Earth's orbital geometry are imprinted on Quaternary glacial cycles.

How the orbital signal appears in glacial cycles has yet to be solved, leaving several outstanding questions about orbital ice-age theory. A major question is: Why do ice ages end with rapid terminations? The benthic $\delta^{18}O$ record has a distinctly asymmetric or "sawtooth" shape, with each cycle containing a long build up to glacial ice volume followed by a relatively rapid termination (Broecker and van Donk, 1970) (Figure 1.1). Though each termination corresponds with rising insolation, there is not a linear correlation between ice volume and Northern Hemisphere summer insolation, indicating that orbital theory alone cannot explain the asymmetric pattern of Late Quaternary ice ages (Broecker and van Donk,

1970; Cheng et al., 2009). Therefore, some other mechanism, or mechanisms, must explain the rapid warming during the transition to interglacial conditions.

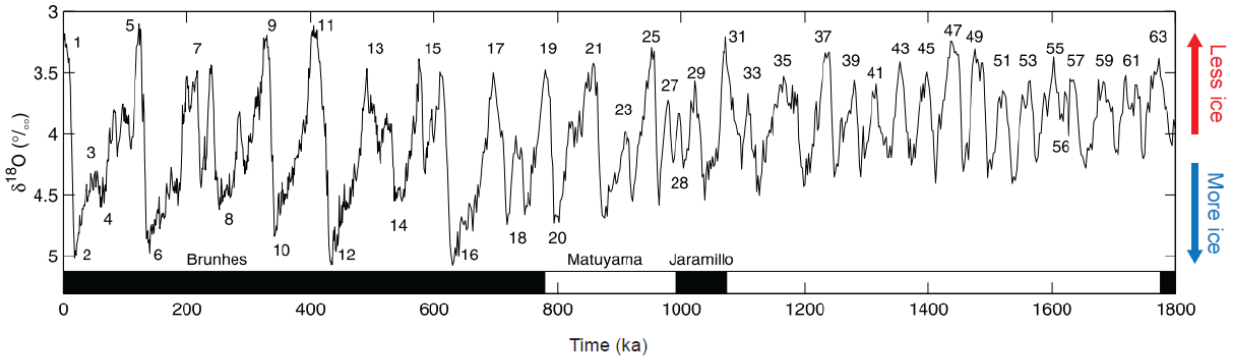

Figure 1.1. Benthic $\delta^{18}O$ (‰) stack from 57 globally distributed records representing global ice volume. Note how ice volume builds up gradually at beginning of a glacial period and disappears rapidly at the termination, creating a "sawtooth" pattern. Modified from Lisiecki and Raymo (2005).

Different hypotheses incorporate various climate drivers as mechanisms that drove deglacial warming. One prominent hypothesis is from Denton et al. (2010), which builds off of Raymo (1997)'s observation that terminations occur when ice sheets reached their maximum extents. The "excess" ice isostatically depressed the crust, creating unstable marine margins. Denton et al. (2010) suggested that rising Northern Hemisphere insolation triggered the collapse of these unstable ice sheets, which led to freshening of the North Atlantic and a decrease in Atlantic meridional overturning circulation (AMOC). Due to the reduced AMOC, extensive sea ice covered the North Atlantic, the Asian monsoon weakened, and the westerlies in both hemispheres shifted southward, pushing the thermal equator south (Cheng et al., 2009). A more southerly position of the southern westerlies resulted in increased upwelling in the Southern Ocean and degassing of CO_2 (Anderson et al., 2009). By the Denton et al. (2010) hypothesis, the CO_2 released into the atmosphere would have been large enough to lock the planet into interglacial conditions.

Alternatively, it has been suggested that degassing of CO_2 from the Southern Ocean was a response to the bipolar seesaw in the Atlantic Ocean from a large Northern Hemisphere meltwater event at 19 ka (Clark et al., 2009; Clark et al., 2012). First, rising insolation drove initial warming in the Northern Hemisphere between 21.5 and 19 ka (Clark et al., 2012). Then, freshwater input from the North Atlantic caused the Northern Hemisphere to cool and the Southern Hemisphere to warm through the bipolar seesaw. Last, changing the strength of the AMOC contributed to the CO_2 degassing from the Southern Hemisphere. It is important to note that both hypotheses call on the destratification of the Southern Ocean and release of CO_2 into the atmosphere as a fundamental factor in driving the termination.

The goal of my thesis research is to compare the chronology for deglaciation of a glacier system in western Mongolia with the climatic forcing mechanisms included in the above hypotheses. These mechanisms are:

1) Rising Northern Hemisphere summer insolation (Milankovitch, 1941; Roe, 2006; Huybers and Denton, 2008).

2) Interhemispheric heat transfer through the Atlantic bipolar seesaw (Crowley, 1992; Broecker, 1998; McManus et al., 2004; Barker et al., 2009; Clark et al., 2009; Clark et al., 2012).

3) Degassing of CO_2 from the Southern Ocean, leading to a rise in atmospheric CO_2 (Denton et al., 2010; Clark et al., 2012; Shakun et al., 2012).

Tracking fluctuations of mountain glaciers is an ideal way to measure climate because summer temperature is a first-order control on glacier mass balance (Oerlemans, 2005). Glaciers of the Mongolian Altai are well situated to record climate change within the interior of the Asian continent, permitting a key test of prominent hypotheses for ice ages. Because these glaciers are geographically isolated from local oceanic influences, they are poised to record the impacts of local radiation forcing from changes in Earth's orbital configuration, greenhouse gases, and heat transfer from the North Atlantic via the westerly wind system.

1.1. Northern Hemisphere summer insolation

The role of Northern Hemisphere summer insolation in the waxing and waning of ice sheets is the original pillar of orbital theory and has precipitated into many subsequent iterations of ice age hypotheses. Milankovitch (1941) posited that periods of summertime insolation minima coincided with glacial advances in Europe. Though there is a lag between global ice volume and insolation, Roe (2006) determined that there is a direct, zero-lag antiphase relationship between the rate of change of global ice volume and summertime insolation in the northern high latitudes. Huybers and Denton (2008) reasoned that Northern Hemisphere ice sheets should respond to summer insolation intensity as opposed to the duration of the seasons because in the Northern Hemisphere, much of ice sheet ablation occurs through surface melt atop land. The Northern Hemisphere is dominated by landmasses rather than the ocean, therefore the heating and cooling of the land by orbital forcing has a strong effect on the continental climate (McKinnon et al., 2013) and thus ice sheets. However, ice sheets have a significantly longer response time to changes in temperature than mountain glaciers. This study aims to examine the effect of local Northern Hemisphere (49°N) summer insolation on a mountain glacier in the Mongolian Altai and determine whether local insolation was a possible driver in deglacial warming.

1.2. Bipolar seesaw

Antiphase mean-annual warming of the Northern and Southern Hemispheres during the last termination, as registered in polar ice cores, led researchers to postulate a role for Atlantic thermohaline circulation in distributing heat between the hemispheres. This has come to be known generally as the 'bipolar seesaw' hypothesis for ocean-heat redistribution. By various versions of this hypothesis, melting ice sheets in the Northern Hemisphere would have contributed fresh water to the high-latitude North Atlantic, decreasing North Atlantic deep-water (NADW) formation. Reduced NADW production and high-northern latitude sea-surface cooling could have impacted cross-equatorial heat transport in the Atlantic leading to warming in the Southern Hemisphere (Crowley, 1992). Alternatively, Broecker (1998) suggested that buoyancy within the interior ocean drives the bipolar seesaw. Meltwater injections from

Northern Hemisphere ice sheets would stratify the North Atlantic and decrease NADW formation. Less NADW formation would create a deep-water 'vacuum' within the interior of the ocean and therefore require more deep-water formation in the Southern Ocean, releasing heat to the atmosphere in the Southern Hemisphere. Therefore, by this hypothesis, an increase in Southern Ocean deep-water formation would warm the Southern Hemisphere middle and high latitudes while cooling the Northern Hemisphere extratropical regions.

Decreasing deep-water formation in the North Atlantic would lead to a shutdown or weakening of the AMOC. McManus et al. (2004) measured $^{231}Pa/^{230Th}$ ratios in North Atlantic sediment cores to track changes in the AMOC. Because radioactive decay of uranium produces ^{231}Pa and ^{230}Th in seawater and because ^{231}Pa is removed more slowly from the water column than ^{230}Th, it is possible to determine the residence time of water masses by measuring the ratio of these two isotopes. McManus et al. (2004) showed that there was preferentially more ^{231}Pa burial in North Atlantic sediments during deglaciation, which they take to indicate that the AMOC shut down during the coldest periods. Sea-surface temperature (SST) records off the coast of Portugal indicate cold surface conditions in the Atlantic during these periods of reduced NADW formation (Bard, 2000). These intervals of cold, stratified conditions in the North Atlantic have been dubbed 'Heinrich Stadials' (Barker et al., 2009). However, terrestrial records from Greenland show that summers may have warmed during Heinrich Stadials, suggesting that the climate in the Atlantic was highly seasonal (Denton et al., 2005; Hall et al., 2008; Bromley et al., 2014; Buizert et al., 2014; Levy et al., 2016; Hall et al., 2017; Koester et al., 2017). If conditions in the North Atlantic were cold, then I predict that there would be a glacial advance in Mongolia until the onset of the Bølling-Allerød at 14.7 ka, due to the location of interior Asia downwind of the North Atlantic. If glacial retreat in Mongolia occurred during North Atlantic stadial conditions (i.e., Heinrich Stadial 1), then this would support the seasonality interpretation.

1.3. Atmospheric CO_2

Ice-core records document an increase in atmospheric CO_2 during the last termination, showing a rise of about 80-ppm from 17.5 ka to 11 ka (Marcott et al., 2013). During the Last Glacial Maximum (LGM), CO_2 was sequestered in the deep ocean until changes in the position of the westerlies, the biological pump, and/or sea-ice position released CO_2 into the atmosphere (Stephens and Keeling, 2000; Toggweiler et al., 2006; Schmittner and Galbraith, 2008; Denton et al., 2010; Shakun et al., 2012). Rising atmospheric CO_2 is a compelling mechanism to drive deglaciation because the effects of CO_2 are globally distributed, and could help to explain why ice ages are synchronous between the two hemispheres despite the Northern Hemisphere orbital signal (Mercer, 1984; Broecker, 2013). If CO_2 was the focal driver of deglaciation, then the main phase of retreat of the glaciers in Mongolia would occur after 17.5 ka, the time at which CO_2 began to increase (Broecker, 2013; Shakun et al., 2015).

1.4. Research objectives

^{10}Be surface-exposure dating allows for high-resolution investigations into climate research by enabling glacial reconstructions on the millennial timescale (Balco, 2011). In this thesis, I present a ^{10}Be chronology for glacier recession in the Tsagaan Gol-Potanin Glacier valley during the last glacial cycle to determine millennial-scale changes. In addition to the chronology, I use paleo-glacier modeling to estimate changes in snowline and atmospheric temperature. I compare the glacial record to time series of insolation rise, North Atlantic sea-surface temperature, and atmospheric CO_2 to test possible drivers of Northern Hemisphere deglaciation. The glaciers of western Mongolia will provide an important test of ice age theories by offering a well-dated constraint on climate in the center of Asia during the termination.

CHAPTER 2

BACKGROUND

2.1. Physical setting

The Altai Mountains of central Asia span Mongolia, China, Russia, and Kazakhstan, extending from the Gobi Desert to the West Siberian Plain (45-52°N to 89-94° E) (Figure 2.1). In western Mongolia, the Altai Mountains are dominated by the Tavan Bogd massif. The mountain range features five major peaks, the tallest of which is Khüiten at 4,374 m a.s.l. (Figure 2.2). The Altai Mountains were formed through subduction zone processes on the margins of the Eurasian continent. This mountain-building event is considered one of the least understood Phanerozoic orogens in the world (Windley et al., 2002). The orogeny occurred approximately from the Neoproterozoic to the Early Devonian, although chronologic constraints are limited and the granitic intrusions are almost entirely undated (Windley et al., 2002). Tavan Bogd massif is composed of metamorphosed quartzo-feldspathic rhythmites and intrusive volcanic lithologies (Windley et al., 2002).

The Mongolian Altai features a semi-arid continental climate characterized by extreme seasonality. Winter temperatures can fall to below -20°C on the Mongolian steppe. In contrast, summer months are warm and July temperatures can reach 20°C (Lehmkuhl et al., 2011). A weather station in the high Altai recorded a mean summer temperature of 3.4°C and a mean annual temperature of -8.8°C from 2007-2008 (Konya et al., 2010). The Altai Mountains block the flow of the Northern Hemisphere westerlies, which deliver moisture to the region (Lehmkuhl et al., 2011). Precipitation at high elevations in western Mongolia is estimated to be greater than 300 mm annually and decreases to about 200 mm/yr on the eastern, leeward side of the mountain range (Lehmkuhl et al., 2011). Precipitation records near Tavan Bogd are limited to low-elevation population centers. In Khovd, about 300 km away from Tavan Bogd, the mean annual precipitation from 1961 to 1990 CE was 138 mm (Kadota and Gombo, 2007). About 70% of annual precipitation occurs in the summer, from June to August (Kadota and Gombo, 2007).

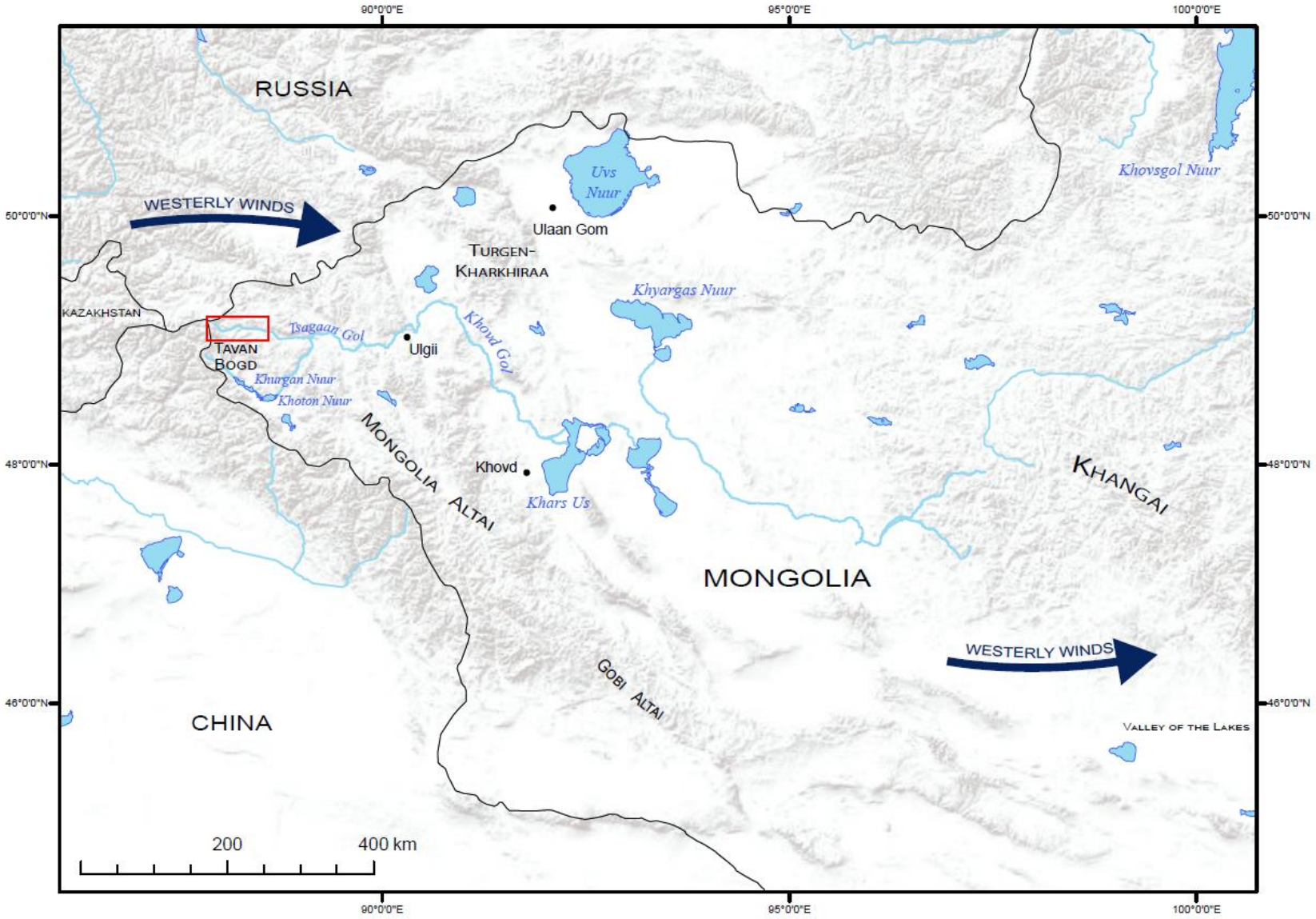

Figure 2.1. Regional map of interior Asia. Red box indicates study area. Base map is World Terrain Base by Esri.

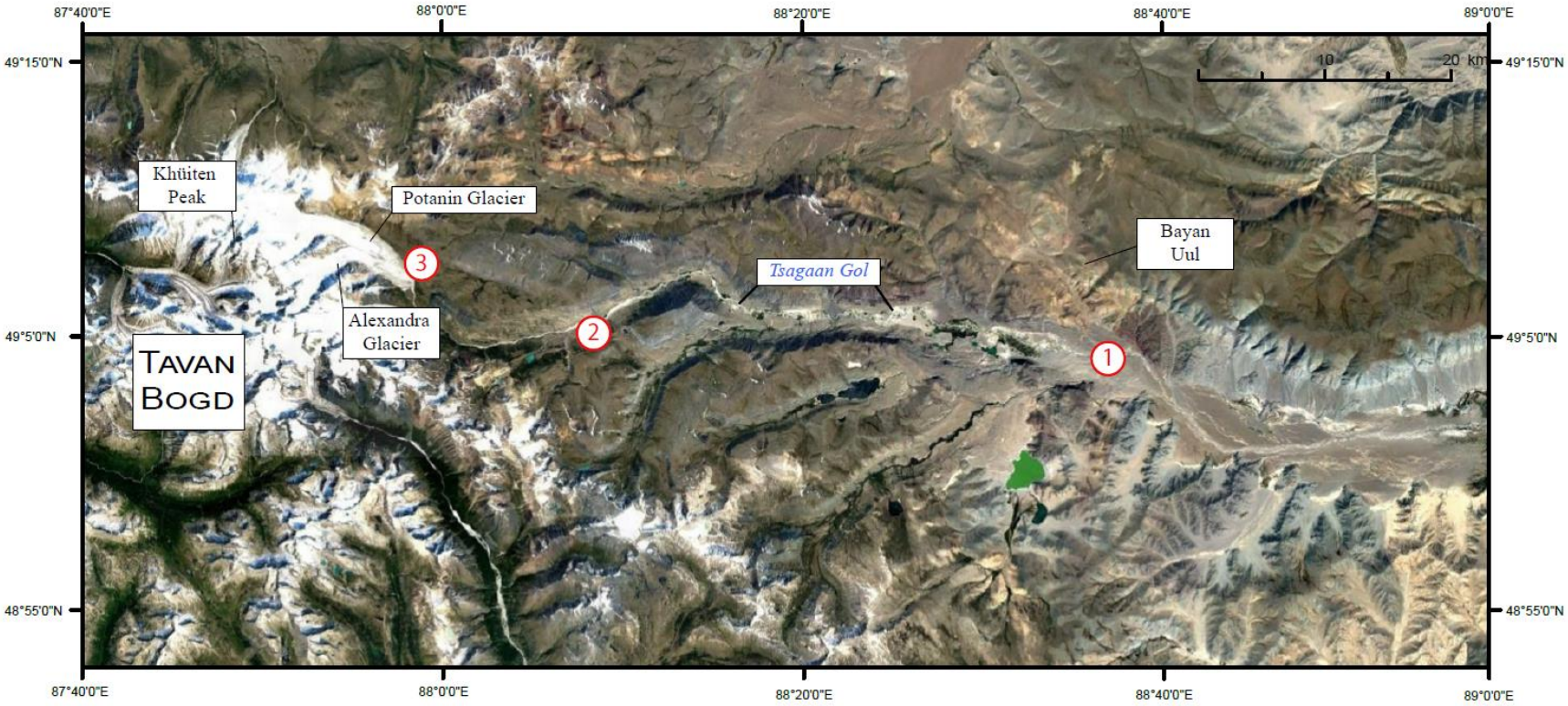

Figure 2.2. Google Earth satellite image of Tsagaan Gol-Potanin Glacier valley. (1) marks Bayan moraine complex, (2) marks Holy Mountain, and (3) marks the Potanin Glacier and moraines.

For my thesis research, I studied the Tsagaan Gol-Potanin Glacier valley, which features the modern Potanin Glacier (49° 8'19"N, 87°56'36"E) at the valley head (Figure 2.2). The Potanin Glacier drains a high icefield of the Tavan Bogd massif and is the largest glacier in Mongolia, with a length of approximately 11 km and an area of 43 km^2 (Kadota and Gombo, 2007). The Alexandra Glacier, a tributary of the Potanin Glacier, is located to the southeast and joins the Potanin Glacier in the terminal region. The valley trends to the east and Tsagaan Gol (transl. "White River"), fed by the meltwater of the Potanin Glacier, flows into Khovd Gol and eventually into Khars Us Nuur, a terminal closed-basin lake located in the central Mongolian great basin.

2.2. Previous studies

Few glacial geomorphic studies have been conducted in the remote Mongolian Altai (Lehmkuhl, 1998). The area was visited by Russian geographers in 1905 CE who photographed the Potanin Glacier when it stood close to its Little Ice Age moraine belt (Figure 2.3) (Sapozhnikov, 1949; Syromyatina et al., 2015). The initial geomorphic studies from the 1980's suggested that the Mongolian Altai experienced two to three phases of glaciation during Marie Isotope Stage (MIS) 2 and MIS 4 (Lehmkuhl, 1998). Devjatkin (1981) obtained absolute dates for glaciations in the Altai using thermoluminescence and radiocarbon dating. Material from glacial landforms yielded ages of 35.3 ± 0.6 ^{14}C ka [39.9 ± 0.7 ka; calibrated using IntCal13 (Reimer et al., 2013) and OxCal v4.3.2 (Ramsey, 2017)] and 32 ± 6 ka with thermoluminescence dating (TL). An older landform yielded an age of 103 ± 12 ka (TL).

Paleo-lake levels from the "Valley of the Lakes", an expanse of closed-basin lakes located between the Khangai and Govi-Altai mountains (Figure 2.1), have also been used to infer the timing of Pleistocene glaciations in western Mongolia (Florensov and Korzhnev, 1982). However, there are only a few dates constraining the timing of Pleistocene high lake levels (Lehmkuhl, 1998). Furthermore, the areas of closed-basin lakes are highly sensitive to catchment-wide runoff from glacial melt, precipitation, and seasonal snowmelt (Broecker, 2010; Barth et al., 2016; Putnam and Broecker, 2017). Thus, any

impact of glacier melt on western Mongolian closed-basin lakes is likely to be obscured by changes in runoff related to precipitation and seasonal snowmelt.

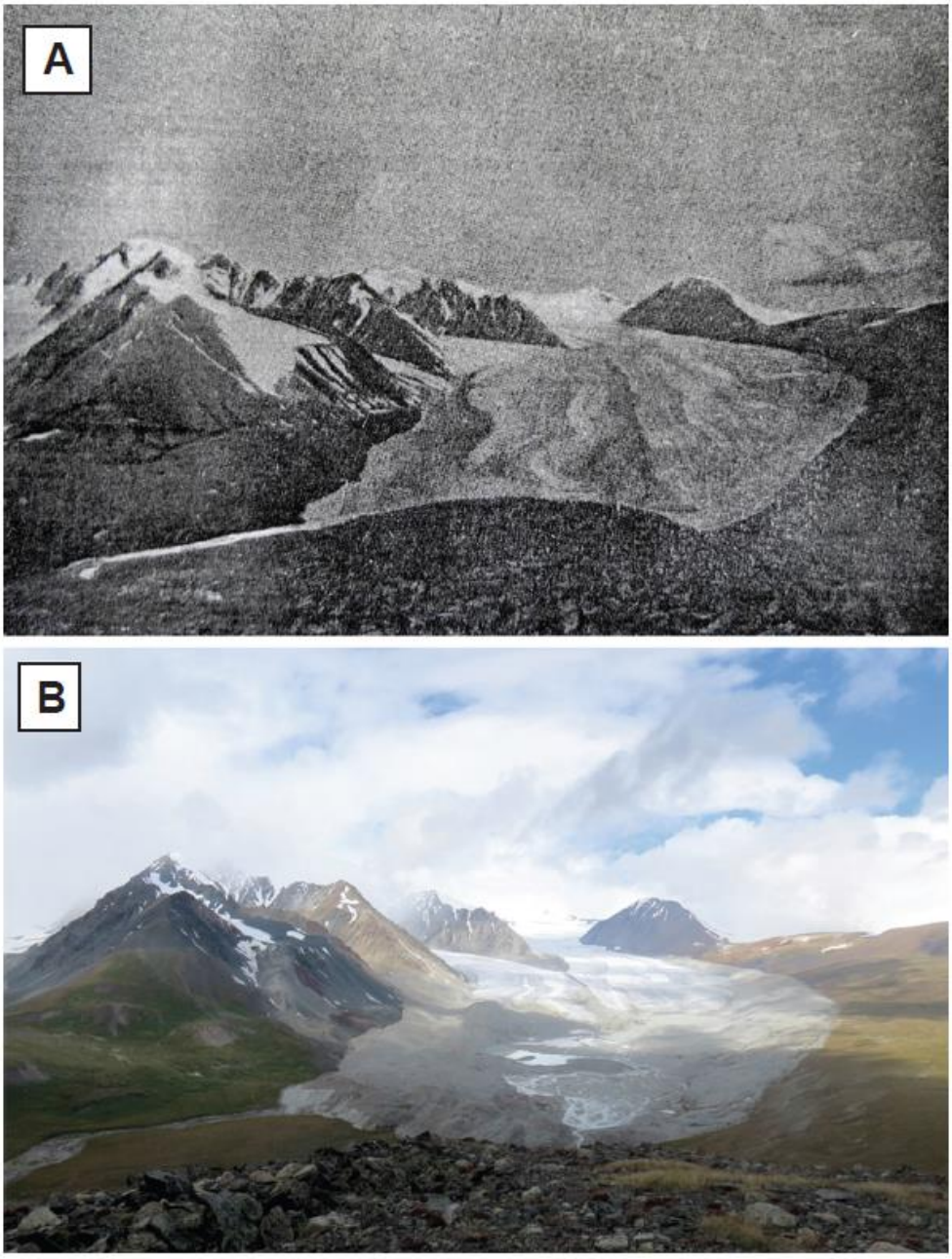

Figure 2.3. Terminus of Potanin and Alexandra Glaciers, vantage to the west. (A) photo by Sapozhnikov, taken in 1905 CE. (B) ground photo taken in 2013 CE. Modified from Syromyatina et al. (2015).

More recent studies have investigated the extent and timing of Late Pleistocene glaciation in the Altai (Klinge, 2001; Lehmkuhl et al., 2004; Lehmkuhl et al., 2011; Lehmkuhl et al., 2016). Lehmkuhl et al. (2007) obtained four optically stimulated luminescence (OSL) ages sampled from fluvial and aeolian sand and silt strata between tills related to the LGM in the Russian Altai. Ages determined from deposits interbedded with multiple tills ranged from 28 -19 ka (Lehmkuhl et al., 2016). A ^{10}Be chronology from the Khangai Mountains in central Mongolia concluded that ice advanced 35-40 ka, 23 ka, and 16-17 ka (Rother et al., 2014). The geographically closest study to the Potanin Glacier valley comes from Lehmkuhl et al. (2016). OSL dates on moraines around the glacial lakes, Khurgan and Khoton Nuur, have minimum limiting ages of 13.6 ± 1.6 ka, 57.8 ± 9.1 ka, and 85.6 ± 10.4 ka.

CHAPTER 3

METHODS

3.1. Glacial geomorphic mapping

I mapped glacial and periglacial landforms, including moraines, rock glaciers, outwash plains, and alluvial deposits, using the symbology from Barrell et al. (2013). In the field, I made hand-drawn maps marking moraine ridges, ground moraine, and terraces. Later, I augmented these maps by interpreting imagery from Google Earth, Shuttle Radar Topography Mission digital elevation models (DEM) at 25.5 m/pixel, and processed drone imagery with ~ 0.3 m/pixel resolution. I used depositional and erosion features to identify landforms and cross-cutting relationships to assign relative ages.

The drone imagery was obtained during the 2016 field season from a DJI Phantom 4 quadcopter (see Appendix A for more detail). I piloted the drone over the Potanin Glacier and Bayan moraine complexes because these two regions contain the majority of boulders sampled for surface-exposure dating. I flew the drone at 100-300 m elevation and set the flight path with an application called "Map Pilot" by Maps Made Easy for iPad. The drone took pictures with 75% overlap to ensure that there were enough tie points among the photographs to develop accurate orthomosaics and DEMs. I then processed the images using Agisoft Photoscan Professional Edition software. In Photoscan, I produced DEMs and orthomosaics. The maps were automatically geo-rectified in Photoscan because of the drone's internal GPS. I improved the spatial accuracy by using sample locations as ground control points, which were measured with a differential GPS and are accurate to ± 10 cm in the horizontal and vertical directions.

3.2. Sample collection

During the summer of 2016, I collected samples from glacially deposited boulders in the Tsagaan Gol-Potanin Glacier valley. I sampled boulders located on glacial moraine ridges, recessional ground moraine, and bedrock. I targeted moraine ridges that appeared stable, showing no evidence of post-

depositional modification, such as mass-wasting, fluvial, and/or anthropogenic processes. Glacial erratic boulders were sampled on ground moraine and on bedrock in regions devoid of constructional landforms.

Boulders were selected based on their geomorphic stability. I assessed the surrounding area for indications of disturbance, including steep-slope angles, fluvial channels, and human activity. I sampled boulders that were embedded in low-angle slopes or located on crests of moraine ridges. I assessed the top surface of each boulder to ensure that I collected samples with minimal surface erosion. Jointed, fractured, exfoliating, pitted, or disintegrating surfaces were avoided in an effort to sample the original surface. I preferentially sampled boulders that had glacial polish, striations, and/or rock varnish because these features indicate minimal surface material loss. In addition, I preferentially sampled flat surfaces on the top of the rocks or sloping upper surfaces. Examples of boulder sampled in this study are in Figure 3.1.

Samples were extracted using wedges and shims (See Appendix A for more detail). This method involves drilling three to five 3/8" holes around the selected sample site. Two shims are inserted into each hole, and wedges are driven between each set of shims until the sample is dislodged from the boulder. After extracting the sample, I measured the geographic location of the sample site, including elevation. The location was measured at each sample site using a Trimble Geo7x, corrected with a Trimble Geo7x base station located less than 10 km away. I used the GeoID application on an iPad to measure the orientation of the sampled surface and a clinometer to record topographic shielding. Shielding corrections were determined using the CRONUS Geometric Shielding Calculator (http://hess.ess.washington.edu/math/general/skyline_input.php). Boulder dimensions were measured with a tape measure, and the boulder was documented photographically from multiple aspects and sketched in a notebook.

Figure 3.1. Examples of boulder sampled for ^{10}Be surface-exposure dating. (A) Sample TGP-16-16 located outboard of Potanin moraines. (B) Sample TGP-16-18 located outboard of Potanin moraines. (C) Sample TGP-16-30 located outboard of Potanin moraines. (D) Sample TGP-16-53 located on Bayan-I moraine. (E) Sample TGP-16-62 located on ground moraine outboard of Bayan-I. (F) Sample TGP-16-70 located on Bayan-II. Photographs by Mariah Radue.

3.3. ^{10}Be surface-exposure dating

^{10}Be surface-exposure dating relies on the accumulation of the cosmogenic isotope, ^{10}Be, in the mineral quartz after it is exposed to Earth's surface. Cosmic rays, high-energy particles from outer space, bombard the silica and oxygen in quartz producing cosmogenic nuclides, including ^{10}Be (Gosse and Phillips, 2001). The amount of ^{10}Be in a rock sample is compared to an independently determined production rate to calculate the exposure age of the sample. For glacially deposited boulders, the accumulation of ^{10}Be begins when the boulder is deposited by the glacier on a moraine or as a glacial erratic. When dating glacial deposits, it is assumed that any previously accumulated ^{10}Be is removed by erosion through glacial quarrying and/or abrasion. In other words, the cosmogenic clock is "reset" by glacial transport and the only exposure history recorded in the sample is post-depositional.

I processed samples at the University of Maine's Cosmogenic Isotope Laboratory (see Appendix A for laboratory procedures). First, I measured the thickness of each rock sample at 4-cm intervals using digital calipers and determined a mass-weighted average thickness value. Then, I crushed samples using a jaw crusher and pulverizer, sieving the sample to a grain size of 710-125 μm. I employed froth flotation to remove most of the feldspars and etched each sample in 1-5% hydrofluoric acid until only quartz remained. Some samples received O-phosphoric boiling treatment to remove cementation. Depending on the mineralogy of each sample, I performed magnetic and heavy liquids separation techniques in addition to hydrofluoric acid etching to further isolate the quartz from other minerals in the sample. I boiled some samples in HCl to remove native or precipitated fluorite. Once samples consisted of pure quartz, I measured the concentrations of Al, Ca, Fe, and Be using an Inductively Coupled Plasma Optical Emission Spectrometer (ICP-OES) to verify purity (Appendix B).

Beryllium extraction was performed using a version of the methods detailed on the Lamont-Doherty Earth Observatory Cosmogenic Dating Group website and included in Appendix A (http://www.ldeo.columbia.edu/cosmo/methods). Beryllium ratios (^{10}Be/^{9}Be) were measured with the CAMS accelerator at the Lawrence Livermore National Laboratory using the 07KNSTD standard,

$^{10}Be/^{9}Be = 2.85e^{-12}$ (Nishiizumi et al., 2007). The $^{10}Be/^{9}Be$ ratios were then corrected for residual boron contamination and ^{10}Be in blanks.

I report ages using two scaling methods: (1) the scaling method of Stone (2000) and (2) a version of the Stone (2000) scaling method that incorporates a high-resolution version of the Lifton et al. (2008) geomagnetic model, labeled 'Lm' (Putnam et al., 2010b). I calculated surface-exposure ages using the sea-level high-latitude ^{10}Be production rate from New Zealand published by Putnam et al. (2010b) of 3.74 ± 0.08 atoms/g/yr (Lm). The New Zealand-based production rate is similar to the rate determined from the Swiss Alps, 3.83 ± 0.24 atoms/g/yr (Lm) (Claude et al., 2014). The production-rate calibration site in the Swiss Alps is at similar latitude (46°N) to the Mongolian Altai (49°N), therefore the more precisely measured New Zealand rate, which is also from a mid-latitude site and yields an indistinguishable rate from the Swiss site, should be appropriate for age calculations in the Mongolian Altai. The average thickness of the samples was used to correct for attenuation of cosmic rays with depth. I incorporated a shielding correction based on the skyline measured with a clinometer at the sample site to account for cosmic rays blocked by the surrounded topography.

^{10}Be production can be affected by the post-deposition environment, by erosion and/or snow cover. Erosion preferentially removes Be atoms and, if left uncorrected, would yield artificially young boulder ages. I did not incorporate erosion rates into the age calculations because preservation of striations and glacial polish on many samples indicates that no erosion had taken place. Thick, prolonged snow cover may also lead to artificially young ages because snow attenuates the cosmic ray flux. I did not apply a snow-cover correction because of the paucity of snow-depth data in the region. In addition, strong winter winds in the Altai would also likely scour prominent moraine features leaving thin or no snow cover (Konya et al., 2010). Additionally, the effects of erosion or snow cover would probably not be consistent among the boulders and would therefore produce noticeable scatter in the dataset.

3.4. Snowline modeling

To reconstruct configurations of the Tsagaan Gol-Potanin paleo-glacier, I employed an ArcGIS toolbox developed by Pellitero et al. (2016) called GlaRe. I reconstructed the paleo-glacier during two periods of moraine deposition, at the Potanin moraines and the Bayan moraine complex. The GlaRe toolbox is based on the method developed by Benn and Hulton (2010), which assumes the glacier has perfectly plastic flow and no basal sliding. The model constrains the glacier surface based on the underlying topography as well as user-defined terminal limits, center flowlines, and basal shear stress. The GlaRe model assumes that the reconstructed glacier is in equilibrium with climate and that the present-day topography represents the glacial basal topography.

I used a 25.5 m/pixel SRTM digital elevation model as the underlying topography of the glacial model. The flowlines were input manually based on visual inspection of the valley center. For the Bayan reconstruction, the Bayan-II moraine was used as the target terminal moraine because it corresponds to the LLGM (see Results section below). I used the outermost moraine, Potanin-I as the terminal limit for the Little Ice Age reconstruction. When reconstructing the Little Ice Age paleo-ice surface, I subtracted the volume of the modern Potanin Glacier using the ice-subtraction tool in GlaRe because the modern ice significantly distorts the underlying topography. The basal shear stress was tuned to make the glacier surface fit with the glacial landforms and ^{10}Be chronology. The basal shear stress for the Bayan reconstruction was 25 kPa in the low-angle terminal area, 50 kPa mid-valley, and 85 up-valley in the steep, mountainous region. The Little Ice Age reconstruction has a basal shear stress value of 50 kPa. Glacial surfaces were interpolated using the inverse-distance weighting method.

The equilibrium line altitude (ELA) is the altitude on the glacier where net accumulation equals net ablation at the end of the melt season. Integrated over many years, the location of the ELA is dictated by climate and topography (Benn and Evans, 2010). The paleo-ELAs were estimated using another ArcGIS toolbox created by Pellitero et al. (2015). I used the accumulation-area ratio (AAR) method for determining the ELA because it is the most commonly used technique for ELA estimation (e.g. Porter, 2001; Benn and Ballantyne, 2005). I chose an AAR value of 0.6 ± 0.5 because these are typical values for

valley glaciers (Bakke and Nesje, 2011). Also, an AAR value of 0.6 ± 0.5 is with the range of the AAR with of the modern Potanin Glacier (Konya et al., 2013). The ELA equates to the snowline at the end of the ablation season (Benn and Evans, 2010), and from here on the ELA will be referred to as the "snowline".

CHAPTER 4

GLACIAL GEOMORPHOLOGY

Surface morphology reveals that during glacial periods, multiple outlet glaciers flowed from an icefield centered on the Tavan Bogd massif. One of the outlet glaciers flowed into the Tsagaan Gol-Potanin Glacier valley, an eastward-trending U-shaped valley (Figure 2.2). The valley is about 300-700 m lower than the surrounding plateau. At the head of the valley lies the Potanin Glacier next to the Little Ice Age moraines. About 50 km down-valley from the Potanin Glacier is a suite of moraines located close to the mountain, Bayan Uul. Another major tributary from the icefield is located about 40 km to the south with terminal and lateral moraines bordering the lakes, Khurgan and Khoton Nuur. A contemporaneous study of the glacial history of the Khoton Nurr valley is being carried out by Strand et al. (in prep.)

I mapped and described three study areas within the valley, the Bayan moraine complex, the Holy Mountain region, and the Potanin Glacier moraine complex (Figure 2.2). Below I describe the glacial geomorphology of each study area in detail.

4.1. Bayan moraine complex

A suite of moraines is located about 50 km down-valley of the present-day Potanin Glacier terminus near the mountain, Bayal Uul (Figures 4.1-2). A large composite constructional moraine belt, Bayan-I, marks the outermost preserved limit of glaciation in the valley (Figure 4.3). This moraine ridge rises about 40 m above the ice-distal outwash plain and 10 m above the moraine on the ice-proximal side. Graded to the Bayan-I moraine complex is a well-developed outwash plain that extends 30 km down-valley. The outwash is composed of rounded clasts, ranging from pebble to boulder and the lithologies are dominated by granitoids, with few quartzites and metavolcanics. Terraces and boulder bars are preserved on the outwash plain. A patch of ground moraine is located outboard of the Bayan-I ridge and projects above the outwash plain. The ground moraine shows no signs of fluvial reworking and features embedded granitoid boulders.

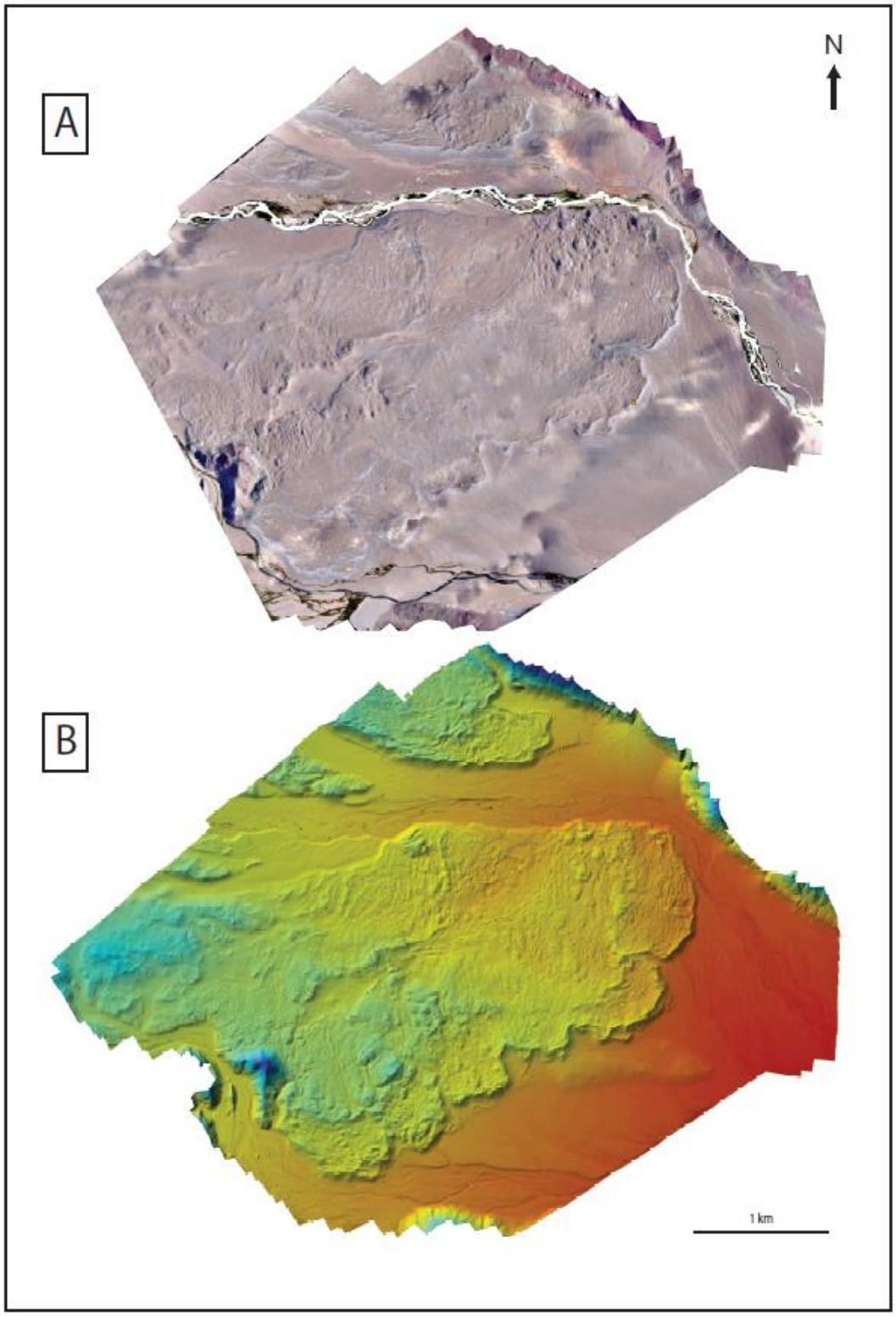

Figure 4.1. Drone imagery of Bayan moraine complex. (A) Orthomosaic and (B) digital elevation model of Bayan moraine complex, with 33.3 cm/pi resolution.

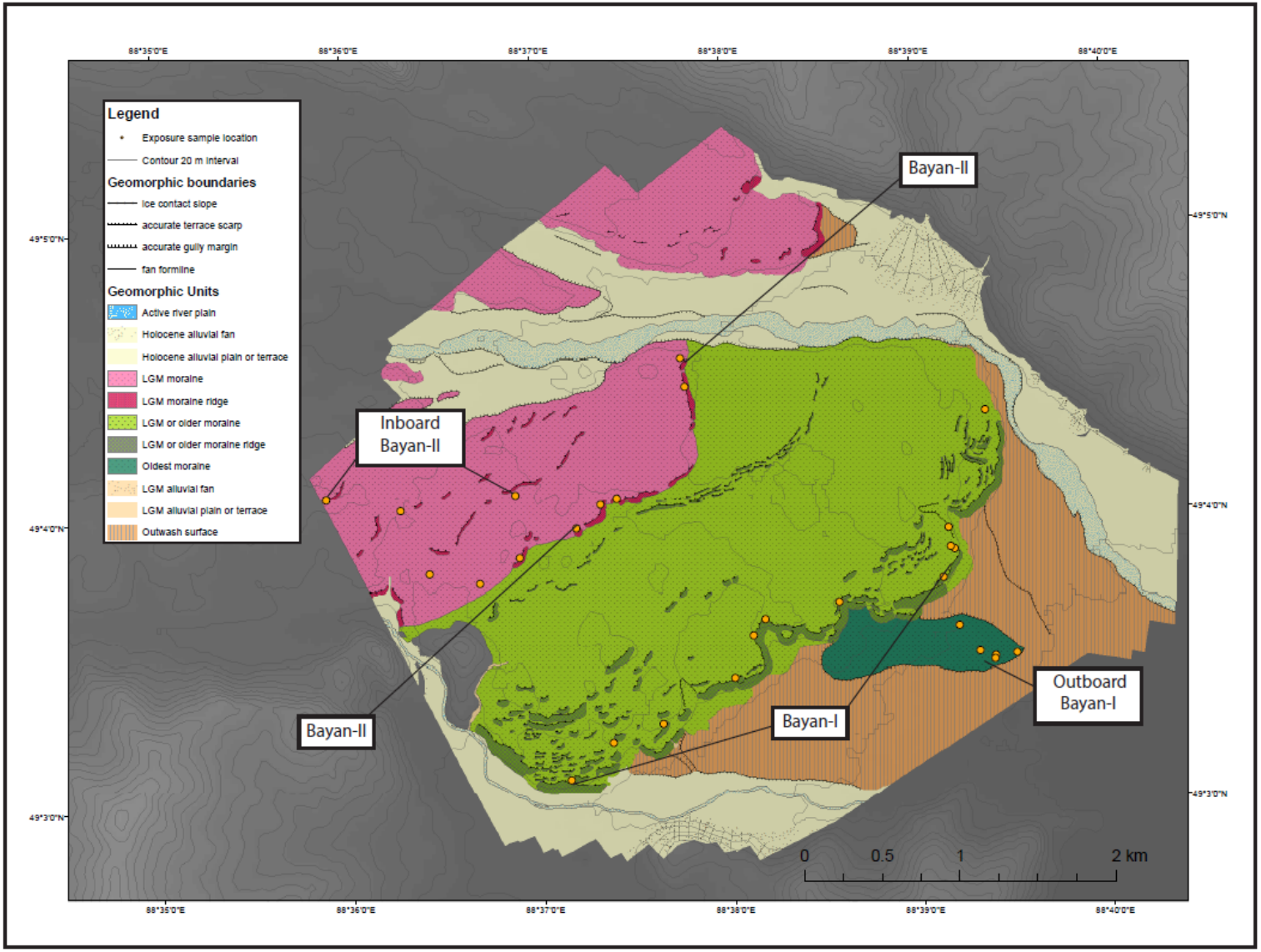

Figure 4.2. Glacial-geomorphic map of Bayan moraine complex, Area 1 in Figure 2.2.

Inboard of Bayan-I, there are many small, discontinuous moraine ridges that range in height from 1-3 m. These landforms are subtle and were difficult to map at ground level in the field. Bayan-II is the next continuous moraine inboard of Bayan-I and shares a similar composition to Bayan-I. Outboard of the moraine there is a narrow (~100 m) outwash plain that is smooth and graded to Bayan-II. Inboard of Bayan-II, there are several small discontinuous moraines and hummocky terrain that grades into ground moraine.

The entire sequence is cut by the Tsagaan Gol (*White River* in Mongolian). The river drains the glaciers and snowfields of Tavan Bogd and has suspended silt or "glacial flour". The river is braided and has several abandoned floodplains. Colluvium from the steep hillsides both cross-cuts and is cross-cut by the river, indicating that they coevolved.

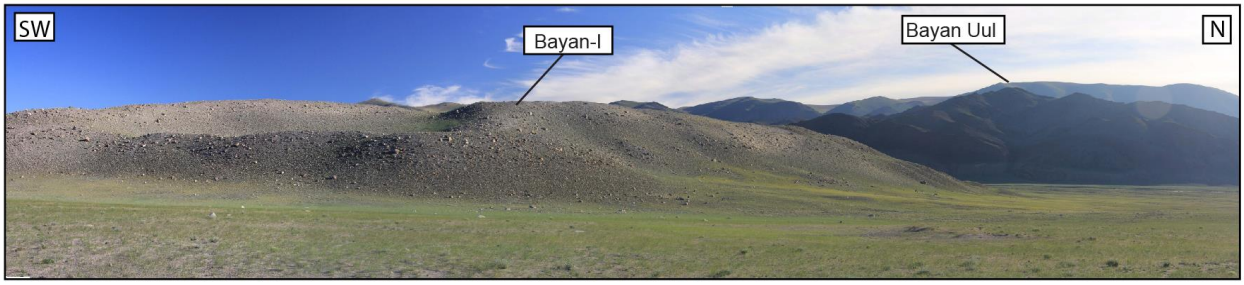

Figure 4.3. Ground photograph Bayan moraine complex. Photograph was taken from the outboard outwash plain, by Aaron Putnam.

4.2. Holy Mountain

Holy Mountain (*Shiveet Khairkhan Uul* in Mongolian) is a partially ice-molded bedrock hill located about 35 km west of the Bayan moraine complex (Figures 4.4-5). The mountain is a UNESCO World Heritage site because early peoples used the glacially-polished bedrock as a canvas for petroglyphs (Jacobson-Tepfer, 2013). The mountain rises 800 m above the valley floor to a maximum elevation of 3200 m a.s.l.. I identified granitoid erratics on the metasedimentary bedrock at least as high as 2966 m a.s.l.. The mountain has a characteristic rôche moutonnée shape with a low-angled stoss side and a steep leeward side. To the west of Holy Mountain, there is a ridge that marks a flow divide where ice diverged around the mountain. North of the flow divide, the bottom of the valley features extensive ground

moraine littered with large granitoid boulders. On the southern side of the valley, there are three subtle (less than 10-m relief) benches (Figure 4.5).

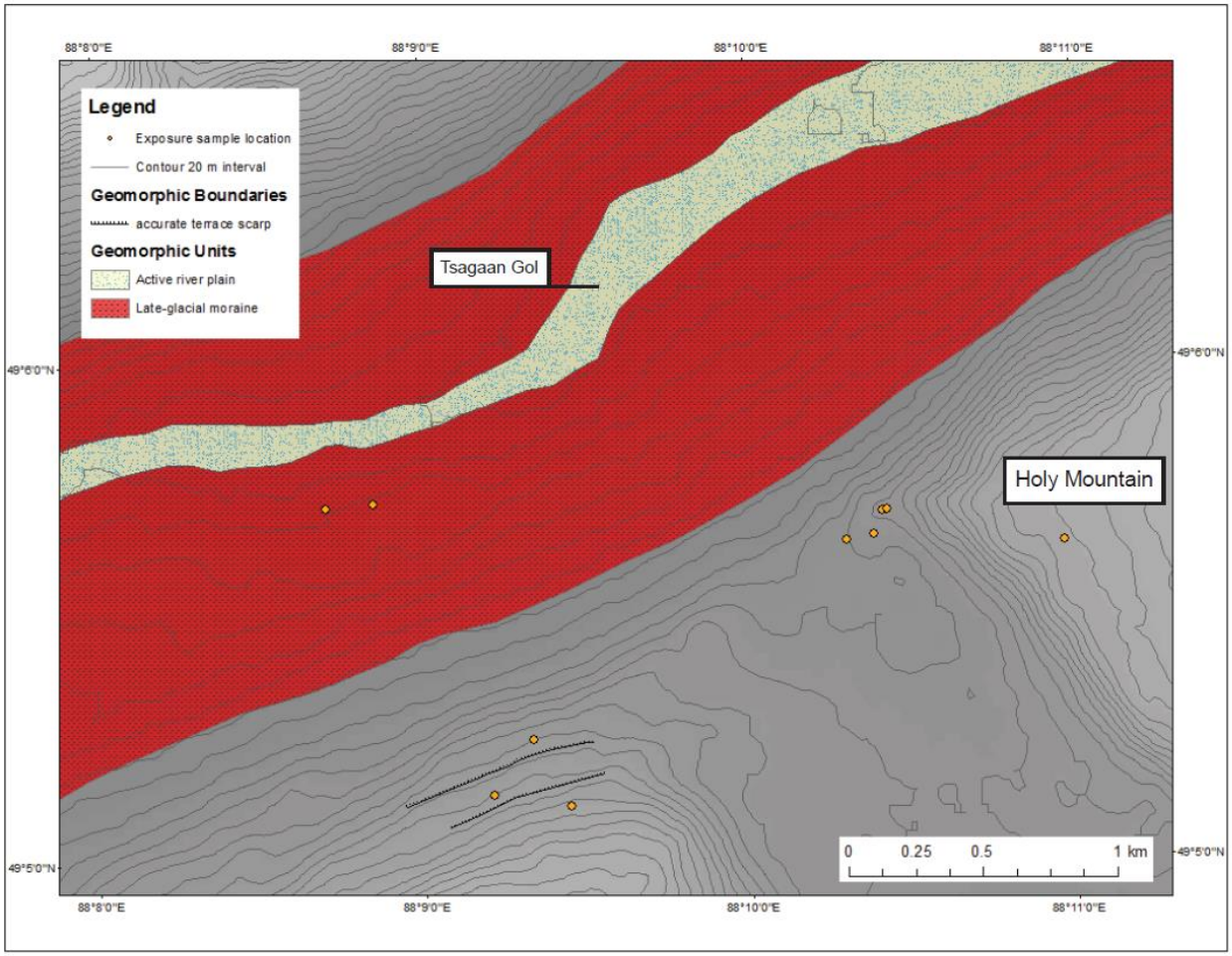

Figure 4.4. Glacial-geomorphic map of Holy Mountain region. Holy Mountain is Area 2 on Figure 2.2.

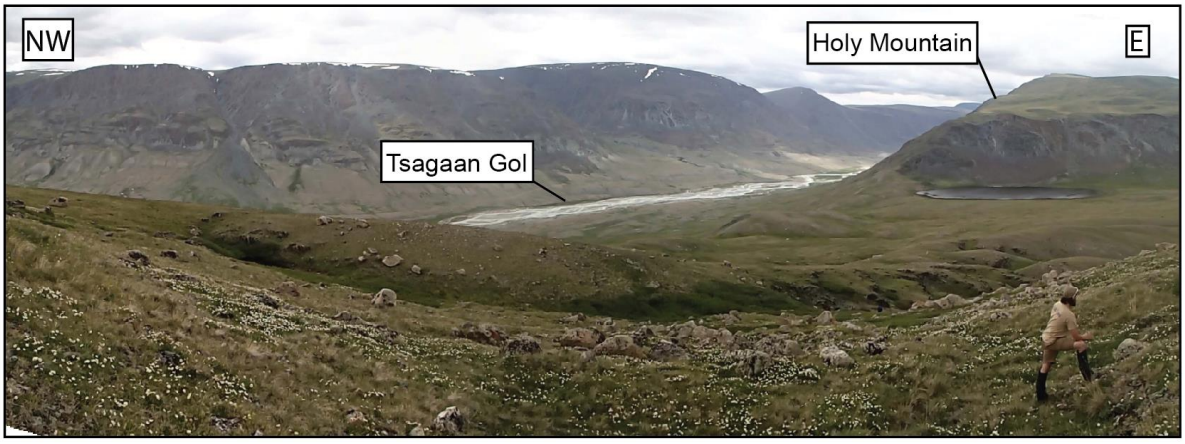

Figure 4.5. Panoramic view of Holy Mountain and Tsagaan Gol. Photograph by Mariah Radue.

4.3. Potanin Glacier moraine complex and outboard landscape

The Potanin Glacier is bordered by a well-developed suite of lateral and terminal moraines presumably formed during the culmination of multiple Little Ice Age advances (Figures 4.6-8). The terminal Potanin moraine is 2 km east of the modern glacial terminus. The moraine ridges extend approximately 40-60 m above the ice surface. There are two prominent moraine ridges in the moraine complex, here referred to as Potanin-I and Potanin-II. Although these ridges were sampled for surface-exposure dating, the samples were not processed for this study. Potanin-II is about 20 m above the modern ice surface and 30 m below the Potanin-I ridge crest. There are also smaller, <10-m relief discontinuous ridges within the moraine complex.

The Potanin moraines are composed predominately of light-gray granitoid lithologies with a few meta-sedimentary rocks. Clast sizes range from ~2 m-diameter boulders to sand. The moraines are poorly consolidated, with approximately 20° slopes dipping toward the glacier. Small, alpine vegetation sparsely covers the moraine and red-colored lichen covers the sides of boulders. Small lakes dot the moraines and have a light blue color. The moraines in the terminal area rise about 70 m above the outboard bedrock, with three distinct discontinuous ridges. The terminal moraines are incised by a meltwater stream, the headwaters of the Tsagaan Gol. The meltwater stream enters a shallow bedrock canyon about 500 m in front of the terminal moraines, incising bedrock composed of fine-grained volcanic lithologies.

The outermost Potanin moraine ridge abuts a vegetated landscape characterized by thin ground moraine mantling glacially-molded granitic bedrock. The ground moraine is comprised of predominately larger clasts ranging from cobble to boulder, and supports generally thin soil (<1 m) and a subalpine steppe vegetation assemblages, including *Cyperaceae*, *Kobresia*, *Artemisia*, and *Chenopodiaceae* (Unkelbach et al., 2017). Exposed bedrock is frost-shattered in bands about 1-m wide and 100-m long. The landscape contains three distinct glacially-carved benches, 0.2-1.2 km outboard of the Potanin-I moraine ridge.

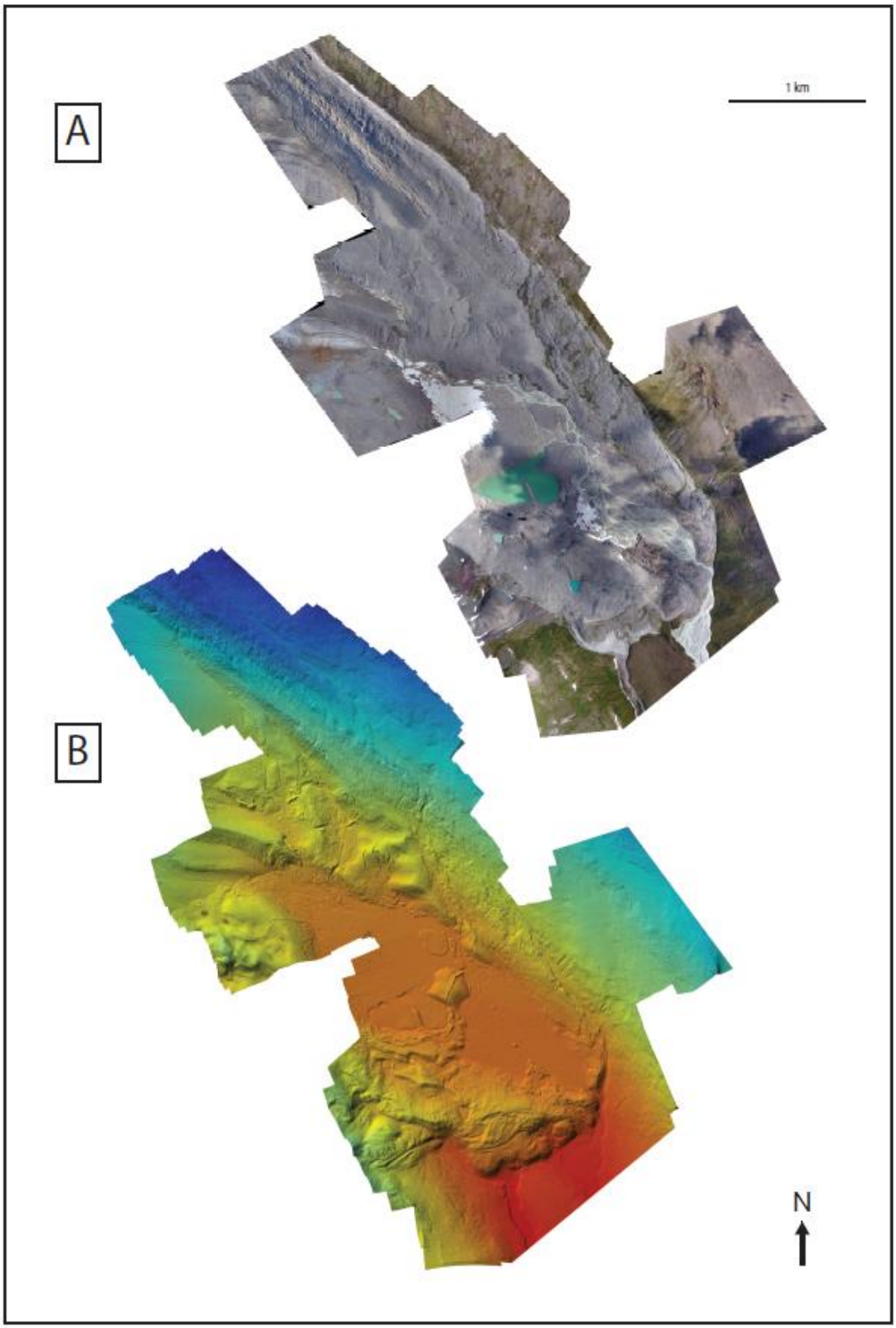

Figure 4.6. Drone imagery of Potanin moraines. (A) Orthomosaic and (B) digital elevation model of Potanin moraine complex, with 34.4cm/ pi resolution.

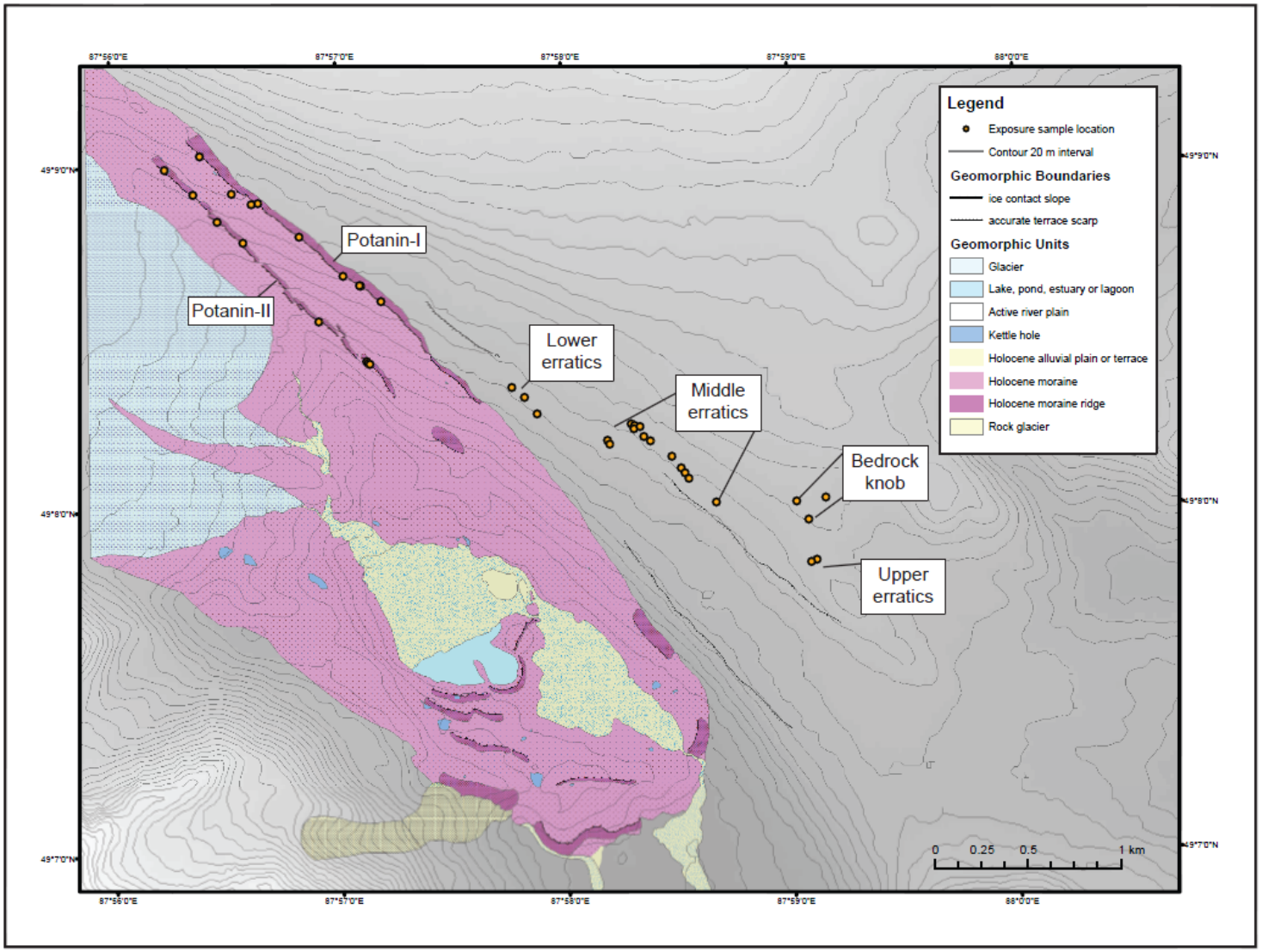

Figure 4.7. Glacial-geomorphic map of Potanin moraines and the outboard landscape. The area is labeled "3" in Figure 2.2.

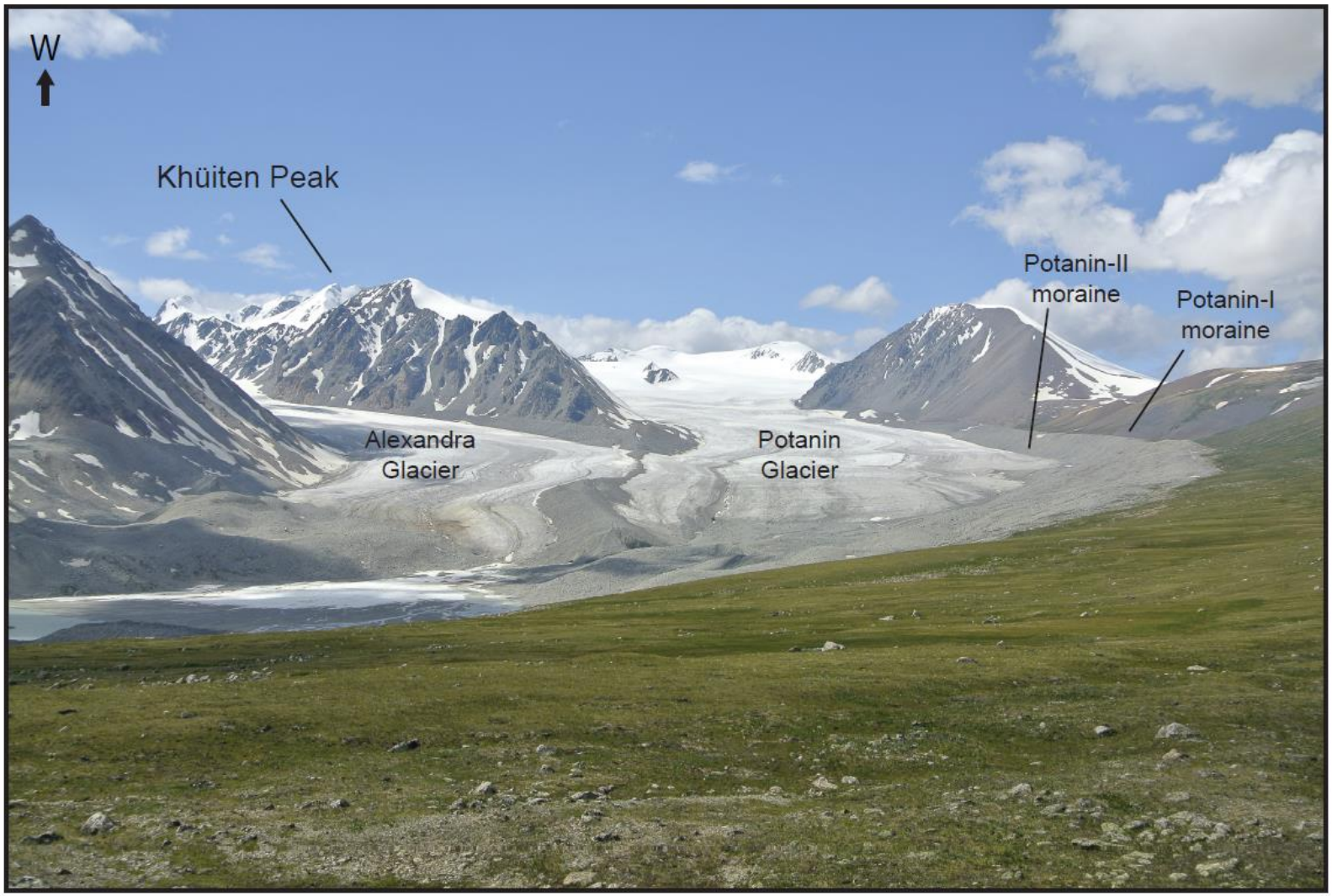

Figure 4.8. Ground photograph of Potanin Glacier and moraines. Photograph by Peter Strand.

CHAPTER 5

RESULTS

I generated 41 ^{10}Be surface-exposure ages out of 76 samples collected in the field (see Appendix C for full sample catalog). I obtained 19 exposure ages from the Bayan complex, 7 from Holy Mountain, and 15 from the recessional landscape outboard of the Potanin moraine complex. Results of ^{10}Be analyses and procedural blanks are given in Table 5.1 and 5.2, respectively. Calculated sample ages are in Table 5.3. For ages obtained from a moraine, I calculated the mean age and the standard error of the mean, using the production rate error of 2.1% associated with the New Zealand production rate (Putnam et al., 2010b). For ages of glacial erratics on ground moraine or bedrock, I summarize the ages as a range. The results of landform statistics are found in Table 5.4. Calculated ages are plotted on glacial-geomorphic maps in Figure 5.1. The probability density functions, hereby called 'camelplots', are shown in Figure 5.2.

Ages marked with a single asterisk (*) are considered outliers and are not included in statistical analysis or age ranges. Outliers were identified in two ways. First, if the surface-exposure age did not agree morphologically with other samples from a sequence of glacial landforms, they are considered outliers. Second, I used Chauvenet's Criterion to test for statistical outliers at the 95 % confidence of samples on one landform (Bevington and Robinson, 1992; Dunai, 2010).

5.1. Bayan moraine complex

I obtained 19 ages from the Bayan moraine complex from the 28 samples collected in this region. Samples are located in four regions: outboard of the Bayan moraines, moraine ridges Bayan-I and II, and inboard of the Bayan moraines. The three analyzed samples from the glacial erratics outboard of Bayan-I have exposure ages of 196.1 ± 1.7 ka, 162.5 ± 1.5 ka, and 132.9 ± 1.2 ka. Seven exposure ages determined from Bayan-I are scattered and range from 9.28 ± 0.19 ka to 56.83 ± 0.71 ka. Five samples were identified as outliers (TGP-16-51, TGP-16-52, TGP-16-53, TGP-16-56, TGP-16-57)

Table 5.1. Results from ^{10}Be sample analysis. In [^{10}Be] calculations, an erosion rate of 0 and a density of 2.7 g/cm^2 are assumed. The standard, 07KNSTD3110 was used for all samples.

LLNL ID	Sample Name	Latitude (DD)	Longitude (DD)	Elevation (m a.s.l.)	Sample Thickness (cm)	Shielding Correction	Quartz Weight (g)	Carrier Added (g)	Carrier [^{9}Be] (ppm)	^{10}Be/^{9}Be ± 1σ (10^{-14})	[^{10}Be] ± 1σ (10^4 atoms/g)	Average ^{9}Be current (μA) (runs)
BE43012	TGP-16-01	49.095195	88.145080	2404.6	2.226	0.99245	5.3533	0.20296	1027	22.886 ± 0.429	59.34 ± 1.11	19.3 (3)
BE43013	TGP-16-02	49.095293	88.147502	2420.4	1.568	0.99335	5.084	0.20233	1027	15.290 ± 0.287	41.54 ± 0.78	28.4 (3)
BE43014	TGP-16-03	49.087360	88.155554	2673.0	1.161	0.98701	5.2688	0.20184	1027	21.840 ± 0.410	57.2 ± 1.08	25.3 (4)
BE43015	TGP-16-07	49.094106	88.173021	2591.4	1.585	0.98783	5.2186	0.20261	1027	17.800 ± 0.372	47.22 ± 0.99	27.3 (4)
BE43016	TGP-16-08	49.094879	88.173475	2608.1	1.335	0.99392	5.0789	0.20184	1027	18.966 ± 0.340	51.51 ± 0.92	25.5 (4)
BE43017	TGP-16-09	49.094944	88.173733	2613.0	2.174	0.99214	5.0716	0.20289	1027	17.663 ± 0.287	48.28 ± 0.79	28.5 (4)
BE43018	TGP-16-10	49.093854	88.182758	2797.1	1.672	0.99880	5.0047	0.20263	1027	46.962 ± 0.762	130.2 ± 2.1	24.2 (3)
BE43713	TGP-16-12	49.138686	87.963735	3008.4	1.841	0.99193	10.3404	0.59663	309.6	51.440 ± 0.956	61.29 ± 1.14	19.1 (3)
BE43714	TGP-16-13	49.137884	87.964663	3002.8	1.581	0.99215	10.1606	0.6524	309.6	32.683 ± 0.593	43.30 ± 0.79	17.6 (4)
BE43715	TGP-16-14	49.136582	87.969812	3013.5	2.216	0.99817	10.0056	0.65112	309.6	47.490 ± 1.065	63.81 ± 1.43	20.9 (4)
BE42291	TGP-16-16	49.137361	87.971589	3034.8	1.936	0.99338	15.4427	0.18164	1027	89.979 ± 1.347	72.56 ± 1.09	25.3 (4)
BE42292	TGP-16-18	49.137102	87.971777	3031.9	1.718	0.99722	15.0073	0.1809	1027	77.754 ± 0.983	64.25 ± 0.81	22.8 (5)
BE42293	TGP-16-19	49.137217	87.972227	3034.7	2.661	0.99802	15.2598	0.18118	1027	86.803 ± 1.302	70.66 ± 1.06	24.7 (4)
BE42294	TGP-16-30	49.136505	87.972969	3028.1	1.271	0.99880	15.0523	0.18183	1027	83.186 ± 0.996	68.89 ± 0.83	22.2 (5)
BE42295	TGP-16-31	49.135759	87.974540	3026.1	1.941	0.99897	15.0811	0.1812	1027	93.057 ± 1.227	76.66 ± 1.01	23.6 (5)
BE42296	TGP-16-32	49.135184	87.975229	3022.7	1.238	0.99888	15.0724	0.18158	1027	86.355 ± 1.372	71.32 ± 1.13	23.5 (5)
BE43716	TGP-16-35	49.133516	87.977797	3014.4	2.131	0.99939	10.293	0.24574	979	44.125 ± 0.823	68.14 ± 1.27	21.4 (3)
BE43717	TGP-16-36	49.133514	87.983721	3047.2	2.119	0.99798	10.3903	0.2447	979	217.985 ± 4.421	335.0 ± 6.8	19.9 (4)
BE43718	TGP-16-37	49.132630	87.984612	3043.8	1.733	0.99940	11.1479	0.24473	979	275.150 ± 3.328	394.4 ± 4.8	21.2 (3)
BE43719	TGP-16-38	49.133685	87.985873	3046.8	2.161	0.99538	10.1048	0.2448	979	97.344 ± 1.323	153.4 ± 2.09	20.8 (3)
BE43720	TGP-16-39	49.130688	87.985177	3039.5	2.486	0.99765	10.3598	0.24498	979	62.682 ± 1.127	96.19 ± 1.73	21.2 (3)
BE43721	TGP-16-40	49.130587	87.984755	3035.8	1.726	0.99865	9.2553	0.2455	979	41.965 ± 0.782	71.95 ± 1.34	23.5 (3)

Table 5.1. continued.

LLNL ID	Sample Name	Latitude (DD)	Longitude (DD)	Elevation (m a.s.l.)	Sample Thickness (cm)	Shielding Correction	Quartz Weight (g)	Carrier Added (g)	Carrier [^{9}Be] (ppm)	^{10}Be/^{9}Be ± 1σ (10^{-14})	[^{10}Be] ± 1σ (10^{4} atoms/g)	Average ^{9}Be current (μA) (runs)
BE43002	TGP-16-51	49.059642	88.635407	2210.0	2.23	0.99629	10.0211	0.18327	1027	30.379 ± 0.699	36.55 ± 0.85	24.6 (4)
BE43722	TGP-16-52	49.057207	88.633698	2201.8	1.563	0.99265	12.4225	0.24404	979	44.091 ± 1.016	56.02 ± 1.29	19 (4)
BE44023	TGP-16-53	49.054660	88.627317	2208.1	1.296	0.99616	15.7383	1.00305	203	65.334 ± 1.019	56.35 ± 0.88	20 (4)
BE43004	TGP-16-56	49.062771	88.652138	2180.1	2.403	0.99935	10.0371	0.18284	1027	17.736 ± 0.346	20.59 ± 0.41	25.6 (3)
BE43005	TGP-16-57	49.064419	88.653214	2172.2	1.877	0.99696	10.8032	0.18326	1027	26.275 ± 0.521	29.12 ± 0.58	18.2 (3)
BE42297	TGP-16-59	49.065663	88.652671	2175.3	2.687	0.99843	15.2096	0.18159	1027	153.409 ± 1.887	125.6 ± 1.55	23.4 (4)
BE43006	TGP-16-60	49.072387	88.656118	2161.7	2.024	0.99901	10.0204	0.18237	1027	91.985 ± 1.154	113.3 ± 1.42	25.7 (4)
BE44024	TGP-16-61	49.059996	88.653505	2142.7	1.14	0.99968	15.8574	1.00264	203	489.543 ± 4.020	419.7 ± 3.45	18.9 (6)
BE44025	TGP-16-62	49.058525	88.655264	2143.4	1.705	0.99964	15.5296	1.00469	203	327.532 ± 2.932	287.3 ± 2.57	19.7 (3)
BE44026	TGP-16-65	49.058356	88.658480	2134.5	1.501	0.99960	11.6454	1.00414	203	296.940 ± 2.655	347.1 ± 3.1	19.5 (3)
BE43008	TGP-16-66	49.064390	88.615017	2227.7	1.424	0.99983	10.0422	0.18265	1027	45.302 ± 0.964	54.97 ± 1.17	25.7 (4)
BE44027	TGP-16-67	49.067667	88.623632	2218.1	2.713	0.99024	15.2689	1.00502	203	158.487 ± 1.766	141.3 ± 1.58	18.7 (3)
BE43009	TGP-16-68	49.074052	88.629759	2193.8	1.736	0.99964	10.0095	0.18302	1027	44.806 ± 0.627	54.64 ± 0.77	24.1 (4)
BE44028	TGP-16-69	49.075702	88.629416	2194.3	3.1	0.99523	15.6223	1.00437	203	57.499 ± 1.069	50.01 ± 0.93	17.8 (3)
BE43010	TGP-16-70	49.067381	88.622170	2222.3	1.93	0.99788	10.2222	0.18302	1027	55.110 ± 0.769	66.16 ± 0.93	25 (4)
BE43723	TGP-16-71	49.066025	88.620041	2220.0	1.159	0.99015	11.0333	0.24395	979	47.304 ± 0.873	67.70 ± 1.25	21.3 (3)
BE44029	TGP-16-73	49.067227	88.604645	2227.9	2.387	0.99944	6.9589	1.00401	203	25.156 ± 0.469	48.93 ± 0.91	19 (3)
BE44030	TGP-16-74	49.067949	88.598131	2252.9	2.526	0.99858	16.6979	1.00569	203	56.441 ± 1.047	45.99 ± 0.85	17.4 (3)
BE44031	TGP-16-75	49.062938	88.611448	2219.5	1.546	0.97948	17.0153	0.99969	203	63.323 ± 1.175	50.34 ± 0.94	21.1 (6)

Table 5.2. Data from procedural blanks. The standard, 07KNSTD3110 was used for every sample.

CAMS Laboratory No.	Sample ID	Carrier Added (g)	Carrier [^{9}Be] (ppm)	^{10}Be/^{9}Be ± 1σ (10^{-14})	^{10}Be ± 1σ (10^{3} atoms)	Average ^{9}Be current (μA) (runs)
BE42298	B32	0.18138	1027	0.086 ± 0.033	10.7 ± 4.1	8.6 (3)
BE43007	B38	0.18290	1027	1.263 ± 0.066	158.5 ± 8.3	24 (2)
BE43019	B40	0.20215	1027	0.079 ± 0.016	11.0 ± 2.2	26.5 (2)
BE43724	B52a	0.65128	309.6	0.091 ± 0.021	12.2 ± 2.8	16.9 (2)
BE43725	B52b	0.24451	979	0.502 ± 0.051	80.3 ± 8.2	16.1 (2)
BE44032	B58	1.00264	203	0.155 ± 0.024	21.1 ± 3.3	25.7 (2)

because they are morphologically inconsistent with inboard moraine ages. The average of the two remaining samples yields a tentative moraine age of 54.1 ± 0.39 ka. Six ages of Bayan-II moraine complex exhibit good internal consistency, with one sample identified as an outlier (TGP-16-67). Excluding the outlier, the five ages form two populations with arithmetic mean ages of 23.24 ± 0.50 ka and 28.08 ±0.58 ka. Three glacial erratics inboard of Bayan-II that bracket small, discontinuous moraine ridges yielded exposure ages of 22.11 ± 0.41 ka, 21.10 ± 0.40 ka, and 19.54 ± 0.36 ka. These ages all occur in morphologic order.

5.2. Holy Mountain

Of the ten samples collected at Holy Mountain, seven samples were analyzed for ^{10}Be surface-exposure ages. Samples were collected from granitic or metasandstone erratics resting on or embedded within ground moraine. The boulders ranged in elevation from 2404 to 2797 m a.s.l., with an elevation range of 393 m. The ages are presented in Table 5.3 and they are plotted as an age vs. elevation plot in Figure 5.3. Exposure ages range from 15.60 ± 0.31 ka to 37.55 ± 0.76 ka, with one morphostratigraphic outlier of 22.67 ± 0.43 ka (TGP-16-01). The age-elevation plot shows that 253 m of ice-surface lowering occurred between 18.23 ± 0.34 ka and 15.69 ± 0.34 ka.

Table 5.3. Calculated sample ages. Ages were calculated using the Stone scaling scheme with a correction for magnetic variation (Lm) and with no magnetic correction (St). Outliers marked with (*).

Sample ID	Lm age (ka) NZ production rate	St age (ka) NZ production rate
Outboard Bayan-I erratics		
TGP-16-61	196.1 ± 1.7	196.6 ± 1.7
TGP-16-62	132.9 ± 1.2	132.9 ± 1.2
TGP-16-65	162.5 ± 1.5	162.6 ± 1.5
Bayan-I moraine		
TGP-16-51*	16.05 ± 0.37	15.76 ± 0.37
TGP-16-52*	24.57 ± 0.57	24.32 ± 0.57
TGP-16-53*	24.47 ± 0.38	24.22 ± 0.38
TGP-16-56*	9.28 ± 0.19	9.04 ± 0.18
TGP-16-57*	13.13 ± 0.26	12.85 ± 0.26
TGP-16-59	56.83 ± 0.71	56.18 ± 0.70
TGP-16-60	51.27 ± 0.65	50.81 ± 0.65
Bayan-II moraine		
TGP-16-66	23.48 ± 0.50	23.22 ± 0.50
TGP-16-67*	62.55 ± 0.71	61.91 ± 0.70
TGP-16-68	23.97 ± 0.34	23.71 ± 0.34
TGP-16-69	22.27 ± 0.42	22.00 ± 0.41
TGP-16-70	28.49 ± 0.40	28.26 ± 0.40
TGP-16-71	27.67 ± 0.52	27.43 ± 0.51
Bayan inboard erratics		
TGP-16-73	21.10 ± 0.40	20.82 ± 0.39
TGP-16-74	19.54 ± 0.36	19.25 ± 0.36
TGP-16-75	22.11 ± 0.41	21.85 ± 0.41
Holy Mountain erratics		
TGP-16-01*	22.67 ± 0.43	22.41 ± 0.42
TGP-16-02	15.69 ± 0.30	15.40 ± 0.29
TGP-16-03	18.23 ± 0.34	17.94 ± 0.34
TGP-16-07	15.95 ± 0.34	15.66 ± 0.33
TGP-16-08	17.06 ± 0.31	16.77 ± 0.30
TGP-16-09	16.08 ± 0.26	15.79 ± 0.26
TGP-16-10	37.78 ± 0.62	37.53 ± 0.62
Bedrock knob erratics		
TGP-16-36	84.04 ± 1.74	83.48 ± 1.73
TGP-16-37	98.82 ± 1.23	98.43 ± 1.22
TGP-16-38	38.17 ± 0.52	37.92 ± 0.52
Upper Potanin outboard erratics		
TGP-16-39	24.04 ± 0.44	23.8 ± 0.43
TGP-16-40	17.98 ± 0.34	17.69 ± 0.33
Middle Potanin outboard erratics		
TGP-16-14	16.26 ± 0.37	15.97 ± 0.36
TGP-16-16	18.27 ± 0.28	17.98 ± 0.27
TGP-16-18	16.14 ± 0.21	15.85 ± 0.20
TGP-16-19	17.81 ± 0.27	17.52 ± 0.26
TGP-16-30	17.25 ± 0.21	16.96 ± 0.20
TGP-16-31	19.28 ± 0.26	19.00 ± 0.25
TGP-16-32	17.90 ± 0.29	17.61 ± 0.28
TGP-16-35	17.31 ± 0.33	17.02 ± 0.32
Lower Potanin outboard erratics		
TGP-16-12	15.73 ± 0.29	15.44 ± 0.29
TGP-16-13	11.18 ± 0.20	10.91 ± 0.20

Table 5.4. Statistics of landform ages. Based on the nature of the landform, different statistics are used to represent the depositional age. Bold ages represent the statistic used for interpretations.

Sample ID	Count (samples excluded)	Age range (ka)	Mean age (ka)	Standard error of the mean (ka)	External uncert. (ka)	Error-weighted mean (ka)	Error-weighted uncert. (ka)	1σ scatter (ka)	Peak age (ka)	Median age (ka)	Interpreted landform age (ka)
Outboard Bayan-I erratics	3 (0)	133-196	163.8	18.30	18.6	157.1	0.80	18.0	132.9	162.5	**133-196**
Bayan-I moraine	2 (5)	51.3 -56.8	54.05	2.78	2.98	53.83	0.48	2.77	51.27	54.05	**54.05 ± 2.78**
Bayan-II moraine	5 (1)	22.3-28.5	25.18	1.22	1.32	25.04	0.19	1.20	23.87	23.97	**22.3-28.5**
Bayan-II (28 ka)	2	27.7-28.5	28.08	0.41	0.70	28.18	0.32	0.40	28.35	28.08	**28.08 ± 0.41**
Bayan-II (23 ka)	3	22.3-24.0	23.24	0.50	0.69	23.33	0.23	0.52	23.88	23.48	**23.24 ± 0.50**
Bayan inboard erratics	3 (0)	19.5-22.1	20.92	0.75	0.86	20.80	0.23	0.76	19.54	21.10	**19.5-22.1**
Holy Mountain erratics	6 (1)	15.7-37.8	20.13	3.55	3.57	17.49	0.13	2.03	15.95	16.57	**15.7-37.8**
Bedrock knob erratics	3 (0)	98.8-38.2	73.68	18.26	18.32	50.14	0.46	16.35	38.17	84.04	**98.8-38.2**
Upper outboard Potanin erratics	2 (0)	24.0-18.0	21.01	3.03	3.06	20.25	0.27	2.93	17.98	21.01	**24.0-18.0**
Middle outboard Potanin erratics	8 (0)	19.3-16.1	17.53	0.37	0.51	17.48	0.09	0.38	17.88	17.56	**19.3-16.1**
Middle erratics (18 ka)	5	17.2-18.3	17.71	0.19	0.40	17.66	0.12	0.20	17.88	17.81	**17.71 ± 0.19**
Middle erratics (16 ka)	2	16.1-16.3	16.20	0.06	0.33	16.17	0.18	0.05	16.16	16.20	**16.20 ± 0.06**
Lower Potanin outboard erratics	2 (0)	11.2-15.7	13.46	2.27	2.29	12.66	0.17	2.13	11.18	13.46	**11.2-15.7**

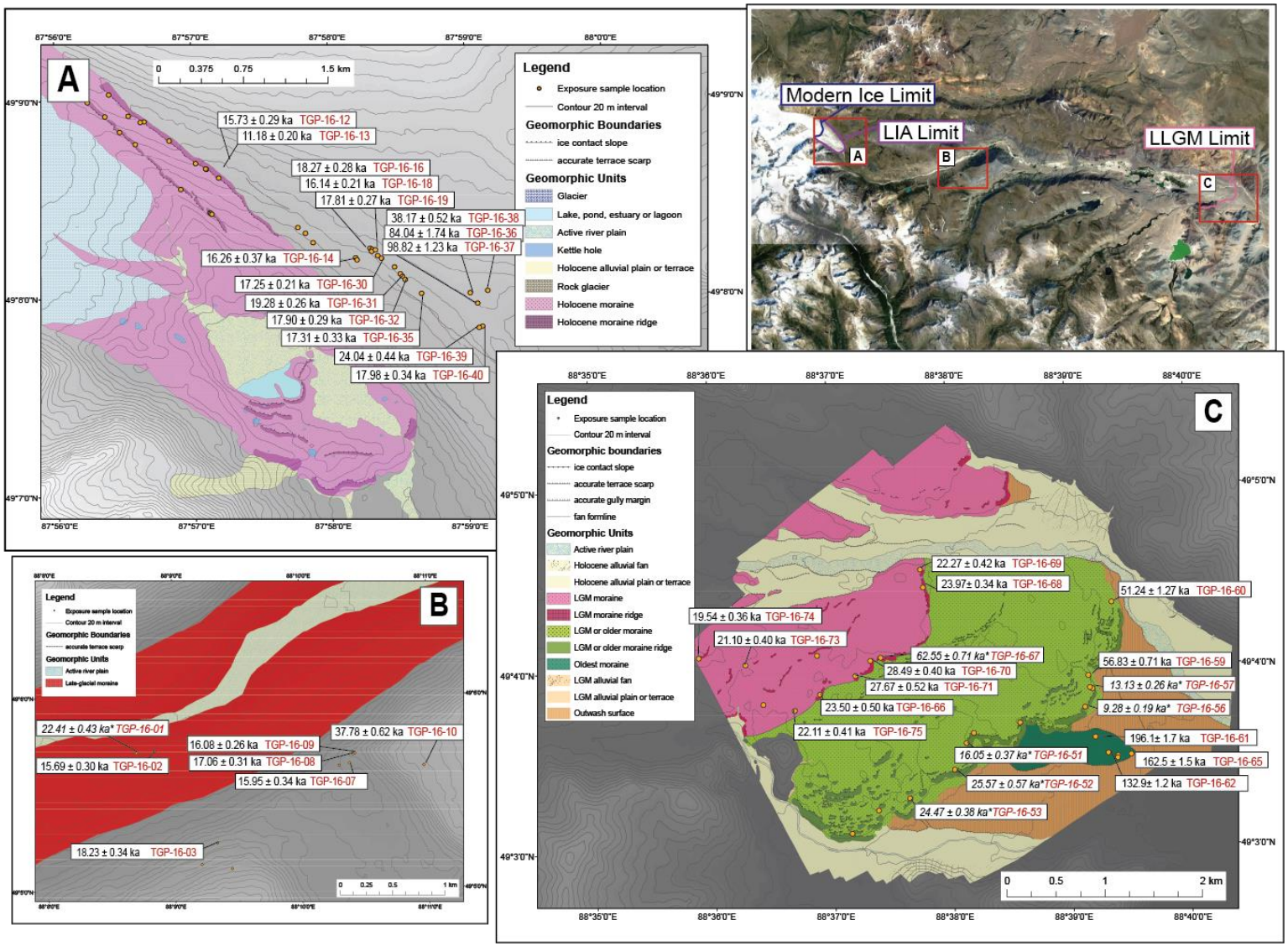

Figure 5.1. ^{10}Be chronology of the Tsagaan Gol-Potanin Glacier valley. The chronology is annotated on glacial geomorphic maps of (A) Potanin moraines and outboard landscape, (B) Holy Mountain, and (C) the Bayan moraine complex. ^{10}Be surface-exposure ages are calculated using the Putnam et al. (2010) production rate with the Lm scaling protocol.

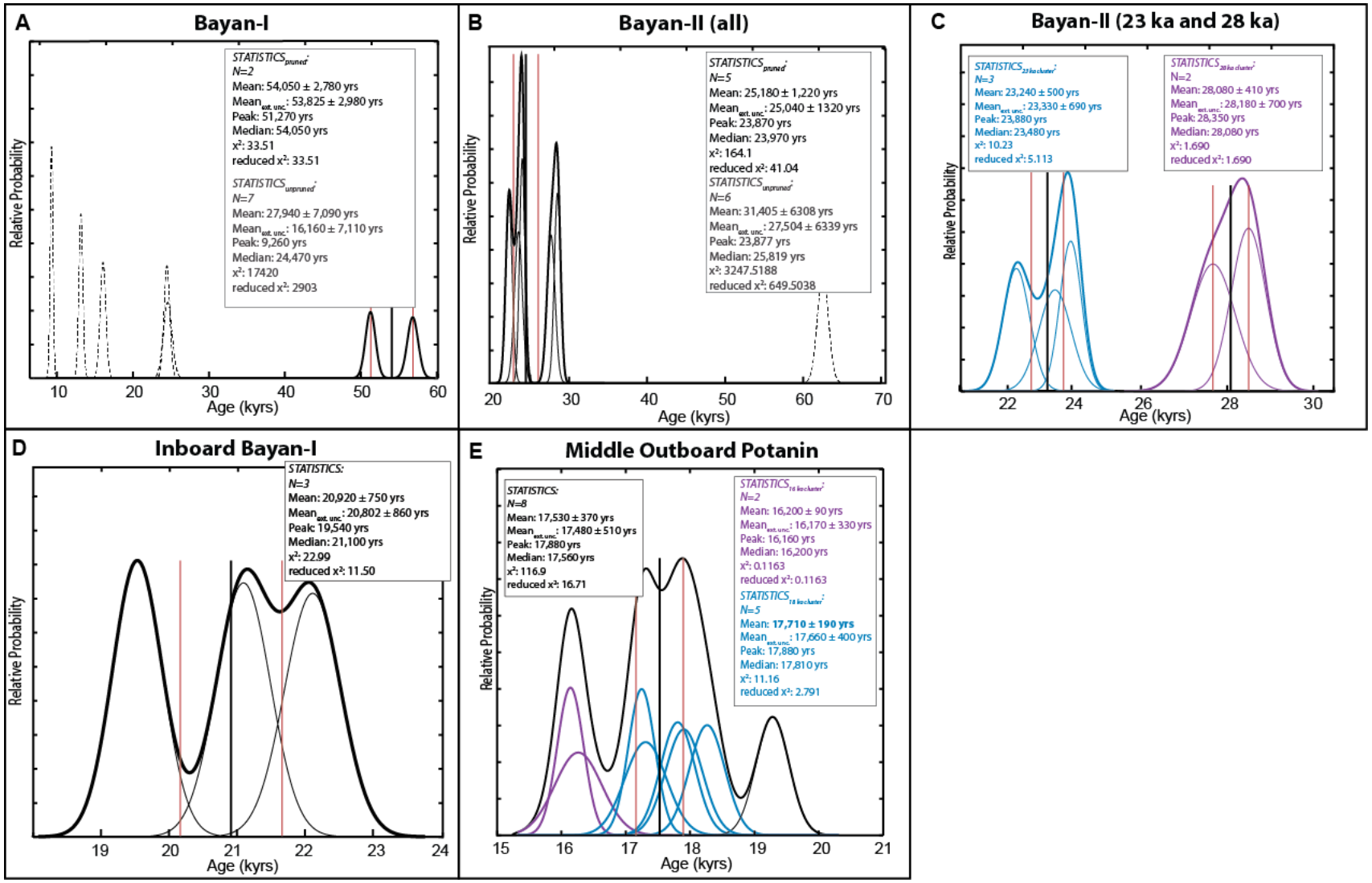

Figure 5.2. Camel plots of selected landforms. Production-rate uncertainty of 2.1% used in error calculations and outliers are represented by dotted lines. See Figures 4.2 and 4.7 for locations of landforms.

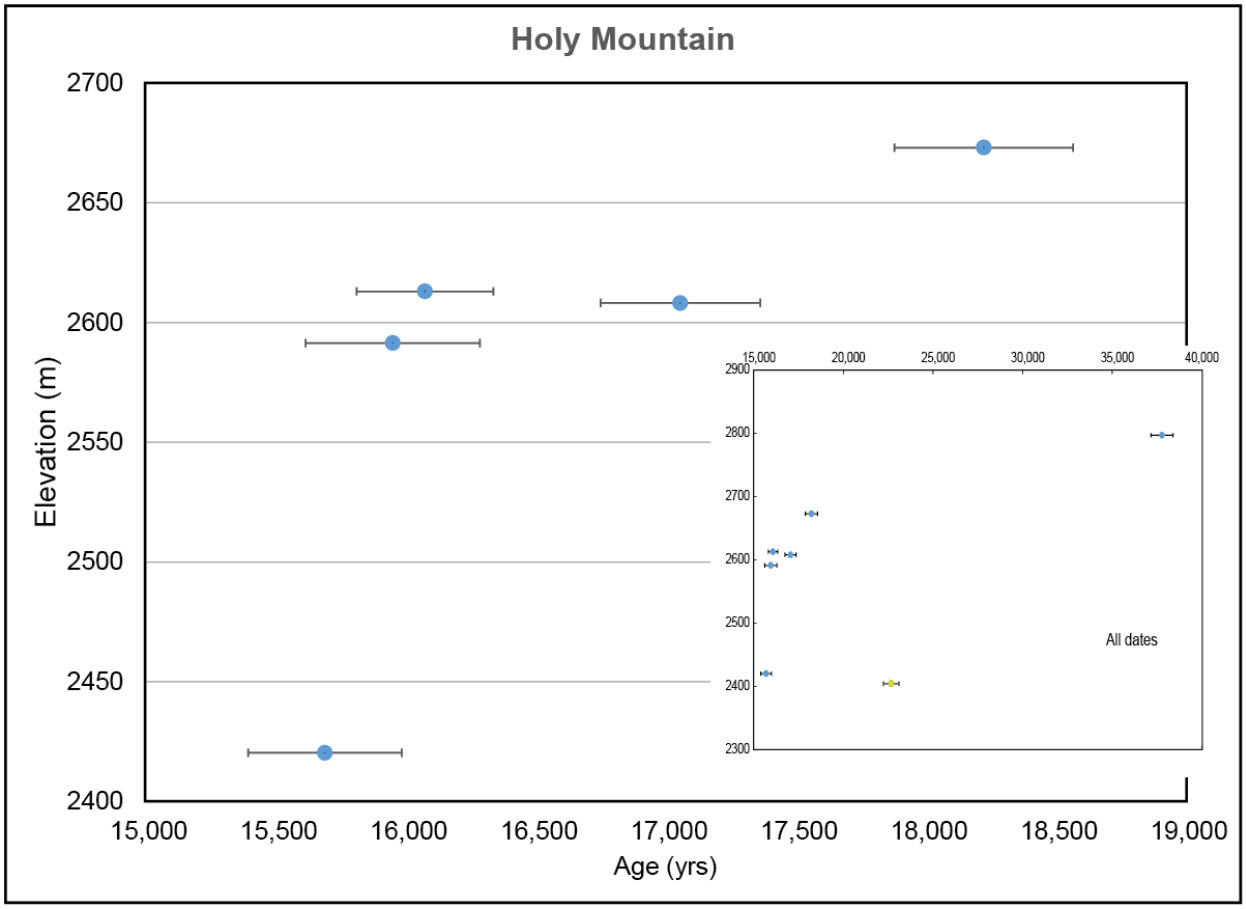

Figure 5.3. Age vs. elevation plot of samples from Holy Mountain. Ages plotted with 1 σ error. Outlier is in yellow.

5.3. Boulders outboard of Potanin moraines

Outboard of the Potanin moraines, there are numerous glacial erratics on a hillside sloping toward the Potanin left-lateral moraines. Of the 21 samples collected, I obtained surface exposure ages of 16. The boulders range in elevation from 3,002 to 3,047 m a.s.l., spanning 45 m. I have clustered the boulders based on location into three groups: lower, middle, and upper erratics. Above the terraces, boulders were collected on the top of the ridge on a flow divide around a series of bedrock knobs.

The lower Potanin erratics group is comprised of two samples that have exposure ages of 15.73 ka ± 0.29 ka and 11.18 ± 0.20 ka. Nine boulders from the middle erratics range in age from 16.26 ka ± 0.37 ka to 19.62 ± 0.26 ka. Excluding the 19.62 ± 0.26 ka age, the surface-exposure ages of the middle erratics create two populations, at 16.20 ± 0.06 ka and 17.71 ± 0.19 ka (Figure 5.2E). Two samples were

dated from the upper region and yielded ages of 24.04 ± 0.44 ka and 17.98 ± 0.34 ka. At the bedrock knob, the ages are older, dating to 37.78 ± 0.62 ka, 84.04 ± 1.74 ka, and 98.82 ± 1.23 ka.

CHAPTER 6

SNOWLINE MODELING

6.1. GlaRe reconstructions

Glacier and snowline reconstruction results are shown in Figures 6.1-2. The Bayan moraine complex reconstruction corresponds with the LLGM, based on the surface-exposure chronology. The Potanin region reconstruction corresponds with the Little Ice Age, based on historical photography (Figure 2.3). The LLGM reconstruction has an area of 310 km^2 and it has a flowline length of 65 km. The maximum ice thickness is 435 m. The snowline, calculated using the AAR method with inputs of 0.60 ± 0.5 yielded a value of 2680 ± 50 m a.s.l.. The Little Ice Age reconstruction yielded a glacier surface area that is 41 km^2 and a flowline length of 12 km. The maximum ice thickness is 444 m and the snowline from glacier reconstructions for the Little Ice Age was 3470 ± 50 m a.s.l..

To verify the results of the GlaRe toolbox, I used both the surface-exposure chronology, glacial landforms, and modern glaciological measurements. The ice thickness of Bayan reconstruction was calibrated to agree with the surface-exposure chronology and moraines, giving confidence that the ice surface is accurate. The modeled ice inundated samples with exposure ages younger than the Bayan-II terminal moraine and regions with older boulders are ice-free. For the Little Ice Age reconstruction, the surface fits within the margins of the Potanin moraines. Also in support of the model's accuracy, the modern snowline of the Potanin Glacier ranged from 3541 to 3714 m a.s.l. from 2005 to 2009 CE and the ELA_0 is 3493 m a.s.l, which is above the modeled Little Ice Age snowline (Konya et al. 2013). However, the ice surface area somewhat disagrees with modern glaciological measurements. The Little Ice Age reconstruction yielded a surface area of 41 km^2, which is 2 km^2 less than estimates of the modern Potanin Glacier by Kadota and Gambo (2007). Perhaps the model underestimated the extent of the glacier near the headwall. In addition, the Little Ice Age reconstruction ice surface has a 100-m step change, the result of an over-deepening formed by the modern-ice subtraction tool.

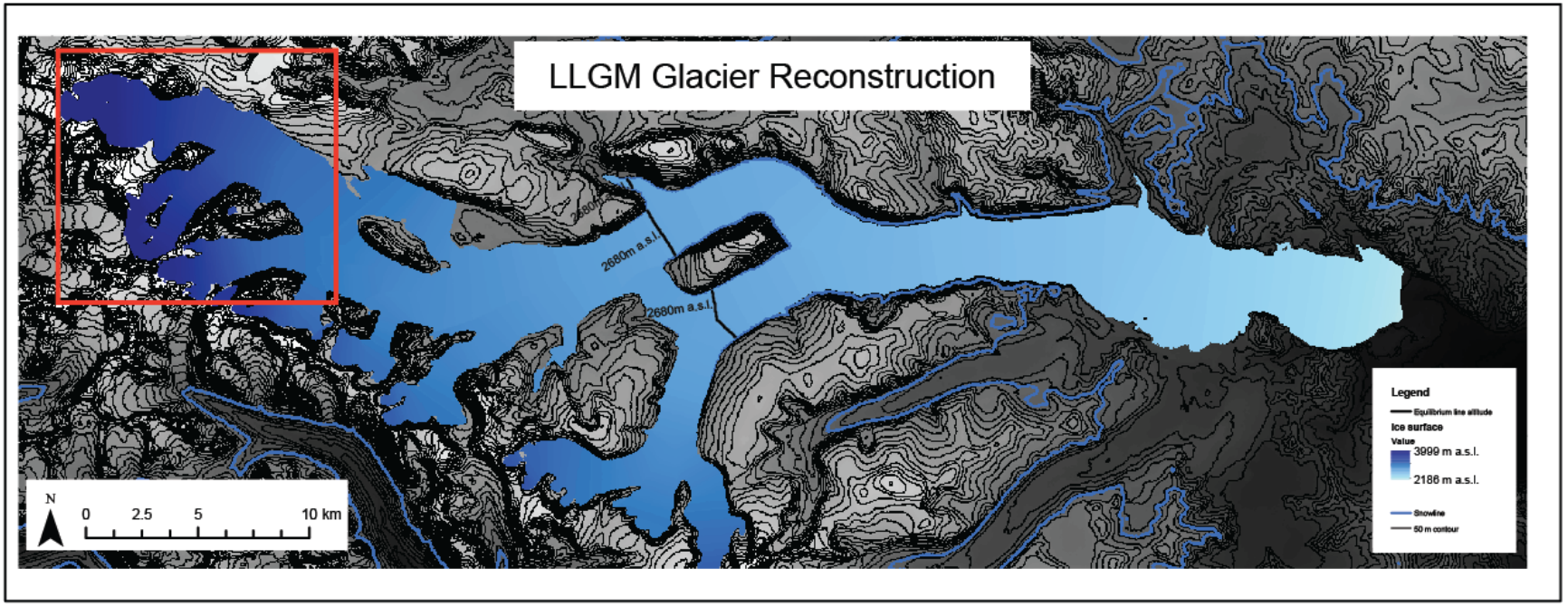

Figure 6.1. Glacier reconstruction and snowline results of Local Last Glacial Maximum. The red box is an inset of the Little Ice Age area shown in Figure 6.2. The black lines represent snowlines calculated using an AAR of 0.6. The blue line represents the elevation of the snowline located on the surrounding topography.

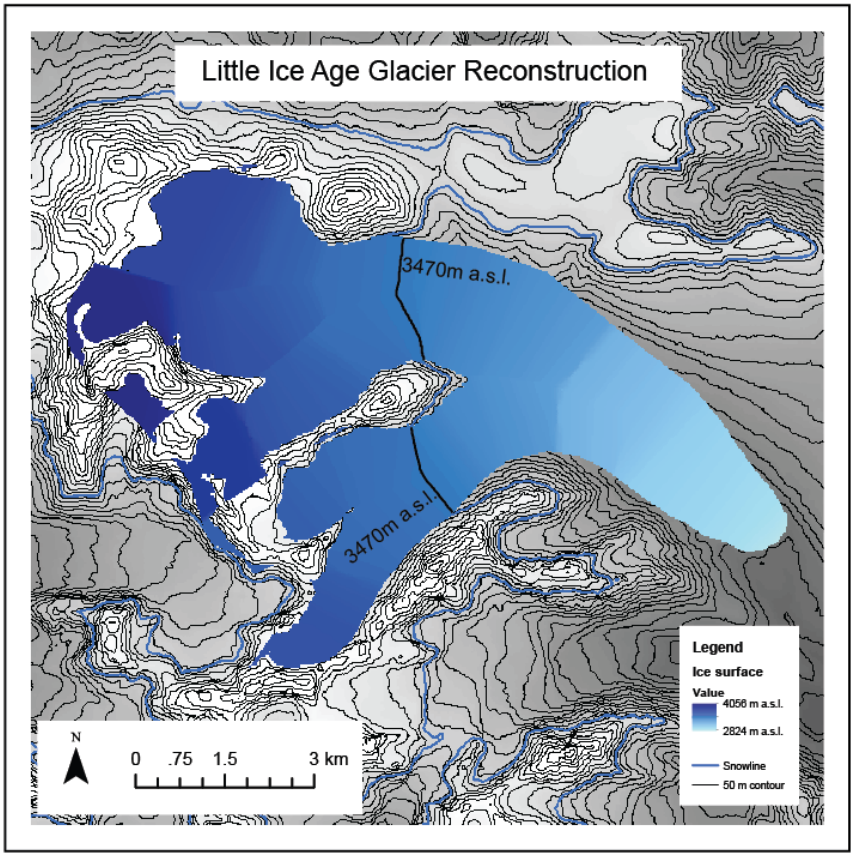

Figure 6.2. Glacier reconstruction and snowline results of Little Ice Age. The black lines represent snowlines calculated using an AAR of 0.6. The blue line represents the elevation of the snowline located on the surrounding topography.

6.2. Sensitivity analysis

In the GlaRe model, basal shear stress is the main variable that will affect the resulting glacier surface, and therefore the snowline. When the basal shear stress increases, the glacier becomes "stickier" and thickens. The thickness of the glacier will affect the calculated snowline because if the glacier surface elevation is higher, the snowline elevation will also increase. In turn, this affects paleoclimate interpretations because a higher snowline suggests warmer climatic conditions. Due to the importance of the basal shear stress to paleoclimate interpretations, I performed a sensitivity test of the basal shear stress on the elevation of the snowline for the LLGM configuration of the Tsagaan Gol-Potanin Glacier valley and a cirque in the Italian Alps named the Ferrere valley (44°20'7.08" N, 6°56'16.44" E). I chose the Ferrere valley because the valley is a similar size to the Potanin Little Ice Age system but there is no

modern glacier in the valley to complicate model assumptions. The data from the Ferrere valley comes from tutorials in the GlaRe supplementary material (https://www.abdn.ac.uk/geosciences/departments /geography-environment/outcomes-442.php).

The valleys are different in two key ways. First, the Tsagaan Gol-Potanin Glacier valley is larger, ~650 km^2 versus the 4.6 km^2 of the Ferrere valley. Second, the Tsagaan Gol-Potanin Glacier is in a low-angle valley. The average slope from the headwall to the terminal moraine is 1.1 degrees. In the Ferrere valley, the average slope is 13.7 degrees.

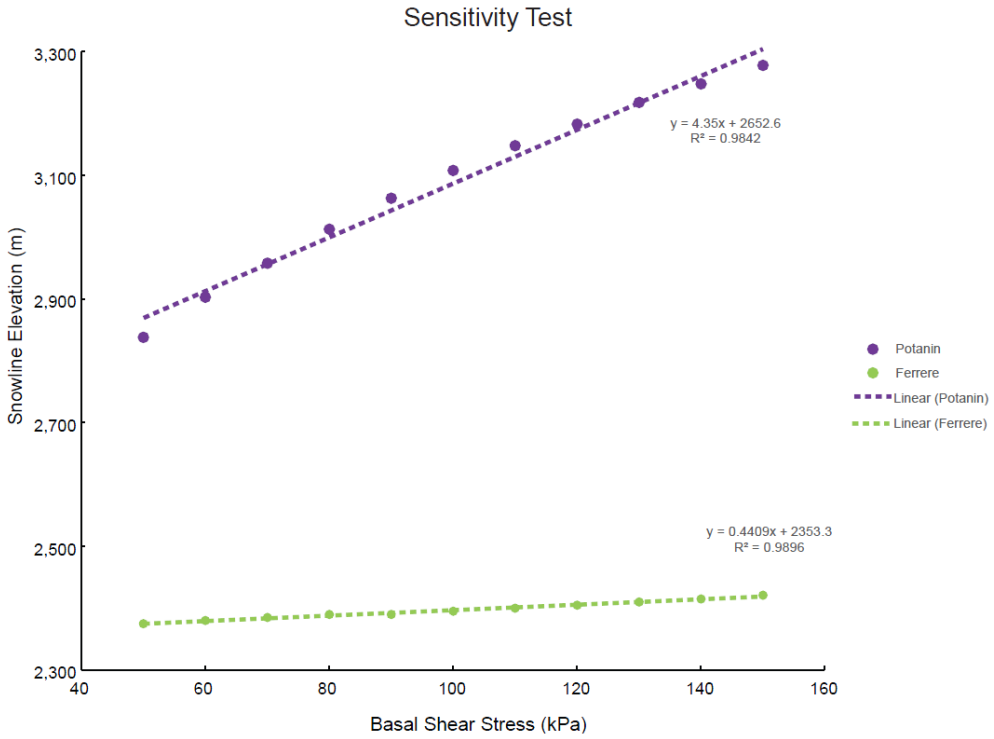

Figure 6.3. Sensitivity analysis of GlaRe model results. The sensitivity of changes in basal shear stress to the elevation of snowline was determined in the Tsagaan Gol-Potanin Glacier system (purple) and the Ferrere valley in the Italian Alps (green). The snowline was calculated using the AAR method (0.6). The linear best fit line and equation are plotted next to the data points.

I iteratively changed the basal shear stress and calculated the associated change in snowline with an AAR value of 0.6. The results are in Figure 6.3. I In the Ferrere system, for every 10 kPa increase in basal shear stress, there is a 4.4 m rise in snowline. For the Tsagaan Gol-Potanin Glacier system, the results changed by an order of magnitude. For every 10 kPa rise in basal shear stress, there is a 43 m rise in the snowline. These results show that knowing the basal shear stress is more important for low-angle

systems, where an equal thickening will result in a greater change in the vertical direction because of the geometry. This test also indicates that if the basal shear stress can be constrained to within 10 kPa, then the error of the snowline is about 40 m for a low-angle system. Because I was able to constrain the basal shear stress to 10 kPa in the Tsgaan Gol-Potanin Glacier reconstructions, I then can compound the error associated with an imprecise basal shear stress value and the possible range of AAR as ± 90 m for the LLGM reconstructions and ± 55 m for the Little Ice Age reconstruction.

6.3. Snowline Changes

I used changes in snowline to compare modern climate with the climate of the LLGM and the Little Ice Age. Snowline generally corresponds to the summertime 0°C isotherm in the atmosphere (Porter, 1979; Porter, 2001; Mackintosh et al., 2017). I calculated the modern 0°C isotherm from meteorological data collected at the Potanin Glacier in 2007-2008 CE by Konya et al. (2010), together with an adiabatic lapse rate of 0.0055°C/m (Konya et al. 2013). The average summer (June, July, August) temperature during the collection interval is 3.4°C at 3040 m a.s.l.. Therefore, the average-summer 0°C isotherm, or snowline, occurs at 3780 m a.s.l.. Comparing the GlaRe results to modern measurements, I found that the snowline rose 1100 ± 90 m from the LLGM to modern. This equates to a temperature difference of 6.0 ± 0.5°C. The snowline rose 310 ± 55 m from the Little Ice Age to modern, representing a 1.7 ± 0.3°C increase in temperature. It is also useful to measure the retreat from the LLGM to the Little Ice Age, two periods of moraine formation. Between the LLGM and Little Ice Age, snowline rose 790 ± 90 m, equating to a temperature increase of 4.3 ± 0.5°C

Table 6.1. Glacier reconstruction results for the LLGM and Little Ice Age.

Reconstruction	Area (km^2)	Flowline length (km)	Maximum thickness (m)	ELA (m a.s.l.)	ΔELA from modern (m)	ΔT from modern (°C)
LLGM	310	65	435	2680 ± 90	1100 ± 90	6.0 ± 0.5
Little Ice Age	41	12	444	3470 ± 55	310 ± 55	1.7 ± 0.3

CHAPTER 7

DISCUSSION

7.1. Glacial chronology

Glacial-geomorphic mapping and ^{10}Be surface-exposure dating show that Tsagaan Gol-Potanin Glacier valley stood at maximum positions within the Bayan moraine complex around 130-190 ka, ~54 ka, and 28-19.5 ka. These periods of extensive ice relate to MIS 6, 3, 2 (Figure 7.1). The boulder ages show that the length of the glacier decreased from MIS 6 to MIS 2. In addition, glacial erratics were deposited at locations that suggest thicker ice during MIS 5 and MIS 3 than during the LLGM. Progressive thinning of the glacier could be the result of warmer climate conditions in MIS 2 than MIS 6, or the result of evolving subglacial topography (Kaplan et al., 2009; Anderson et al., 2012; McKinnon et al., 2012).

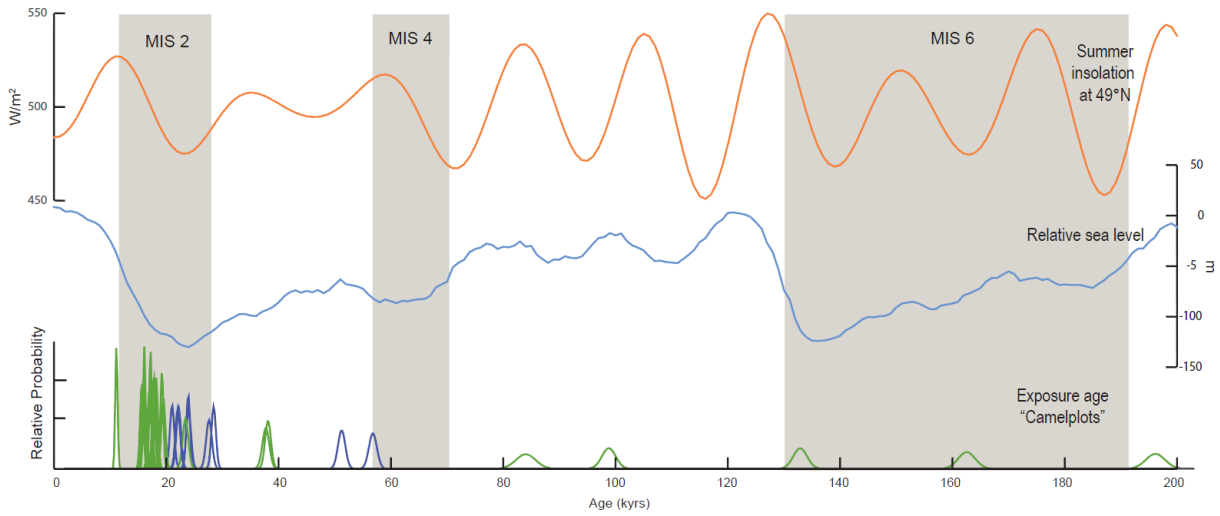

Figure 7.1. Boulder deposition in the Tsagaan Gol-Potanin Glacier valley compared to local insolation (orange) and relative sea level (blue). Sea level data from Spratt and Lisiecki (2016). Boulder ages are plotted in terms of their relative probability. Green represents glacial erratics, interpreted to mean stagnant or retreating ice and blue indicates boulders on a moraine, representing the culmination of an advance.

The oldest moraine deposited in the valley is moraine ridge Bayan-I. The boulders on Bayan-I possibly correspond to moraine formation during early MIS 3, but these interpretations are based on only two exposure ages. The remaining five ages from that moraine complex are classified as outliers because they do not fit morphologically with Bayan-II. I interpret the age scatter to indicate boulder exhumation

on Bayan-I, which is supported by observations of varying amounts of rock varnish on the boulders (see Appendix C). Possibly, all the boulders on Bayan-I were exhumed, even the samples not identified as outliers, and the 54.05 ± 2.78 ka moraine age is a minimum value for moraine deposition. Bayan-II is a composite moraine belt that was formed during two episodes of moraine construction at 23.24 ± 0.50 ka and 28.08 ± 0.58 ka. Inboard of Bayan-II, there are three exposure ages that bracket small-discontinuous moraines. These ages range from 19.54 ± 0.36 ka to 22.11 ± 0.41 ka and mark the last glacier resurgence within the Bayan moraine complex. Up-valley of these samples is unstructured ground moraine deposited as the glacier margin receded.

Exposure ages at Holy Mountain record a history of thinning of the Tsagaan Gol-Potanin paleo-glacier. An age of 37.78 ± 0.62 ka of the highest boulder indicates that the glacier was more extensive during MIS 3 than MIS 2, which is similar to the age distribution at the Bayan moraine complex. From 18.23 ± 0.34 ka to 15.69 ± 0.30 ka, the glacial erratics at Holy Mountain record 253 m of thinning. Sample TGP-16-02 is located on the valley floor, which indicates that the glacier terminus was near the base of Holy Mountain by the time of boulder deposition at 15.69 ± 0.30 ka.

Deglaciation of the valley is also recorded by glacial erratics outboard of the Potanin moraines. All boulders are erratics on bedrock or ground moraine, therefore they are interpreted as representing transient ice positions. The middle glacial erratics that are located about 500 m outboard and 100 m above the Potanin moraines form a straight line parallel to the modern ice margin. The boulders range in age from 16-19 ka, with two populations clustering around 16.20 ± 0.06 ka and 17.71 ± 0.19 ka. These erratic boulders indicate that the termination was underway by at least 17.7 ka because the glacier must have been retreating to deposit boulders on ground moraine. The glacial erratics outboard of the Potanin moraines span a small elevation range in this region, with boulders that date to 99 to 16 ka within 10-20 meters of each other. The large age range is to be expected because the Tsagaan Gol-Potanin Glacier valley is low-angle, meaning that changes in the thickness near the glacier head are minimal.

7.2. The Last Glacial Maximum and Termination

My glacier reconstruction affords a constraint on the climate of central Asia during the global LGM, 26.5 to 19.0 ka (Clark et al., 2009; MARGO Project Members, 2009). The ^{10}Be chronology indicates that the LLGM in the Tsagaan Gol-Potanin Glacier valley was achieved as early as 28.08 ± 0.41 ka and sustained until 19.54 ± 0.36 ka (Figure 7.2). My chronology agrees with other studies in western Mongolia which found ice advances from 28-19 ka (Lehmkuhl et al., 2011; Rother et al., 2014). The chronology also agrees with mountain-glacier records from North America and Europe, where the LGM began at about 30 ka (Clark et al., 2009). In addition, there is correspondence with the timing of mountain glaciers in New Zealand, where the LLGM moraine deposition occurred at about 27 ka, 22 ka, 20 ka, and 18 ka (Putnam et al., 2013; Doughty et al., 2015). The contemporaneous advances of mountain glaciers indicate that the Tsagaan Gol-Potanin Glacier valley system was tracking a global signal during the last ice age. It is important to note that the Laurentide ice sheet did not reach its maximum position until 26.5 ka (Clark et al., 2009). Thus, an ice sheet-albedo mechanism for spreading cooling throughout the planet is inconsistent with the pattern of global mountain glacier advance.

The post-LLGM samples give clues about the nature of the last termination in two ways: first, erratics give limits on glacier length. Sample TGP-16-02, the lowest elevation sample from Holy Mountain is located at the bottom of the valley (Figure 7.2). Therefore, when the glacier deposited this boulder at 15.69 ± 0.30 ka, the ice must have terminated below the NW face of Holy Mountain. Second, erratics give us a minimum-limiting value for snowline because they must be deposited in ablation zones, below the snowline, where ice flow is divergent. The middle outboard Potanin erratics bear the mark of glacial erosion, with polish and striations preserved, indicating that they traveled through the glacier and were deposited in the ablation zone, below the snowline. Therefore, it is possible to take the highest elevation boulder at 3,334 m a.s.l. as a minimum-limiting elevation of the snowline at 17.71 ± 0.19 ka.

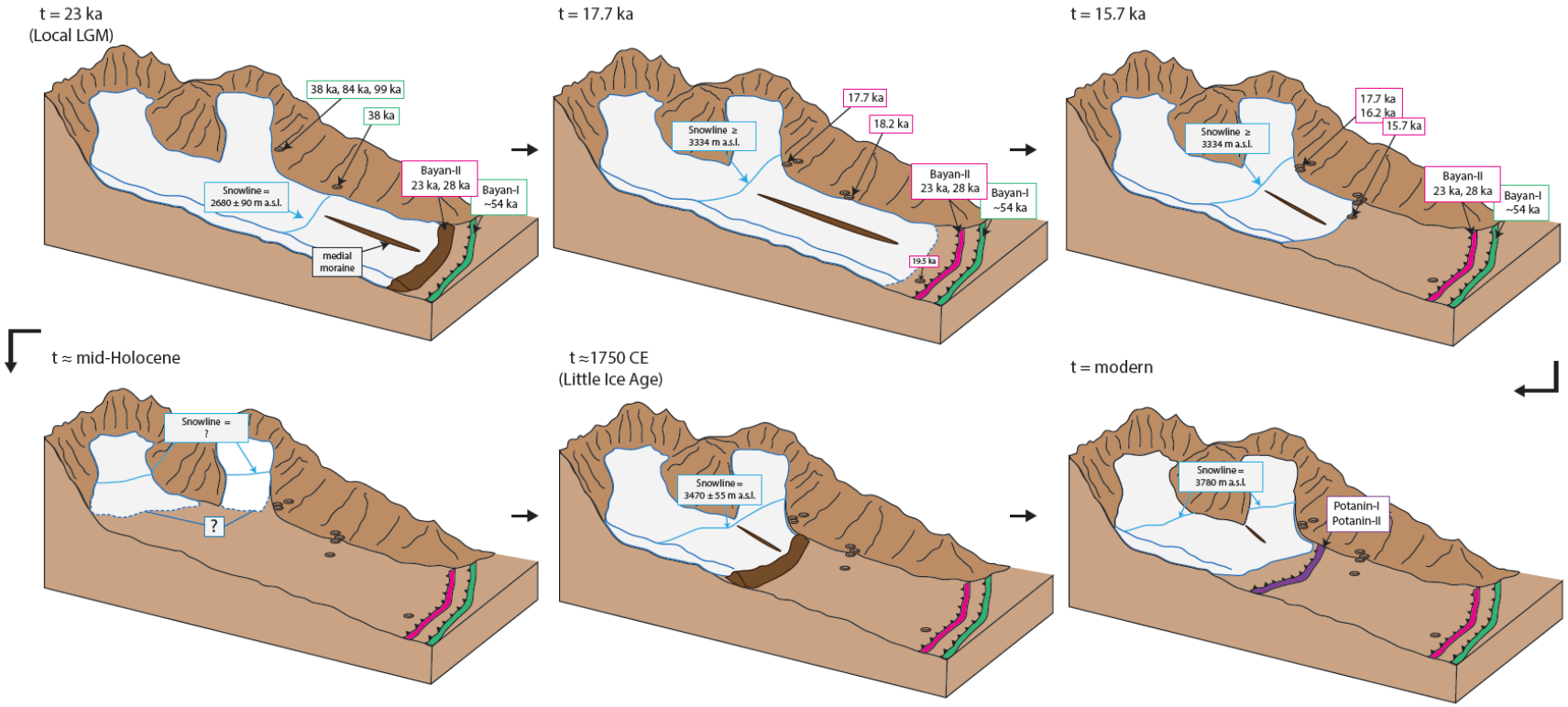

Figure 7.2. Schematic diagram of the glacial history of Tsagaan Gol-Potanin Glacier valley. At 23 ka, the glacier had achieved the LLGM position (Bayan-II). By 17.7 ka, the glacier had retreated from the LLGM moraine ridge and snowline increased by 640 ± 90 m. The glacier retreated to a mid-valley position by 15.7 ka, documented by a glacial erratic at the bottom of the valley near Holy Mountain. The position of the glacier during the mid-Holocene is unknown. The next period documented by glacial moraines was during the Little Ice Age (~1750 CE) when snowline was 310 ± 55 m lower than modern. Presently, the glacier has retreated from the Potanin moraines and the snowline is 3780 m a.s.l..

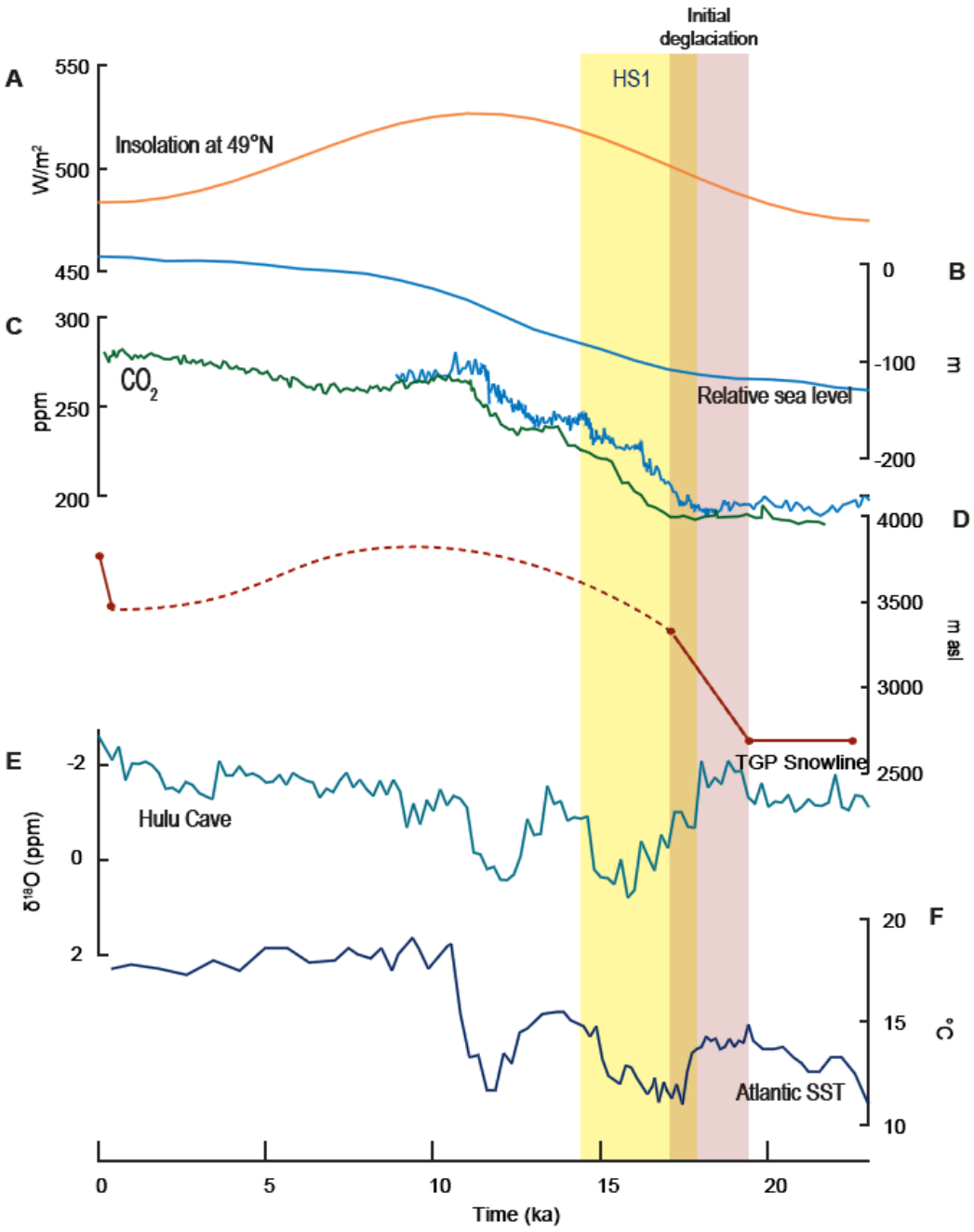

Figure 7.3. Comparison of paleoclimate indicators during the last termination. (A) Local June 21 insolation at 49°N, (B) relative sea level from Spratt and Lisiecki (2016). (C) CO_2 from Marcott et al. (2013) (blue) and Epica Dome C from Monnin et al. (2004) (orange). (D) Results of this study: snowline change in Tsagaan Gol-Potanin (TGP) glacier valley. (E) Hulu Cave isotope record from Cheng et al. (2016). (F) Atlantic SST from Bard (2000). Pink bar delineates initial deglaciation in Tsagaan Gol-Potanin Glacier valley. Yellow bar delineates Heinrich Stadial 1 from 14.7-17.5 ka.

Tracking changes in snowline is a fundamental way to use the glacial record to reconstruct past climate (Mackintosh et al., 2017). Here, I used three methods to determine changes in snowline during the termination. First, I calculated the LLGM and Little Ice Age snowlines of 2680 ± 90 m a.s.l. and 3470 ± 55 m a.s.l., respectively using the AAR method from glacial reconstructions (Table 6.1). A minimum value for snowline was estimate from a cluster of five glacial erratics outboard of the Potanin moraines, which are located at 3,334 m a.s.l. (Figure 5.2E). Last, I estimate modern snowline of 3780 m a.s.l from a weather stations on the Potanin-I moraine (see Chapter 6). With these three methods, I determine snowline rise during the termination and Holocene, which is documented schematically in Figure 7.2 and graphically in Figure 7.3. The snowline rose 1100 ± 90 m from the LLGM to modern, equaling 6.0 ± 0.5°C. Between the LLGM and Little Ice Age, snowline rose 790 ± 90 m, equating to a temperature increase of 4.3 ± 0.5°C. At least 640 ± 90 m of snowline rise, or 3.5 ± 0.5°C of warming, occurred by 17.71 ± 0.19 ka, which represents up to ~60% of the snowline rise from the LLGM to modern.

My chronology demonstrates that the Tsagaan Gol-Potanin paleo-glacier retreated during Heinrich Stadial 1 (HS1) (Figure 7.3). During this period of mean-annual cooling in the North Atlantic, glaciers in Mongolia record summer warming. The chronology agrees with evidence that North Atlantic stadials were periods of strong seasonality, during which glaciers in Europe and Greenland were retreating in response to warming summers (Denton et al., 2005; Buizert et al., 2014; Wirsig et al., 2016). Like glaciers in Europe, the Tsagaan Gol-Potanin paleo-glacier registered summertime warming, despite cooler temperatures in the North Atlantic region.

The moraine chronology developed in this study permits direct comparison between the timing of deglaciation and summertime atmospheric warming in the Mongolia Altai with the rise in atmospheric CO_2. Deglaciation in the Tsagaan Gol-Potanin Glacier valley was well underway by 17.71 ± 0.19 ka. The snowline had risen by at least 640 meters, which corresponds to ~60% of the snowline rise from the LGM to modern, or 3.5 ± 0.5°C of warming. From 23.0 to 18.0 ka, atmospheric CO_2 was about 194 ppm on average, fluctuating between 200 and 189 ppm (Marcott et al., 2013). CO_2 rose steadily after 18.0 ka and was 196 ppm at 17.5 ka. The change in CO_2 by 17.5 ka was only 3% of the full deglacial CO_2 rise of 80

ppm. Thus, these results indicate that CO_2 was not the primary driver of glacier recession in the Mongolian Altai from the LLGM to 17.7 ka (Figure 7.3).

7.3 Implications

North Atlantic warming and CO_2 rise both lag the timing and rates of deglaciation and atmospheric warming in the Mongolian Altai from 19.5 ka to 17.1 ka. Therefore, other mechanisms are needed to explain the pronounced warming in the Mongolian Altai. First, let us consider rising local summer insolation. The termination coincides with rising summer insolation at 49°N, yet is this sufficient to account for 640 ± 90 m of snowline rise by 17.7 ka? Heating of large landmasses by solar radiation has substantial effects on the continental climates (McKinnon et al., 2013). Therefore, summer insolation may have had an important role in deglaciation at the beginning of the termination and needs to be explored further.

Next, I consider the possibility that a shift in the position of the Northern Hemisphere westerly winds played a role in the deglaciation of the Potanin Glacier system. The westerlies mark the boundary between the sub-tropical high and sub-polar low, so a more northerly position would bring warmer air temperatures to the Mongolian Altai. The Tsagaan Gol-Potanin glacier could be registering a summertime poleward shift in the westerlies during the termination, which has also been suggested for glaciers in New Zealand and Scotland (Putnam et al., 2010a; Bromley et al., 2014). Last, let us turn to the tropical Pacific and the role it plays in Earth's climate. The global atmosphere is very sensitive to changes in changes in tropical SST because tropical water masses provide heat and water vapor to higher latitudes (Visser et al., 2003). The timing of the LLGM in Mongolia coincides with minimum Pacific SST values, reached at 38-30 ka (Lea et al., 2000; Feldberg and Mix, 2003; Martínez et al., 2003). The coincidence of the LLGM in Mongolia and minimum Pacific SST values points towards a tropical mechanism as a possible component of glacial cycles. Deglaciation also coincides with warming Pacific water masses during the termination (Visser et al., 2003).

One major question that emerges from this research is whether summer insolation intensity alone could have caused deglaciation and summer warming from 19.5 ka to 17.7 ka or is it necessary to call on the far-field effects of the tropical Pacific and/or a shift in the Northern Hemisphere westerlies?

CHAPTER 8

CONCLUSIONS

This study of the glacial history of the Tsagaan Gol-Potanin Glacier valley in the Mongolia Altai has contributed to our knowledge of the climate history in central Asia, a sparsely-studied region. The key findings of this research are:

1) I produced a precise, high-resolution ^{10}Be surface-exposure chronology, composed of 41 dates on glacial landforms and erratic boulders, underpinned by glacial-geomorphic mapping from field observations and drone imagery. Moraine formation occurred at 54.05 ± 2.78 ka, 23.24 ± 0.50 ka, and 28.08 ± 0.58 ka. Glacial erratics were deposited at 133-196 ka and 19.5-22.1 ka in the Bayan region, 37.8-15.7 ka at Holy Mountain, and 98.8-11.2 ka in the Potanin region. In the Potanin region, boulder ages cluster into two groups, dating to 17.71 ± 0.19 ka and 16.20 ± 0.09 ka.
2) Glacial snowline reconstructions show that the temperature during the peak of the LLGM was 6.0 ± 0.5°C lower than modern and 4.3 ± 0.5°C lower than the Little Ice Age. The temperature during the Little Ice Age the temperature decreased 1.7 ± 0.3°C from modern.
3) Deglaciation in the Tsagaan Gol-Potanin Glacier valley was well underway by 17.7 ± 0.19 ka, with 640 ± 90 m of snowline rise occurring by this time. This represents ~60% of the snowline rise from the LLGM to modern and a 3.5 ± 0.5°C temperature increase.
4) Summer warming in the Altai occurred during Henrich Stadial 1, which is consistent with amplified seasonality during a period of mean annual cooling. Deglaciation in the Mongolia Altai preceded the rise in atmospheric CO_2. Thus, CO_2 is likely not the primary mechanism for driving the initial pulse of deglacial warming in the Mongolian Altai.
5) I suggest that the glacial chronology can be explained by rising local summer insolation, increased heat export out of the tropical Pacific, and/or a northward shift of the summertime westerly jet. The relative importance of the above mechanisms remains to be answered.

BIBLIOGRAPHY

Adhémar, J.A., 1842, Revolutions de la mer: Déluges Périodiques, Carilian-Goeury et V. Dalmont: Paris.

Anderson, R.F., Ali, S., Bradtmiller, L.I., Nielsen, S.H.H., Fleisher, M.Q., Anderson, B.E., and Burckle, L.H., 2009, Wind-Driven Upwelling in the Southern Ocean and the Deglacial Rise in Atmospheric CO2: Science, v. 323, no. 5920, p. 1443–1448, doi: 10.1126/science.1167441.

Anderson, R.S., Dühnforth, M., Colgan, W., and Anderson, L., 2012, Far-flung moraines: Exploring the feedback of glacial erosion on the evolution of glacier length: Geomorphology, v. 179, p. 269–285, doi: 10.1016/j.geomorph.2012.08.018.

Bakke, J., and Nesje, A., 2011, Equilibrium-Line Altitude (ELA), *in* Encyclopedia of Snow, Ice and Glaciers, p. 268–277.

Balco, G., 2011, Contributions and unrealized potential contributions of cosmogenic-nuclide exposure dating to glacier chronology, 1990-2010: Quaternary Science Reviews, v. 30, no. 1–2, p. 3–27, doi: 10.1016/j.quascirev.2010.11.003.

Bard, E., 2000, Hydrological Impact of Heinrich Events in the Subtropical Northeast Atlantic: Science, v. 289, no. 5483, p. 1321–1324, doi: 10.1126/science.289.5483.1321.

Barker, S., Diz, P., Vautravers, M.J., Pike, J., Knorr, G., Hall, I.R., and Broecker, W.S., 2009, Interhemispheric Atlantic seesaw response during the last deglaciation: Nature, v. 457, no. 7233, p. 1097–1102, doi: 10.1038/nature07770.

Barrell, D.. J.A., Anderson, B.G., Denton, G.H., and Smith Lyttle, B., 2013, Glacial geomorphology of the central South Island, New Zealand - digital data: Lower Hutt.

Barth, C., Boyle, D.P., Hatchett, B.J., Bassett, S.D., Garner, C.B., and Adams, K.D., 2016, Late Pleistocene climate inferences from a water balance model of Jakes Valley, Nevada (USA): Journal of Paleolimnology, v. 56, no. 2–3, p. 109–122, doi: 10.1007/s10933-016-9897-z.

Benn, D.I., and Ballantyne, C.K., 2005, Palaeoclimatic reconstruction from Loch Lomond Readvance glaciers in the West Drumochter Hills, Scotland: Journal of Quaternary Science, v. 20, no. 6, p. 577–592, doi: 10.1002/jqs.925.

Benn, D., and Evans, D.J.A., 2010, Glaciers and glaciation: Hodder Education, London.

Benn, D.I., and Hulton, N.R.J., 2010, An ExcelTM spreadsheet program for reconstructing the surface profile of former mountain glaciers and ice caps: Computers and Geosciences, v. 36, no. 5, p. 605–610, doi: 10.1016/j.cageo.2009.09.016.

Bevington, P.R., and Robinson, D.K., 1992, Data Reduction and Error Analysis for the Physical Sciences, 2nd edn.: Computers in Physics, v. 7, no. 4, p. 324, doi: 10.1063/1.4823194.

Broecker, W.S., 2010, Long-Term Water Prospects in the Western United States: Journal of Climate, v. 23, p. 6669–6683, doi: 10.1175/2010JCLI3780.1.

Broecker, W.S., 1998, Paleocean circulation during the last deglaciation: A bipolar seesaw? Paleoceanography, v. 13, no. 2, p. 119–121.

Broecker, W., 2013, What Drives Glacial cycles: Eldigio Press, , no. 1, p. 1–5, doi: 10.1007/s13398-014-0173-7.2.

Broecker, W.S., and van Donk, J., 1970, Insolation changes, ice volumes, and the O18 record in deep-sea cores: Reviews of Geophysics, v. 8, no. 1, p. 169–198, doi: 10.1029/RG008i001p00169.

Bromley, G.R.M., Putnam, A.E., Rademaker, K.M., Lowell, T. V, Schaefer, J.M., Hall, B., Winckler, G., Birkel, S.D., and Borns, H.W., 2014, Younger Dryas deglaciation of Scotland driven by warming summers.: Proceedings of the National Academy of Sciences of the United States of America, v. 111, no. 17, p. 6215–9, doi: 10.1073/pnas.1321122111.

Buizert, C., Gkinis, V., Severinghaus, J.P., He, F., Lecavalier, B.S., Kindler, P., Leuenberger, M., Carlson, a. E., Vinther, B., Masson-Delmotte, V., White, J.W.C., Liu, Z., Otto-Bliesner, B., and Brook, E.J., 2014, Greenland temperature response to climate forcing during the last deglaciation: Science, v. 345, no. 6201, p. 1177–1180, doi: 10.1126/science.1254961.

Cheng, H., Edwards, R.L., Broecker, W.S., Denton, G.H., Kong, X., Wang, Y., Zhang, R., and Wang, X., 2009, Ice Age Terminations: Science, v. 326, no. 5950, p. 248–252, doi: 10.1126/science.1177840.

Cheng, H., Edwards, R.L., Sinha, A., Spötl, C., Yi, L., Chen, S., Kelly, M., Kathayat, G., Wang, X., Li, X., Kong, X., Wang, Y., Ning, Y., and Zhang, H., 2016, The Asian monsoon over the past 640,000 years and ice age terminations: Nature, v. 534, no. 7609, p. 640–646, doi: 10.1038/nature18591.

Clark, P.U., Dyke, A.S., Shakun, J.D., Carlson, A.E., Clark, J., Wohlfarth, B., Mitrovica, J.X., Hostetler, S.W., McCabe, A.M., Mix, A.C., Bard, E., Schneider, R., Lambeck, K., Chappell, J., et al., 2009, The Last Glacial Maximum.: Science, v. 325, no. 5941, p. 710–4, doi: 10.1126/science.1172873.

Clark, P.U., Shakun, J.D., Baker, P.A., Bartlein, P.J., Brewer, S., Brook, E.J., Carlson, A.E., Cheng, H., Kaufman, D.S., Lui, Z., Marchitto, T.M., Mix, A.C., Morrill, C., Otto-Bliesner, B.L., et al., 2012, Global climate evolution during the last deglaciation: Proceedings of the National Academy of Sciences of the United States of America, v. 109, no. 19, p. 1134–1142, doi: 10.1073/pnas.1116619109/-/DCSupplemental.www.pnas.org/cgi/doi/10.1073/pnas.1116619109.

Claude, A., Ivy-Ochs, S., Kober, F., Antognini, M., Salcher, B., and Kubik, P.W., 2014, The Chironico landslide (Valle Leventina, southern Swiss Alps): age and evolution: Swiss Journal of Geosciences, v. 107, no. 2–3, p. 273–291, doi: 10.1007/s00015-014-0170-z.

Croll, J., 1867, LV. On the change in the obliquity of the ecliptic, its influence on the climate of the polar regions and on the level of the sea: The London, Edinburgh, and Dublin Philosophical Magazine and Journal of Science, v. 33, no. 225, p. 426–445.

Crowley, T., 1992, North Atlantic deep water cools the southern hemisphere: Paleoceanography, v. 7, no. 4, p. 489–497, doi: 10.1029/92PA01058.

Denton, G.H., Alley, R.B., Comer, G.C., and Broecker, W.S., 2005, The role of seasonality in abrupt climate change: Quaternary Science Reviews, v. 24, no. 10–11, p. 1159–1182, doi: 10.1016/j.quascirev.2004.12.002.

Denton, G.H., Anderson, R.F., Toggweiler, J.R., Edwards, R.L., Schaefer, J.M., and Putnam, A.E., 2010, The Last Glacial Termination: Science, v. 328, no. June, p. 1652–1656, doi: 10.1126/science.1184119.

Doughty, A.M., Schaefer, J.M., Putnam, A.E., Denton, G.H., Kaplan, M.R., Barrell, D.J.A., Andersen, B.G., Kelley, S.E., Finkel, R.C., and Schwartz, R., 2015, Mismatch of glacier extent and summer insolation in Southern Hemisphere mid-latitudes: Geology, v. 43, no. 5, p. 407–410, doi: 10.1130/G36477.1.

Dunai, T., 2010, Cosmogenic Nuclides: Principles, Concepts and Applications in the Earth Surface Sciences: Annals of Physics, v. 54, p. 258, doi: 10.1017/CBO9780511804519.

Feldberg, M.J., and Mix, A.C., 2003, Planktonic foraminifera, sea surface temperatures, and mechanisms of oceanic change in the Peru and south equatorial currents, 0-150 ka BP: Paleoceanography, v. 18, no. 1, p. 1016, doi: 10.1029/2001PA000740.

Florensov, N.A., and Korzhnev, S.S., 1982, Geomorphology of Mongolian People Republic: Joined Sovjet-Mongolian scientific research geological expeditions,.

Gosse, J.C., and Phillips, F.M., 2001, Terrestrial in situ cosmogenic nuclides: Theory and application: Quaternary Science Reviews, v. 20, no. 14, p. 1475–1560, doi: 10.1016/S0277-3791(00)00171-2.

Hall, B., Baroni, C., Denton, G., Kelly, M.A., and Lowell, T., 2008, Relative sea-level change, Kjove Land, Scoresby Sund, East Greenland: Implications for seasonality in Younger Dryas time: Quaternary Science Reviews, v. 27, no. 25–26, p. 2283–2291, doi: 10.1016/j.quascirev.2008.08.001.

Hall, B.L., Borns, H.W., Bromley, G.R.M., and Lowell, T. V., 2017, Age of the Pineo Ridge System: Implications for behavior of the Laurentide Ice Sheet in eastern Maine, U.S.A., during the last deglaciation: Quaternary Science Reviews, v. 169, p. 344–356, doi: 10.1016/j.quascirev.2017.06.011.

Hays, J.D., Imbrie, J., and Shackleton, N.J.J., 1976, Variations in the Earth's Orbit : Pacemaker of the Ice Ages: Science, v. 194, no. 4270, p. 1121–1132, doi: 10.1126/science.194.4270.1121.

Huybers, P., and Denton, G., 2008, Antarctic temperature at orbital timescales controlled by local summer duration: Nature Geoscience, v. 1, no. 11, p. 787–792, doi: 10.1038/ngeo311.

Jacobson-Tepfer, E., 2013, Late Pleistocene and Early Holocene Rock Art from the Mongolian Altai: The Material and its Cultural Implications: Arts, v. 2, no. 3, p. 151–181, doi: 10.3390/arts2030151.

Kadota, T., and Gombo, D., 2007, Recent glacier variations in Mongolia: Annals of Glaciology, v. 46, p. 185–188, doi: 10.3189/172756407782871675.

Kaplan, M.R., Hein, A.S., Hubbard, A., and Lax, S.M., 2009, Can glacial erosion limit the extent of glaciation? Geomorphology, v. 103, no. 2, p. 172–179, doi: 10.1016/j.geomorph.2008.04.020.

Klinge, M., 2001, Glacial-geomorphologic Investigations in the Mongolian Altai: a Contribution to the Late Quaternary Landscape and Climate History of Western Mongolia: Aachen: Aachener Geographische Arbeiten, v. 35, p. 125.

Koester, A.J., Shakun, J.D., Bierman, P.R., Davis, P.T., Corbett, L.B., Braun, D., and Zimmerman, S.R., 2017, Rapid thinning of the Laurentide Ice Sheet in coastal Maine, USA, during late Heinrich Stadial 1: Quaternary Science Reviews, v. 163, p. 180–192, doi: 10.1016/j.quascirev.2017.03.005.

Konya, K., Kadota, T., Davaa, G., Yabuki, H., and Ohata, T., 2010, Meteorological and ablation features of Potanin Glacier, Mongolian Altai: Bulletin of Glaciological Research, v. 28, p. 7–16, doi: 10.5331/bgr.28.7.

Konya, K., Kadota, T., Nakazawa, F., Gombo, D., Kalsan, P., Yabuki, H., and Ohata, T., 2013, Surface mass balance of the Potanin Glacier in the Mongolian Altai Mountains and comparison with Russian Altai glaciers in 2005, 2008, and 2009: Bulletin of Glaciological Research, v. 31, p. 9–18.

Lea, D.W., Pak, D.K., and Spero, H.J., 2000, Climate impact of late quaternary equatorial Pacific sea surface temperature variations: Science, v. 289, no. 5485, p. 1719–1724, doi: 10.1126/science.289.5485.1719.

Lehmkuhl, F., 1998, Quaternary Glaciations in Central and Western Mongolia: Quaternary Proceedings, v. 13, no. 6, p. 153–167.

Lehmkuhl, F., Klinge, M., Rother, H., and Hülle, D., 2016, Distribution and timing of Holocene and late Pleistocene glacier fluctuations in western Mongolia: Annals of Glaciology, v. 57, no. 71, p. 169–178, doi: 10.3189/2016AoG71A030.

Lehmkuhl, F., Klinge, M., and Stauch, G., 2011, The extent and timing of Late Pleistocene Glaciations in the Altai and neighboring mountain systems, *in* Ehlers, J., Gibbard, P.L., and Hughes, P.D. eds., Developments in Quaternary Science— Extent and Chronology — A Closer Look, Elsevier, Oxford, p. 967–979.

Lehmkuhl, F., Klinge, M., and Stauch, G., 2004, The extent of Late Pleistocene glaciations in the Altai and Khangai Mountains, *in* Ehlers, J. and Gibbard, P.L. eds., Quaternary Glaciations — Extent and Chronology, Part III: South America, Asia, Africa, Australia, Antarctica, Elsevier, Oxford, p. 243–254.

Lehmkuhl, F., Zander, A., and Frechen, M., 2007, Luminescence chronology of fluvial and aeolian deposits in the Russian Altai (Southern Siberia): Quaternary Geochronology, v. 2, no. 1–4, p. 195–201, doi: 10.1016/j.quageo.2006.04.005.

Levy, L.B., Kelly, M.A., Lowell, T. V., Hall, B.L., Howley, J.A., and Smith, C.A., 2016, Coeval fluctuations of the Greenland ice sheet and a local glacier, central East Greenland, during late glacial and early Holocene time: Geophysical Research Letters, v. 43, no. 4, p. 1623–1631, doi: 10.1002/2015GL067108.

Lifton, N., Smart, D.F., and Shea, M.A., 2008, Scaling time-integrated in situ cosmogenic nuclide production rates using a continuous geomagnetic model: Earth and Planetary Science Letters, v. 268, no. 1–2, p. 190–201, doi: 10.1016/j.epsl.2008.01.021.

Lisiecki, L.E., and Raymo, M.E., 2005, A Pliocene-Pleistocene stack of 57 globally distributed benthic δ18O records: Paleoceanography, v. 20, no. 1, p. 1–17, doi: 10.1029/2004PA001071.

Mackintosh, A.N., Anderson, B.M., and Pierrehumbert, R.T., 2017, Reconstructing Climate from Glaciers: Annual Review of Earth and Planetary Sciences, v. 45, no. 1, p. annurev-earth-063016-020643, doi: 10.1146/annurev-earth-063016-020643.

Marcott, S.A., Shakun, J.D., Clark, P.U., and Mix, A.C., 2013, A Reconstruction of Regional and Global Temperature for the Past 11,300 Years: Science, v. 339, no. 6124, p. 1198–1201, doi: 10.1126/science.1228026.

MARGO Project Members, 2009, Constraints on the magnitude and patterns of ocean cooling at the Last Glacial Maximum: Nature Geoscience, v. 2, no. 2, p. 127–132, doi: 10.1038/ngeo411.

Martínez, I., Keigwin, L., Barrows, T.T., Yokoyama, Y., and Southon, J., 2003, La Niña-like conditions in the eastern equatorial Pacific and a stronger Choco jet in the northern Andes during the last glaciation: Paleoceanography, v. 18, no. 2, p. 1–18, doi: 10.1029/2002PA000877.

McKinnon, K.A., Mackintosh, A.N., Anderson, B.M., and Barrell, D.J.A., 2012, The influence of sub-glacial bed evolution on ice extent: A model-based evaluation of the Last Glacial Maximum Pukaki glacier, New Zealand: Quaternary Science Reviews, v. 57, p. 46–57, doi: 10.1016/j.quascirev.2012.10.002.

McKinnon, K.A., Stine, A.R., and Huybers, P., 2013, The spatial structure of the annual cycle in surface temperature: Amplitude, phase, and lagrangian history: Journal of Climate, v. 26, no. 20, p. 7852–7862, doi: 10.1175/JCLI-D-13-00021.1.

McManus, J.F., Francois, R., Gherardi, J.-M., Keigwin, L.D., and Brown-Leger, S., 2004, Collapse and rapid resumption of Atlantic meridional circulation linked to deglacial climate changes: Nature, v. 428, no. 6985, p. 834–837, doi: 10.1038/nature02494.

Mercer, J.H., 1984, Simultaneous climatic change in both hemispheres and similar bipolar interglacial warming: Evidence and implications: Climate Processes and Climate Sensitivity, v. 29, p. 307–313, doi: 10.1029/GM029.

Milankovitch, M., 1941, Kanon der Erdbestrahlung und seine Andwendung auf das Eiszeiten-problem: Belgrade.

Monnin, E., Steig, E., Siegenthaler, U., Kawamura, K., Schwander, J., Stauffer, B., Stocker, T., Morse, D., Barnola, J., Bellier, B., and Others, A., 2004, EPICA Dome C ice core high resolution Holocene and transition CO2 data: IGBP PAGES/World Data Center for Paleoclimatology Data Contribution Series # 2004-055. NOAA/NGDC Paleoclimatology Program, Boulder CO, USA., v. 55.

Nishiizumi, K., Imamura, M., Caffee, M.W., Southon, J.R., Finkel, R.C., and McAninch, J., 2007, Absolute calibration of 10Be AMS standards: Nuclear Instruments and Methods in Physics Research, Section B: Beam Interactions with Materials and Atoms, v. 258, no. 2, p. 403–413, doi: 10.1016/j.nimb.2007.01.297.

Oerlemans, J., 2005, Extracting a climate signal from 169 glacier records.: Science (New York, N.Y.), v. 308, no. 5722, p. 675–7, doi: 10.1126/science.1107046.

Pellitero, R., Rea, B.R., Spagnolo, M., Bakke, J., Hughes, P., Ivy-Ochs, S., Lukas, S., and Ribolini, A., 2015, A GIS tool for automatic calculation of glacier equilibrium-line altitudes: Computers & Geosciences, v. 82, no. April 2016, p. 55–62, doi: 10.1016/j.cageo.2015.05.005.

Pellitero, R., Rea, B.R., Spagnolo, M., Bakke, J., Ivy-Ochs, S., Frew, C.R., Hughes, P., Ribolini, A., Lukas, S., and Renssen, H., 2016, Glare, a GIS tool to reconstruct the 3D surface of palaeoglaciers: Computers & Geosciences, v. 94, p. 77–85, doi: 10.1016/j.cageo.2016.06.008.

Porter, S.C., 1979, Hawaiian glacial ages: Quaternary Research, v. 12, no. 2, p. 161–187, doi: 10.1016/0033-5894(79)90055-3.

Porter, S.C., 2001, Snowline depression in the tropics during the last glaciation: Quaternary Science Reviews, v. 20, no. 10, p. 1067–1091, doi: 10.1016/S0277-3791(00)00178-5.

Putnam, A.E., and Broecker, W.S., 2017, Human-induced changes in the distribution of rainfall: , p. 1–15.

Putnam, A.E., Denton, G.H., Schaefer, J.M., Barrell, D.J.A., Andersen, B.G., Finkel, R.C., Schwartz, R., Doughty, A.M., Kaplan, M.R., and Schlüchter, C., 2010a, Glacier advance in southern middle-latitudes during the Antarctic Cold Reversal: Nature Geoscience, v. 3, no. 10, p. 700–704, doi: 10.1038/ngeo962.

Putnam, A.E., Schaefer, J.M., Barrell, D.J.A., Vandergoes, M., Denton, G.H., Kaplan, M.R., Finkel, R.C., Schwartz, R., Goehring, B.M., and Kelley, S.E., 2010b, In situ cosmogenic 10Be production-rate calibration from the Southern Alps, New Zealand: Quaternary Geochronology, v. 5, no. 4, p. 392–409, doi: 10.1016/j.quageo.2009.12.001.

Putnam, A.E., Schaefer, J.M., Denton, G.H., Barrell, D.J.A., Birkel, S.D., Andersen, B.G., Kaplan, M.R., Finkel, R.C., Schwartz, R., and Doughty, A.M., 2013, The Last Glacial Maximum at 44 degrees S documented by a Be-10 moraine chronology at Lake Ohau, Southern Alps of New Zealand: Quaternary Science Reviews, v. 62, p. 114–141, doi: 10.1016/j.quascirev.2012.10.034.

Ramsey, C.B., 2017, Methods for Summarizing Radiocarbon Datasets, *in* Radiocarbon, p. 1809–1833.

Raymo, M.E., 1997, The timing of major climate terminations: Paleoceanography, v. 12, no. 4, p. 577–585, doi: 10.1029/97PA01169.

Reimer, P.J., Bard, E., Bayliss, A., Beck, J.W., Blackwell, P.G., Ramsey, C.B., Buck, C.E., Cheng, H., Edwards, R.L., Friedrich, M., Grootes, P.M., Guilderson, T.P., Haflidason, H., Hajdas, I., et al., 2013, IntCal13 and Marine13 Radiocarbon Age Calibration Curves 0–50,000 Years cal BP: Radiocarbon, v. 55, no. 4, p. 1869–1887, doi: 10.2458/azu_js_rc.55.16947.

Roe, G., 2006, In defense of Milankovitch: v. 33, no. August, p. 1–5, doi: 10.1029/2006GL027817.

Rother, H., Lehmkuhl, F., Fink, D., and Nottebaum, V., 2014, Surface exposure dating reveals MIS-3 glacial maximum in the Khangai Mountains of Mongolia: Quaternary Research (United States), v. 82, no. 2, p. 297–308, doi: 10.1016/j.yqres.2014.04.006.

Sapozhnikov, V., 1949, On Russian and Mongolian Altai: Geografgiz, Moscow (in Russian),.

Schmittner, A., and Galbraith, E.D., 2008, Glacial greenhouse-gas fluctuations controlled by ocean circulation changes: Nature, v. 456, no. 7220, p. 373–376, doi: 10.1038/nature07531.

Shakun, J.D., Clark, P.U., He, F., Lifton, N.A., Liu, Z., and Otto-Bliesner, B.L., 2015, Regional and global forcing of glacier retreat during the last deglaciation.: Nature communications, v. 6, p. 8059, doi: 10.1038/ncomms9059.

Shakun, J.D., Clark, P.U., He, F., Marcott, S.A., Mix, A.C., Liu, Z., Otto-bliesner, B., Schmittner, A., and Bard, E., 2012, Global warming preceded by increasing carbon dioxide concentrations during the last deglaciation: Nature, v. 484, no. 7392, p. 49–54, doi: 10.1038/nature10915.

Spratt, R.M., and Lisiecki, L.E., 2016, A Late Pleistocene sea level stack: Climate of the Past, v. 12, no. 4, p. 1079, doi: 10.5194/cp-12-1-2016.

Stephens, B.B., and Keeling, R.F., 2000, The influence of Antarctic sea ice on glacial–interglacial CO2 variations: Nature, v. 404, no. 6774, p. 171–174, doi: 10.1038/35004556.

Stone, J.O., 2000, Air pressure and cosmogenic isotope production: Journal of Geophysical Research: Solid Earth, v. 105, no. B10, p. 23753–23759, doi: 10.1029/2000JB900181.

Strand, P.D., Putnam, A.E., Denton, G.H., Putnam, D.E., Sambuu, O., and Radue, M.J. The Last Glacial Termination in the Altai Mountains of Western Mongolia, in prep.:

Syromyatina, M. V., Kurochkin, Y.N., Bliakharskii, D.P., and Chistyakov, K. V., 2015, Current dynamics of glaciers in the Tavan Bogd Mountains (Northwest Mongolia): Environmental Earth Sciences, v. 74, no. 3, p. 1905–1914, doi: 10.1007/s12665-015-4606-1.

Toggweiler, J.R., Russell, J.L., and Carson, S.R., 2006, Midlatitude westerlies, atmospheric CO2, and climate change during the ice ages: Paleoceanography, v. 21, no. 2, doi: 10.1029/2005PA001154.

Unkelbach, J., Dulamsuren, C., Punsalpaamuu, G., Saindovdon, D., and Behling, H., 2017, Late Holocene vegetation, climate, human and fire history of the forest-steppe-ecosystem inferred from core G2-A in the “Altai Tavan Bogd” conservation area in Mongolia: Vegetation History and Archaeobotany, v. 0, no. 0, p. 0, doi: 10.1007/s00334-017-0664-5.

Visser, K., Thunell, R., and Lowell, S., 2003, Magnitude and timing of temperature change in the Indo-Pacific warm pool during deglaciation: Nature, v. 421, no. 6919, p. 152–155, doi: 10.1038/nature01331.1.

Windley, B.F., Kröner, A., Guo, J., Qu, G., Li, Y., and Zhang, C., 2002, Neoproterozoic to Paleozoic Geology of the Altai Orogen, NW China: New Zircon Age Data and Tectonic Evolution: The Journal of Geology, v. 110, no. 6, p. 719–737, doi: 10.1086/342866.

Wirsig, C., Zasadni, J., Ivy-Ochs, S., Christl, M., Kober, F., and Schlüchter, C., 2016, A deglaciation model of the Oberhasli, Switzerland: Journal of Quaternary Science, v. 31, no. 1, p. 46–59, doi: 10.1002/jqs.2831.

APPENDIX A

METHODS

A.1 Sampling Methods

Sampling is most easily carried out in groups of 3-5 people. One person can extract the sample while others make observations in field notebooks. Once the sample is extracted, then the driller can make notes while others set up the GPS and measure boulder dimensions.

1. Identify boulder for sampling. Boulder should be glacially deposited and show no signs of post-depositional movement. Avoid boulders on steep slopes or at the bottom of a steep slope. Also, note any human and fluvial alteration near the boulder.

2. Identify the sampling site on the boulder. Aim to sample from a flat surface on the top of the boulder, dipping less than 30°. If there is glacial polish or striations preserved on the boulder, then try to sample those surfaces.

3. Mark the intended sample location with a permanent marker and take a picture of the unsampled surface with a scale. Then, measure the orientation of the sample surface. Record the dip and dip direction.

4. Don safety protections: eyewear, gloves, and ear plugs/earmuffs.

5. Drill 3-5 holes into the boulder about 10° dipping from horizontal with a carbide 3/8" drill bit, using a concrete-grade drill (e.g., Hilti TE-6A). Make the holes about 5 cm apart and arc around the desired sample location. Apply gentle pressure to the drill to guide the bit in. If drilling into a low-angle surface, it can help to make a small vertical divot with the drill to start the hole.

6. Clean the holes with a puffer and insert wedges and shims - one wedge and two shims for each hole. Make the flat surface of the shims parallel to horizontal and place the shims so that the tips are flush with the edge of the boulder. Then insert the wedge between the shims, ensuring that the wedge faces are also parallel to horizontal.

7. Using a hammer, drive in the shims steadily. Make sure that the wedges are going in evenly so that all wedges are experiencing the same amount of pressure. You will hear the wedges ring the same pitch if the pressure is even. Continue to hammer until the sample "pops" off the rock. If the sample does not come off, then you may have to remove wedges and start new holes. This frequently happens if the holes are drilled too steeply. Vice grips are useful when removing wedges and shims. If there is enough sample extracted (usually 600-1000 g), continue with the procedure, as outlined below. If not, repeat by drilling new holes adjacent to the extracted sample.

8. Place a Trimble Geo 7x GPS (or antenna) on the sample location and let the GPS record at least 500 points. The GPS can record positions while the remaining steps are completed.

9. Sketch the boulder and surrounding geomorphic features. Make written notes of boulder features, such as polish, striations, exfoliation, lichen, chicken heads, etc, and proximal surface features.

10. Measure the length, width, and height of the boulder (measure height from ground to sample surface on N, E, S, and W sides).

11. Measure the shielding from the sample location using a clinometer. Make sure to determine whether any portion of the boulder is shielding the sample. Record in notebook.
12. All information about the boulder (dimensions, rock type, shielding) should be input into the data dictionary in the GPS.

13. On a canvas sampling bag, write the sample name, date, location, and short description of sample on the bag.

14. With the sample bag on the boulder, and a hammer for scale, photograph the boulder from multiple aspects. Then place sample into the bag (only rock fragments with the rock surface preserved).

15. Once the sample and bag are removed, extend a measuring tape to 2 m and place on the ground near the base of the boulder. Then take a video of the boulder with a GoPro mounted on a monopod, making sure to capture every surface of the boulder.

A.2 Drone Mapping and Map Generation

A.2.1 Drone Mapping

When drone mapping, we use a DJI Phantom 4 quadcopter with a gimble camera. We use the app "Map Pilot" by Maps Made Easy for iPad. Be sure to check local regulations about drone flying before you map.

1. Determine area for drone mapping. While you have access to the internet, create a flight in Map Pilot and save map for offline use.

2. In the field, determine a flying location. The drone can only survey an area with a radius of 2 km from the starting point, so it is most efficient to start flights in the middle of the study area.

3. Set up the drone and controller. Take the case off the camera. Connect the iPad to the console. Put the sun shield on the iPad. Put the parabolic extenders on the console antennas. Turn on the console. Place the drone on the drone carrying case lid.

4. Make sure that there is an SD card in the drone with sufficient memory and a fully charged battery. Turn on the drone and open the DJI app. Wait for the drone to connect with the iPad. Once it has connected, close the DJI app and open Map Pilot.

5. The drone should appear as an arrow on the Map Pilot App. Create a new flight plan that is one battery-life long. This usually includes three transects and 1 km long for each transect (but this will vary depending on chosen altitude). Plan the flights so they are parallel or perpendicular to your entire flight swath. Tap on the iPad to create new point for flight plan, hold the point down to move it, and double tap to delete. Make sure that there is 70% overlap for the pictures and that the drone is flying at 300 m (or the regulated max height for the area in which you are flying).

6. Save the flight plan. Upload the flight to the drone. Turn the console to P mode. Then clear the drone area and press start.

7. The drone flight will take about 12-14 minutes. Make sure that the wind doesn't change and that it doesn't rain. If it does start raining, bring the drone home. The drone will fly along the course and a dot will appear on the flight path when the drone takes a picture. Pay attention to if the drone misses a photograph. If there are too many missing images, you will need to re-fly that segment.
8. The drone will return to the home point when the flight plan is complete. When the drone is about 20 m above the home point, take control of the drone by toggling to the S mode on the console. Lower the drone to a person so that they can catch the drone above their head. They should keep the drone above their head until the drone is shut down (the way to shut down the drone depends on the initial calibrations).

9. Fly as many flights as possible with the available batteries until the entire field area is covered. Make sure to back up flight images on another drive at the end of each day. It is also advisable to periodically swap out memory cards in case the drone crashes and is irretrievable.

A.2.2 Map Generation with PhotoScan

The manual for PhotoScan by Agisoft is found at http://www.agisoft.com/pdf/photoscan-pro_1_3_en.pdf and the tutorial followed when creating DEMs and orthomosaics http://www.agisoft.com/pdf/PS_1.3%20Tutorial%20(BL)%20%20Orthophoto,%20DEM%20(GCPs).pdf. Below is a modified version of the PhotoScan tutorial.

1. PhotoScan Preferences: Open PhotoScan "Preferences" dialog using corresponding command from the "Tools" menu. Set the following values for the parameters on the "General" tab:
    a. Stereo Mode: Anaglyph (use Hardware if your graphic card supports Quad Buffered Stereo)
    b. Stereo Parallax: 1.0
    c. Write log to file: specify directory where Agisoft PhotoScan log will be stored (in case of contacting the software support team it could be required)

2. Set the parameters in the GPU tab as following: Check on any GPU devices detected by PhotoScan in the dialog. Check on "Use CPU" option when less than two GPU are used. Set the following values for the parameters on the Advanced tab:
    a. Project compression level: 6
    b. Keep depth maps: enabled
    c. Store absolute image paths: disabled
    d. Check for updates on program startup: enabled
    e. Enable VBO support: enabled

3. Add Photos: To add photos select "Add Photos" command from the Workflow menu or click "Add Photos" button located on Workspace toolbar. In the Add Photos dialog browse the source folder and select files to be processed. Click "Open" button. "Load Camera Positions". At this step, the coordinate system for the future model is set using camera positions. Note: the camera position is included in the picture meta-data, so we do not have to add camera positions. Add all photos from study area into one group.

4. Align Photos: At this stage PhotoScan finds matching points between overlapping images, estimates camera position for each photo and builds sparse point cloud model. Select "Align Photos" command from the Workflow menu. Set the following recommended values for the parameters in the Align Photos dialog:

a. Accuracy: High (lower accuracy setting can be used to get rough camera positions in a shorter time)
b. Pair preselection: Reference + Generic (in case camera positions are unknown – only Generic preselection mode should be used)
c. Constrain features by mask: Disabled (Enabled in case any areas have been masked)
d. Key point limit: 40,000
e. Tie point limit: 4,000
f. Adaptive camera model fitting: Enabled (to let PhotoScan distortion parameters estimation).

5. Click "OK" button to start photo alignment. In a short period of time (depends on the number of images in the project and their resolution) you will get sparse point cloud model shown in the Model view. Camera positions and orientations are indicated by blue rectangles in the view window.

6. Place Markers: Markers are used to optimize camera positions and orientation data, which allows for better model output. Select the marker on the Reference pane. Then filter images in Photos pane using "Filter by Markers" option in the context menu available by right-clicking on the markers label in the Workspace pane. Now you need to check the marker location on every related photo and refine its position if necessary to provide maximum accuracy. Open each photo where the created marker is visible. Zoom in and drag the marker to the correct location while holding left mouse button. Repeat the described step for every ground control point (GCP). (Note: this step is much easier once an ortho photo of the area is already made. I recommend proceeding without entering the markers, make an orthophoto, import the orthophoto into Google Earth and find the boulder sample sites based on GPS data. Then redo the following steps).

7. Input Marker Coordinates: Finally, import marker coordinates from a file. Click "Import" button on the Reference pane toolbar and select file containing GCP coordinates data in the "Open" dialog. The easiest way is to load simple character-separated file (*.txt) that contain markers name, x-, y- coordinates and height. In "Import CSV" dialog indicate the delimiter according to the structure of the file and select the row to start loading from. Note that # character indicates a commented line that is not counted while numbering the rows. Indicate for the program what parameter is specified in each column through setting correct column numbers in the "Columns" section of the dialog. Also, it is recommended to specify a valid coordinate system in the corresponding field for the values used for camera center data. Check your settings in the sample data field in "Import CSV" dialog: Click "OK" button. The data will be loaded into the Reference pane.

8. Optimize Camera Alignment: To achieve higher accuracy in calculating camera external and internal parameters and to correct possible distortion (e.g. "bowl effect" and etc.), an optimization procedure should be run. This step is especially recommended if the GCP coordinates are known almost precisely – within several centimeters accuracy (marker-based optimization procedure). Click the "Settings" button in the Reference pane and in the Reference Settings dialog select the corresponding coordinate system from the list according to the GCP coordinates data. Prior to optimization it is also possible to remove the points with the highest reprojection error values using corresponding criterion in "Edit Menu" → Gradual Selection dialog. Set the following values for the parameters in Measurement accuracy section and check that valid coordinate system is selected that corresponds to the system that was used to survey GCPs: Marker accuracy: 0.005 (specify value according to the measurement accuracy).
    a. Scale bar accuracy: 0.001

b. Projection accuracy: 0.1
c. Tie point accuracy: 1

9. Click “OK “button. On the Reference pane uncheck all photos and check on the markers to be used in optimization procedure. The rest of the markers that are not taken into account can serve as validation points to evaluate the optimization results. It is recommended to perform the optimization procedure since camera coordinates are usually measured with considerably lower accuracy than GCPs, also it allows to exclude any possible outliers for camera positions caused by the onboard GPS device failures. Click “Optimize” button on the Reference pane toolbar. Select camera parameters you would like to optimize. Click “OK” button to start optimization process. (For DJI drone cameras it is usually suggested to optimize the rolling shutter).

10. Set Bounding Box: Bounding Box is used to define the reconstruction area. Bounding box is resizable and rotatable with the help of Resize Region and Rotate Region tools from the Toolbar. Important: The colored side of the bounding box indicates the plane that would be treated as ground plane and has to be set under the model and parallel to the XY plane. This is important if mesh is to be built in Height Field mode, which is reasonable for aerial data processing workflow.

11. Build Dense Point: Cloud Based on the estimated camera positions the program calculates depth information for each camera to be combined into a single dense point cloud. Select “Build Dense Cloud” command from the Workflow menu. Set the following recommended values for the parameters in the Build Dense Cloud dialog:
    a. Quality: Medium (higher quality takes quite a long time and demands more computational resources, lower quality can be used for fast processing)
    b. Depth filtering: Aggressive (if the geometry of the scene to be reconstructed is complex with numerous small details or untextured surfaces, like roofs, it is recommended to set Mild depth filtering mode, for important features not to be sorted out) Points from the dense cloud can be removed with the help of selection tools and Delete/Crop instruments located on the Toolbar.
12. Build Mesh (optional: can be skipped if polygonal model is not required as a final result): After dense point cloud has been reconstructed it is possible to generate polygonal mesh model based on the dense cloud data. Select “Build Mesh” command from the Workflow menu. Set the following recommended values for the parameters in the Build Mesh dialog:
    a. Surface type: Height Field
    b. Source data: Dense cloud
    c. Polygon count: Medium (maximum number of faces in the resulting model. The values indicated next to High/Medium/Low preset labels are based on the number of points in the dense cloud. Custom values could be used for more detailed surface reconstruction).
    d. Interpolation: Enabled Click “OK” button to start mesh reconstruction.

13. Edit Geometry: Sometimes it is necessary to edit geometry before building texture atlas and exporting the model. Unwanted faces could be removed from the model. Firstly, you need to indicate the faces to be deleted using selection tools from the toolbar. Selected areas are highlighted with red color in the Model View. Then, to remove the selection use “Delete Selection” button on the Toolbar (or Del key) or use “Crop Selection” button on the Toolbar to remove all but selected faces. If the overlap of the original images was not sufficient, it may be required to use “Close Holes” command from the Tools menu at geometry editing stage to produced holeless model. In Close Holes dialog select the size of the largest hole to be closed (in percentage of the total model size). PhotoScan tends to produce 3D models with excessive geometry resolution. That's why it is recommended to decimate mesh before exporting it to a

different editing tool to avoid performance decrease of the external program. To decimate 3D model select “Decimate Mesh...” command from the Tools menu. In the Decimate Mesh dialog specify the target number of faces that should remain in the final model. For PDF export task or web-viewer upload it is recommended to downsize the number of faces to 100,000 - 200,000. Click “OK” button to start mesh decimation procedure.

14. Build Texture (optional; applicable only to polygonal models): This step is not really needed in the orthomosaic export workflow, but it might be necessary to inspect a textured model before exporting it or it might be helpful for precise marker placement. Select “Build Texture” command from the Workflow menu. Set the following recommended values for the parameters in the Build Texture dialog: Mapping mode: Orthophoto Blending mode: Mosaic Texture size/count: 8192 (width & height of the texture atlas in pixels) Enable color correction: disabled (the feature is useful for processing of data sets with extreme brightness variation, but for general case it could be left unchecked to save the processing time) Click “OK” button to start texture generation.

15. Build DEM: Digital elevation model can be generated based on the dense cloud or mesh model. Usually first option is preferred, as it provides more accurate results (low-poly model, being used as a source data, may result in inaccurate DEM) and allows for faster processing, since mesh generation step can be skipped. Select “Build DEM” command from the Workflow menu: Coordinate system should be specified in accordance with the system used for the model referencing. At the export stage it will be possible to project the results to a different geographical coordinate system. After DEM generation process is finished, it is possible to open the reconstructed model in Ortho view by double-clicking on the DEM label in the chunk's contents on the Workspace pane.

16. Build Orthomosaic: Select “Build Orthomosaic” command from the Workflow menu: Select desired surface for orthomosaic generation process: mesh or DEM, and blending mode. Pixel size will be suggested according to the average ground sampling resolution of the original images. According to the surface size and the input pixel size the total size of the orthomosaic (in pixels) will be calculated and shown in the bottom of the dialog box. Generated orthomosaic can be reviewed in Ortho mode similar to the digital elevation model. It can be opened in this view mode by double-clicking on the orthomosaic label in the Workspace pane.

17. Export Orthomosaic: Select “Export Orthomosaic” → Export JPEG/TIFF/PNG command from File menu. Set the following recommended values for the parameters in the Export Orthomosaic dialog: Projection: Desired coordinate system Pixel size: desired export resolution (please note that for WGS84 coordinate system units should be specified in degrees. Use Meters button to specify the resolution in meters). Export as TIFF.

18. Export DEM: Select “Export DEM” → Export GeoTIFF/BIL/XYZ command from File menu. Set the following recommended values for the parameters in the Export DEM dialog. Export as GeoTIFF with WGS84 projection.

A.3 Quartz Separation

Detailed below are methods for obtaining clean quartz from a whole rock and Be extraction. The preparation of the rock involves both physical and chemical separation methods. The procedure detailed below is a modified version of the Lamont-Doherty Earth Observatory Laboratory methods (http://www.ldeo.columbia.edu/cosmo/methods).

A.3.1 Rock Crushing

Safety information: The crushing, grinding, and sieving of rocks produces high amounts of dust, and inhalation of dust particles should be avoided. Review the procedures for operating the ventilation systems for these pieces of equipment and procedures. ALWAYS WEAR A DUST MASK (NIOSH approved, N95), safety goggles, work gloves, long pants, and closed shoes.

1. Ensure that work area and machinery are thoroughly cleaned.

2. Rock samples may need to be cut using a saw to fit in jaw crusher.

3. The samples are crushed into small pieces using a jaw crusher. Use a piece of wood to guide samples into crusher to ensure that they do not fly away.

4. Samples are then crushed using a disk mill. Place the nozzle of the vent into the whole at the top of the box around the disk mill. This will remove the majority of the dust particles from the source area. Crush rock pieces into sand-sized grains (generally < 0.7mm). It is necessary to put the sample through the disk mill numerous times and progressively move the disks closer together to achieve the desired grain size without producing excess fine-grained sediment.

5. The crushed rock can then be put through a column of sieves to sort the sample by grain size. Use 125-710 µm size sieves.

Cleaning: Saws and rock crushing machines should be thoroughly cleaned after each sample. Rinse saws with water and dry them completely afterward. Use methanol to protect the metal pieces from oxidation. Clean the disk mill using a vacuum, air compressor, and small broom or brush. After cleaning the disk mill, turn it on and let it run for a few seconds without putting a sample in and observe to see if grains are in the pan. Clean sieves with a brush and put in a small ultrasonic bath. Then, dry sieves in an oven and inspect them for cleanliness. If grains are still present in sieves, clean further with a brush or air compressor.

A.3.2 Phosphoric Acid Boiling

Samples are boiled in O-phosphoric acid to dissolve a whole host of minerals in many rock types.

1. Check the beakers thoroughly for cracks and clearly label them.

2. Be careful of cross contamination if you are boiling more than 1 sample.

3. Set up the hotplates in the hood with the metal cages, ensuring that the hotplates are steady on the hood floor.

4. Weigh up to 115 g of non-magnetic sample into 1000 ml beakers. Weight the sample directly into the beaker in the fume hood both to avoid inhaling dust and contaminating the lab with dust.

5. While in the fume hood, add some DI-water to each beaker (to keep the dust down). Then, at the sink rinse them thoroughly with DI-water to wash off the fines.

6. In the fume hood, add up to 400 ml of concentrated (85%) O-phosphoric acid to each beaker and cover the beakers with a watch glass. Set the hotplate to about 325°C and bring the samples to a boil. The boiling can be very vigorous at first, so you must stay in the lab until it has reached a steady rolling boil. Make sure that vigorous boiling isn't causing the beakers to "walk" off the hotplate. After about 1 hour the boiling will become gentle. Boil for 1-2 hours longer or until the volume reaches 300 ml. After a while, usually a total of about 2-3 hours, the rolling boil subsides, and the surface can become quite flat. This a good time to take off the samples.

CAUTION: Sometimes when the sample has boiled too long the acid will become very thick and jelly-like. (It seems to happen more with samples that have a lot of fines and organics, such as lichens from the surface of the rocks—another reason to rinse well.) To reduce the amount of lost in thick gel, pour it off before stirring the sample up and suspending it in this dense liquid. If the samples boil for too long, a dense gel can form which can be difficult to remove without losing a lot of sample.

1. Remove the beakers from the hotplate. You can remove the watch glasses, so they cool faster, but then rinse them with DI-water into a container in the hood. Do not squirt water into the hot acid! Let the samples cool for about an hour. The acid may form a gel around the sample and on the side of the beaker (this film of supersaturated silica solution), which will dissolve during the sodium hydroxide cleaning.

2. Once the beakers are cool (lukewarm is ok), pour off the acid into the Phosphoric Acid waste container. In the hood, squirt down the sides of the beaker with ~200 ml of DI-water and stir the samples with a clean metallic spatula. Allow the samples to settle and decant the water off into the waste container. Then add another 500 ml of DI-water. You can now take the samples over to the sink without risk of inhaling acid fumes. Rinse them 3 more times with DI-water in the sink.

3. Add 300 ml of DI-water to each beaker. In the fume hood, add 100 ml 50% NaOH (sodium hydroxide) to each beaker. The NaOH will dissolve the silicate coating around the quartz grains left by the phosphoric acid leach. Cover the beakers with the watch glasses and boil for ten minutes. (Use the same watch glass for the same sample as before, otherwise thoroughly rinse off any sample grains so as to avoid cross contamination of your samples.)

4. **DO NOT LEAVE THE SAMPLES! At this step the boiling is usually very vigorous and beakers can "walk" off the hotplate!** Start the hotplate at 300°C. If the boiling is too vigorous, reduce the heat. One hour after the samples boil, take the samples off the hotplate. Allow the samples to cool, about 30 minutes. You can remove the watch glasses immediately, rinsing the lids directly into the beaker. Once, cool, pour off the solution into NaOH waste container. Rinse w/ ~100 ml DI-water and pour off into the waste container and then rinse three times with DI-water and in the sink.

5. Either proceed directly to the HF/HNO_3 leaching steps or dry the sample in the oven overnight. If you are drying the samples, transfer them to small beakers, combining the same sample into one beaker. Once the sample is dry let it cool, weigh it, and record the weight in the notebook. Cover the sample with parafilm. If you are going directly to the HF step, combine 2 beakers of the sample into each bottle for the leaching step on the shaker table.

Beaker Cleaning: Scrub the beakers in the sink using a brush if necessary and rinse thoroughly so that no sample grains remain in the beakers. If they are really filthy, you can soak them in a soapy solution. Use DI-water for the final rinse. Dry beakers on the drying rack.

A.3.3 Froth Flotation

This method is used to separate feldspar and mica from quartz. It is based on the froth flotation method developed at the PRIME lab (http://www.physics.purdue.edu/primelab/MSL/froth_ floatation.html).

Grain size typically 125-710 µm but you should evaluate your sample and select a size that minimizes poly-mineral grains. We have successfully processed 63-125 µm. Quartz with attached feldspars or mica will float, in which case smaller is better. You can froth as much as 300 g in one bottle, otherwise split it into 2 bottles.

Preparation and Pretreatment -- 1% HF leach

1. Record all information in the froth flotation log.

2. Weigh the sample and record the weight (weigh it directly into a tared 2000 ml leaching bottle. Pour the sample in the hood to reduce dust inhalation and lab contamination).

3. Rinse the sample with DI-water to remove dust.

4. Take a small split (<1g) of the rinsed sample with a spatula and place it in a labeled petri dish for examination under the microscope (it is easier to look at the minerals after the sample has been rinsed of dust). Set the sample aside to describe while the sample is leaching.

5. Add 1% HF solution to the jar filling it approximate 2x the depth of the sample. Place it on the shaker table for 45-60 minutes. Do one sample at a time so the sample isn't sitting in the HF solution for too long. You can start the next sample leaching when you begin frothing the current sample.

6. Meanwhile describe the sample and record this in the log. Roughly estimate the percent composition of quartz and feldspar and any other significant minerals. If you don't know the mineral, at lead describe color, luster, shape, etc.

Frothing Set Up

1. Fill the 10-liter carboy next to the carbonator with the frothing solution: the final should contain 0.01 ml/1 glacial acetic acid and 0.01 ml/ lauryl amine (surfactant).

2. A concentrated solution is stored in the cabinet below the hood. Add 10 ml of concentrate per liter of DI-water and mix well (this does not have to be precise).

3. Rinse off the carbonator tube before placing it into the frothing solution in the carboy. Make sure it is completely submerged. The solution will be sucked into the carbonator after it's been dispensed. Keep at lead a few liters in the carboy so the carbonator does not suck up air.

4. Hard open the CO_2 tank. It is pre-set to ~100 psi (it should not exceed 100 psi).

5. Plug in the carbonator. There is no on/off switch.

Frothing Process

1. After 45-50 minutes, decant the 1% HF solution from the sample into a labeled waste container. DO NOT rinse the sample.

2. Keep the sample in the 2L leaching bottle and add a few drops of mineral oil to the sample and swirl it around. All mineral oil seems to work-pine, eucalyptus, tea tree (Do not use vegetable oils. Although they will work, they are impossible to clean up. Mineral oils are aromatic hydrocarbons and will evaporate as opposed to vegetable oils that are long chain fatty acids.

3. Dispense some frothing solution onto the sample. Carefully swirl around the bottle at the same time. Decant the solution with the floating grains into a plastic collection jar or directly into a filter funnel hooked up to the pump. The first 2-3 additions might not work very well but with each repetition the frothing with get "foamier" and more grains will float. The floating minerals will look clumpy, fluffy, and bubbly and after a few repetitions of froth and decanting, the sinking fraction and floating fraction will look distinct. If the frothing seems to slow down yet you can see there is still feldspar to remove, try added more oil. (An easy granitic sample needs 5-10 repetitions. Usually the quartz looks more grayish than the feldspar. Note that usually granite has much more feldspar than quartz so it is normal that the quartz fraction is smaller than the feldspar fraction. Use your original quartz estimate as a guide and if you are unsure, take a split and check under the microscope before you finish.

4. When you think the separation is complete, take a split from the sinking quartz fraction and check under the microscope to see if any feldspar remains. Difficult samples can be deceiving, so use this as a guide to check what you naked eye sees. Do not finish the sample without looking at this split or you may quit too early.

Once the separation is complete…

1. Take a tiny split from the floating fraction and record what is in it. Take note of any quartz that floated off with the feldspar fraction. It appears that very fine grain quartz can pour off with the floating fraction and in some cases where the quartz yields are small, it will be important to try and reduce this, or to recover it. Also, poly-mineral grains of quartz and feldspars will float.

2. Rinse the floating fraction in the filter with DI-water.

3. Finish filter the floating fraction, neutralize it with baking soda, and pour down the sink.

Sinking and Floating Fractions

Quartz & Recovery:

1. Rinse the sinking fraction with D-I water.

2. Proceed to HF/HNO_3 leaching

3. Dry the rinsed floating fraction in the filter in the oven.

4. Once dry, transfer it to a plastic bag and weigh it. Record the weight and calculate the sinking fraction wt. (total wt.-floating wt./floating wt.). If your original quartz estimate was good, it should be very close to the sinking (assuming a clean separate).

RECORD ALL WEIGHTS IN THE LOG

A.3.4 Chemical Preparation Steps

The following steps require the use of strong acids that present skin and inhalation exposure risks, and for HF, systemic toxicity. Review the MSDS sheets and any other documentation provided. Understand the risks associated with handling the chemicals you are working with, the procedures for reducing any risks, and emergency procedures in the event of an accident.

- Always work in a fume hood with the sash as low as is practical.
- Wear safety/splash goggles and use a full-coverage face shield if there is any risk of splashing.
- Wear appropriate gloves: for work with hot acids, use heavyweight (22 mil) neoprene gloves. For work with HF, you must wear HF-resistant gloves- not all materials are HF resistant (for example, latex). Check your gloves regularly for holes and excessive wear and replace as needed.
- You must wear long pants and closed shoes. Shorts, skirts, and open-toed or fabric shoes are not permitted when working with chemicals.
- Know where the eyewash stations, safety showers, spill kits, and tubes of calcium gluconate gel are located. Small spills contained in a hood can be cleaned up. In the event of a large spill or accident, call your institution's building manager.
- All HF exposures must be treated as medical emergencies. Flush the exposed area with water until medical help arrives.
- All chemical waste is collected in labeled containers and picked up as hazardous waste. Understand the procedures for collecting, labeling, and disposing of your waste.
- Empty bottles must be thoroughly rinsed out. Fill the bottle with water in the hood to avoid breathing vapors, and then rinse out at least 3 times in the sink. Deface the label, and write very clearly on the bottle, "RINSED."

Hydrofluoric/Nitric Acid Leach:

Samples are leached in a dilute hydrofluoric/nitric acid solution in order to dissolve minerals other than quartz and to remove meteoric ^{10}Be. Samples are generally leached twice in 1000 ml of a 5% HF/HNO_3 solution and placed on the shaker table, each time for 2 day, and once in a 2% HF/HNO_3 solution in a heated ultrasonic bath for 24 hours. Some samples require additional (4-10) leaching steps before they are sufficiently clean.

Shaker Table Leach

You can put ~150 g of sample in a bottle, though this will vary from sample to sample. Most samples dissolve a lot after the first leaching step, but you might want to adjust the amount of sample for samples that don't dissolve as much at this step.

- For a 5% HF+5% HNO_3 solution- Add 500 ml MQ-H_2O. Then, working in the fume hood, add 50 ml concentrated (49%) HF and 35 ml concentrated (79%) HNO_3, making sure to use the ACS grade bottles. NOTE: ALWAYS ADD WATER FIRST! NEVER ADD WATER TO ACID!

- Place bottles on the shaker table overnight. Make sure there are no drips of acid on the sides of the bottles. The samples do not need to be on for a full 24 hours. If you put them on in the afternoon, it is okay to change them the next morning. For a 5% HF+ 2% HNO_3 solution, use 875 ml MQ-H_2O, 100 ml HF, and 25 ml HNO_3.

- In the hood, pour the acid solution into a properly labeled waste container being careful not to pour out your sample.

- While working in the fume hood, add -1000 ml of MQ-H_2O to each bottle. Shake them vigorously, and then decant the water into the sink, again being careful not to spill any sample. The acid is dilute enough to now work outside of the hood. Rinse the samples two more times, filling the bottles about a third of the way and shaking them vigorously each time. The vigorous shaking will work to break up weaker feldspar grains.

- Repeat this shaker table leach step until the sample is clean.

Ultrasonic Leach in 2% HF + 2% HNO_3:

- Fill the bottle with 800 ml MQ- H_2O

- In the hood, add 30 ml HF and 21 ml HNO_3.

- Put the lids on tight when putting into the ultrasonic bath.

- Fill the bath to the brim with water.

- Turn on both the sonicator. You will need to check the level of the water from time to time. Even without the heat on, the water will evaporate. Keep it full to the brim.

- Remove the bottles from the bath and allow them to cool for about 30 minutes.

- Decant the acid into a waste container.

- Under the hood, fill the bottles with MQ- H_2O to rinse in the waster container.

- As with the shaker table leach, shake these up vigorously, decant into the sink, and repeat for a total of 3-4 rinses.

- Transfer sample into a very clean and labeled beaker for storage. Dry in oven. When sample is dry, cover with parafilm.

- Wash your bottles. Make sure you remove all sample grains from the bottles before adding a new sample! Rinse the bottles thoroughly and scrub with brush. You can turn the bottle upside down and forcefully clean off any grains that may be stuck to the bottom and sides. Once your bottles are cleaned, remove all labels and put them away.

A.3.5. Magnetic Mineral Separation

- An initial rough magnetic separation can be achieved by putting the sample through a chute magnet. The grain size generally is between 0.125-0.7 mm. If the samples have been etch, dry them in the oven in a small beaker.

- The non-magnetic fraction attained using the chute magnet is then put through a frantz isodynamic separator (usually 0.5 Amps and a 5-degree tilt) until few magnetic grains remain. This may take two cycles through the frantz. Collect the magnetic fraction in a plastic bag and return the non-magnetic grains to the beaker.

- Cleaning: Clean the chute magnet thoroughly after each sample. Wipe the frantz and the collection cups with the brush and then with the air hose.

A.4 Extraction of Beryllium from Quartz Method

Version: This version was created by Peter Strand, September 2016. It is an adaptation of the following two procedures, modified for the University of Maine cosmogenic isotope laboratory:
1. John Stone's Be-10/Al-26 method (http://depts.washington.edu/cosmolab/chem) as modified by Brenda Hall.
2. Roseanne Schwartz's Lamont Doherty Be-extraction method (http://www.ldeo.columbia.edu/cosmo/methods).
Where applicable, I've included notes from the two methods.

The method that follows is used to separate Beryllium from pure quartz for AMS measurement.

John says: The procedure described below will cope with up to ~10 mg of Fe and 3-5 mg of Ti, assuming the total amount of Al, Be and other metals is less than 3-5 mg. It can be modified to accommodate larger samples by increasing the size of vessels, ion exchange columns, etc.

"ICP" Aluminum check for quartz purity:
John says: Check the trace-element content of the quartz separate before dissolving it for ^{26}Al-^{10}Be analysis. It is important to obtain low concentrations of Al, Ti, Mg, Ca and alkalis. High Al levels decrease the $^{26}Al/^{27}Al$ ratio and limit the number of ^{26}Al ions that can be counted. This will reduce the statistical precision of the measurement. High levels of Ti and other trace elements may complicate the chemical separation described below.
Careful quartz clean-up usually (though not always) results in Al and Ti concentrations of <100 ppm. Higher levels of Al may indicate the presence of impurities such as feldspar, muscovite, garnet, or sparingly soluble fluorides from the HF treatment. Note, a 99.5% pure quartz separate containing ~0.5% feldspar still has an Al concentration of ~1000 ppm.

"ICP" Al-Check

- Select and label a set of small, 8ml Teflon ICP beakers, one for each sample.
- Weigh and record the weight of each beaker with lid on.
- With a clean spatula, transfer 0.05-0.35g of sample into the beaker. (0.1 g of sample is a good target) *Doing this in front of the anti-static machine helps keep quartz grains from being flung about by static.*
- Weigh and record the weight of the beaker and sample with lid on.
- Add a small amount of 1% HNO_3 with squirt bottle, enough to wet the grains, then cap the beaker.
- Thoroughly clean the spatula with isopropanol and a KimWipe after each sample.
- Uncap ICP beakers and place on the large hotplate in the fume hood.
- Don the HF safety gear and get a clean 100 ml Teflon reagent beaker. Carefully pour enough concentrated HF into the reagent beaker for for 2-3ml for each ICP-check beaker.
- Add 2-3 ml of this HF to each sample with a disposable pipette.
- Add 1 ml of 8% H_2SO_4 to each beaker and set hotplate to ~275 °F. The samples will dry down to a droplet of H_2SO_4 overnight.
- Cool the samples.

John says: Check the samples for solid material. An opaque, white, crystalline material indicates that the quartz is not clean enough for Be/Al chemistry. Fluffy white bits may indicate garnet. Samples may have a dark material which is probably illmenite or organic material, both of which can be HF-resistant. Illmenite or organic material can be ignored as they will not interfere with the chemistry and will only slightly contribute to the total error via an overestimation of the quartz weight.

- Add 5 ml of 1% HNO_3 to each beaker with the repeat pipettor, and then cap beakers. The solutions are now ready for ICP analysis, and should be not be weighed and recorded until immediately before being sent for ICP analysis.
- Weigh and record the weight of the beaker and solution with lid on. *Solution weight = weight of beaker w/ solution - beaker tare weight*
- Transfer to cleaned and labeled ICP-check centrifuge tubes once weighed.

To get ppm of sample, take measured ppm of solution and multiply by weight of solution (here, ~5.1 g). Divide by g in sample.
i.e., 3.6 ppm Al in ICP solution x 5.1 g of ICP solution = ~18 micrograms of Al in ICP solution, obtained from dissolving 0.1 g of rock. Thus, ~180 ppm Al in rock.

To calculate mg in sample, take ppm of sample (from above) and multiple by weight of quartz to be dissolved for chemistry. Divide by 1000.
i.e. 180 ppm Al in sample x 8 g quartz weight = 1.44 mg in sample

Sample Weighing, Spiking & Blank Preparation

- Determine the amount of quartz and carrier needed for each sample.
- For a batch of 6-11 samples of similar size, prepare 1 process blank.
- Label Jars with tape or Teflon marker.

Select a Savillex jar large enough so you only fill the beaker 1/2 full. Estimate space for 5mls HF per gram of sample, the sample itself, and some water.
Roseanne says: samples <10g use 90ml Savillex, samples ≥10g use 180ml+ Savillex.
Use the same size beaker for the blank as for the samples. Name the blank based on the batch number (check the master book): B25, B26, etc.

- To reduce static, wrap Al foil around the beakers and use anti-static gate.

- If you are not using the entire sample, make sure the sample is well mixed so that the split taken is representative of the entire sample.

Weighing Sample

METHOD 1: *Weighing directly into Savillex jar. (For a sample size < 25g and Savillex jar < 180ml.)*
- Place a clean labeled Teflon jar wrapped w/ Al foil on the analytical balance (the Al foil reduces static).
- Tare the balance.
- Add desired amount of sample to the jar with clean spatula. Record the weight to 4 decimal places.
- Remove the jar from the balance and cover grains with MQ-water.

Optional weighing method:
METHOD 2: Weight by difference. (If the Savillex beaker + Sample will be > 200g.)
- *Wrap the Savillex jar w/ Al foil.*
- *Weigh the entire sample in its storage container. Record this weight as "Sample + Tare wt.".*
- *Empty the entire contents of the container into the Savillex jar.*
- *Weigh the empty container. Record this weight as "Tare wt."*
- *You will calculate your sample weight – "Sample + Tare" – "Tare".*
- *Cover the sample w/ MQ-water.*

Be very careful not to spill any sample in this transfer, since your sample weight is being determined by weighing the amount removed from the sample container.

- Clean your spatula and work area between samples!

Adding Carrier (^{9}Be)

Since the natural concentration of ^{10}Be in rock is too low to be detected by AMS we add a known amount of ^{9}Be to each sample.

Record the initial weight of the working carrier bottle confirm that it is equal the final weight from the previous use. Remove all the Parafilm before weighing the bottles and invert the bottles a few times to homogenize the solution. When you are finished spiking all your samples, record the final weight of the carrier bottle.

Everyone's work depends on the integrity of the carrier. NEVER RISK CONTAMINATING THE CARRIER!

- We calculate the amount of carrier added to a sample by weighing the carrier bottle before and after each addition to a sample, rather than directly weighing the amount delivered to the sample.

- Tare the balance.

- Invert carrier bottle a few times to homogenize the solution. Be sure drops of condensation around the lid are taken up and mixed in. Weigh the carrier bottle and confirm that it equals the final weight from the previous use. Record this weight in both the log and your notebook.

- Remove the cap and pipette ^{9}Be carrier into your sample. Use the "Carrier only" 100 – 1000µL pipette and MAKE SURE THE PIPET IS SET AT THE CORRECT VOLUME!

- Immediately recap the carrier bottle and reweigh it. Work quickly, but carefully. Do not leave the carrier bottle open longer than necessary. We want to reduce evaporation as much as possible.

- Check the pipette tip to ensure that the entire amount removed from the bottle, which is what we are weighing, is delivered to your sample and no drops were left behind in the tip.

- If a drop remains in the pipette tip, remove the pipette tip and rinse it out with some MQ-H_2O directly into the sample beaker. Discard the tip and use a new tip.

- Reweigh the carrier bottle and record the weight. Calculate the amount of carrier added to your sample as you go along to ensure you have added the amount of carrier you think you have added.

- When finished, check that the carrier bottle cap is screwed on firmly and seal with Parafilm.

- Record all final weights in the Log Book and in your notebook. Record which carrier you used.
- All of the necessary data (sample and carrier weights) must end up in the database and a printed copy should be taped into the lab book.
- Print the chemistry tracking sheet and tape it to the bench in the Al-Be lab.

Blanks

Roseanne says:
The primary use of blank is to correct the sample ^{10}Be concentration for any ^{10}Be contamination occurring during the sample preparation.

As a general rule, prepare 1 blank per 8-10 samples if all samples are of similar size and are spiked with the same amount of carrier and you expect they will go through the exact same column chemistry. If sample weights should vary by a factor of 3, make up 2 blanks, one to represent small samples and one for large samples, or if you know or even just suspect some of your samples will require more column chemistry, prepare an extra blank.

The blanks are treated exactly like a sample. Use the same size Savillex jar as you used for your samples, rinse the sides down w/ MQ-water as you did for the quartz, and add the carrier in the exact same manner. Prepare blanks at the same time you weigh out and spike samples.

Sample Dissolution

SAFETY INFORMATION*: You will be using very large volumes of concentrated HF in this step. Follow all safety precautions. Do not work alone in the lab while pouring large volumes of HF. The sample may react upon addition of concentrated HF, so add the HF slowly and use extra caution with a large sample. Do not swirl your samples for a few hours.*

Don gloves, sleeve guards, face shield, and apron. Weighed and spiked samples are taken to the hood. In the fume hood, for each sample:

- Add ~5 ml HF per gram of quartz from the bottle-top dispenser. (Reagent A.C.S. grade is ok)

- Screw the caps on the beakers, loosely at first, to allow for any release of gas if the samples are reactive. After a few hours, tighten the lids.
  Roseanne says: If quartz is clean, samples will not react when HF is added.

- If you have the time, just let the samples sit until they're dissolved, rather than putting them on a hotplate. It's the easiest and cleanest way to handle them. You eliminate having to deal with condensation on the lids, and the deposition of silica and fluoride salts on the lid. *A 5 gram sample will dissolve in about a day while a 50 gram sample will need several days. Swirling them several times/day helps. Make sure the caps are on tightly! Wear full protective gear including face shield when handling the bottles*

You can speed the dissolution up with heat, but first allow the samples to sit overnight before placing them on the hotplate. You can heat them initially with the lids off and at a very low temperature (~125 °F) for a few hours so you are sure they won't react violently. Then, put the lids on tightly and turn the heat up to ~300 °F. It is the combination of heat and pressure that really speeds things up. It is important that you used a large enough jar so there is enough headspace to accommodate the buildup of pressure.

Note: Savillex Teflon melts at 260 °C (500 °F). Keep the temperature below 220 °C (420 °F).
(The pancake griddles should not get this hot)
DO NOT put Savillex containers on the ceramic hotplate

If you are measuring Al, this is where you would take a split for stable Al measurement. Otherwise, continue with the dry down.

Evaporation & Dry Down w/ HCl

Once the samples have dissolved, or are nearly dissolved, you will evaporate off all the HF. Fe, Ti, Al, Be, and other ions are left as chloride salts ready for anion exchange clean up. Drying down the solutions eliminates F^- and Si via the reactions:
$H_2SiF_6(l) \rightarrow (heating) \rightarrow SiF_4(g) + 2HF(g)$ and $HF(l) \rightarrow (heating) \rightarrow HF(g)$

- Open beakers, rinse droplets off of lids into jars with MQ-water
- Place the vessels on the hotplate and evaporate at ~400 °F
  If leaving overnight, turn hotplate down to ~300 °F

VERY IMPORTANT! Until the sample is completely dissolved, do not spill a drop! If you lose any solution at this point you are preferentially losing ^{9}Be (the carrier). Once the sample has completely dissolved, ^{9}Be and ^{10}Be are in equilibrium, and a spill will not affect the 10/9 ratios.

Small vessels that contain < 100 ml will dry down in a day. Larger volumes may take two days or more. Sometimes there are minerals that won't dissolve which you'll centrifuge out later.
Place a sign on the front lab door indicating that a HF evaporation is in progress.

Chloride Conversion

- Once all HF is evaporated, remove the Savillex jars from the hotplate and cool slightly before adding HCl.
  Note: HCl tends to splatter when added to a very hot beaker.

- Add ~2-3 ml 6M HCl (amount not critical). Wet all sample and dry down again at ~275 °F.
  Use the larger amount for samples with a very large residue. Rinse down the sides of the beaker with the HCl addition and/or a little MQ-water. The residue should re-dissolve almost instantaneously.
  Samples can be moved to recirculating hood after first HCl conversion

- Repeat the HCl addition (using ~2-3 ml 6M HCl) and evaporation step 2 more times (for a total of three HCl additions).

- Cool the samples completely. Then add 2 ml 6M HCl to each sample. Close the lid, and allow them to dissolve.

  Roseanne says: The final solution may be a deep yellow-green color due to $FeCl_3$. Some samples may also have thrown a fine, powdery white precipitate that will not re-dissolve. This is probably TiO_2. No Al or Be is co-precipitated with the Ti and it can be removed by centrifuging before the anion exchange.

Anion Exchange Columns

- Rinse 15-ml centrifuge tubes w/ MQ-water and label them w/ sample ID and "Anion"

- Transfer the samples to the labeled centrifuge tubes. You can pour it in, or transfer with a disposable pipette. If the sample is thick, sticky and full of residue it is easier with a pipette.

- Add another 1 ml of concentrated 6M HCl to the jar as a rinse and transfer to the centrifuge tube. There should be 3 ml in the tube. Samples are now ready for Anion columns.

The anion exchange columns remove Fe^{III} (and some Ti) in the sample.

Resin = AG-1 X8 200-400# mesh. This procedure uses 3 ml of resin (=filled to the 4cm mark)

The anion columns can be reused many times. Inspect the columns before use. When the anion resin gets too old it will take on a darker color and/or contains bubbles in it. If you need to repack columns, follow the procedure for column packing (see Appendix).

**You can reuse the Savillex jars you dissolved your sample in if they are 90 ml or smaller, and if they are clean. Sometimes the digestion leaves black residue behind. This can be wiped out w/ a KimWipe, but should then be followed by a quick leach w/ some dilute HCl or HNO3 (~5% is fine) on the hotplate. Use a new clean KimWipe for each jar.*

Prep SAMPLES:

- Centrifuge the samples for 10 minutes at 3500 RPM to remove solids.

Prep COLUMNS:

- Place waste containers under columns and drain water from columns. Discard water
- Examine resin for bubbles and look on top for dirt from previous samples
- Add 15 ml 1.2M HCl (fill headspace 1 ½ times). This washes the resin
- Add 9 ml 6M HCl (fill headspace 1x). This conditions of the resin

Anion Exchange Columns

COLLECT Beryllium fraction:

- Place labeled 30 ml Savillex vials (or 90ml Savillex) under columns.

- Load samples with disposable pipette. Use a new pipette for each sample. Drip the solution down the column wall, reaching as far as possible into the column with the pipette. Do NOT pour the sample into the column. Try not to disrupt the top surface of the resin. Allow them to drain through completely.

(Elute the Beryllium fraction with a total of 9 ml 6M HCL added in 3 aliquots – 3x resin volume, allowing the acid to drain through before the next addition.

- Add 1 ml 6M HCL
- Add 4 ml 6M HCL
- Add 4 ml 6M HCL

Clean columns:
Strip of Fe & Discard (you don't need to keep this)

- Replace waste containers
- Add 9 ml 1.2M HCl
- Add 9 ml MQ-water
- fill columns with MQ-water, cap, and store

John says: In strong HCl, Fe(III) forms a range of anionic Cl^- complexes $FeCl_4^-$, $FeCl_5^{2-}$ and $FeCl_6^{3-}$, which bind tightly to the anion exchange resin. These will form a yellow-brown band at the top of the resin column. Al and Be do not form strong Cl^- complexes and elute from the column with the HCl. Some Ti in the form of $Ti^{(IV)}Cl_6^{2-}$ will bind, but most will drain through as cationic or neutral species, ending up with the Al + Be.

Sulfate Conversions

- Add 1 ml of **0.5M H_2SO_4** to each Be/Al fraction and dry-down at ~275 °F. This will take ~ 4-6 hours. NEVER EXCEED THIS VOLUME OF H_2SO_4! *The dried residue from this step may turn an alarming dark-brown to black color due to organics which bled from the anion resin. Don't worry - it will disappear over the next couple of steps.*
  Note: Do NOT add peroxide with the sulfuric acid in this step as it will form Cl gas!

- Once dried down, cool the beakers and add 2 drops of **~2% H_2O_2** (hydrogen peroxide) (if using 30% H_2O_2, just use the smallest drop you can – though note that 30% H_2O_2decreases strength rapidly with time - we used 2 drops of 30% for a year-old bottle). Then add **2-3 ml of MQ-water** with disposable pipette. *The cakes will begin to dissolve, taking on an amber/gold - red color ($TiO[H_2O_2])^{2+}$) if Ti is present. Reheat the vials. The black charry material will disperse and disappear after a while. Dry the samples down again. Red may creep up walls.*

- Cool, repeat the **H_2O_2/water (2 drops ~2% H_2O_2+ 2-3 ml of MQ-water)** addition, and dry the samples a second time. At the end of this procedure, the samples should end up either as compact white cakes or small, syrupy droplets of involatile H_2SO_4. *Samples may be slightly yellow. If they remain charry or dark-colored, repeat the peroxide/water addition and dry them down a third time.*

- Take the samples up in **4 ml of MQ water**, containing a couple drops of **30% H_2O_2**or trace of 2% H_2O_2. *Warm them a little if necessary to get them back in solution. Don't risk evaporating too much water - keeping the acid strength low for column loading gives a sharper elution and cleaner Ti-Be cut. The samples are now in ~0.2 M H_2SO_4, ready for loading on the cation exchange columns. They can be stored indefinitely in this form.*

John says: Ca^{2+} can be problematic during sulfate conversion (before cation columns) because crystalline calcium sulfate ($CaSO^4$ – same composition as gypsum) may form, which is difficult to re-dissolve. Also, during cation exchange, Ca^{2+} (and other cations) compete for adsorption sites with other cations and causes cations to elute faster (e.g. Ti may elute with only 4-5 ml of acid rather than 10 ml, and Be elutes right after Ti).

John says: The cation column separates Al, Be and Ti. The column procedure using 2 ml of resin can handle 3-5 mg of Ti, if the total amount of Al and other metals is less than 3-5 mg. The method easily scales up and the volume of resin can be doubled or tripled.

Cation Exchange Columns

COLUMN SETUP

If reusing columns, simply setup and drain, if not reusing columns, follow below:

- *Place waste collection cups. Using a disposable pipette, add 2 ml of DOWEX-50 X8 200-400# cation exchange resin to each column. Fill the column with a little MQ-water and before it drains, slurry in a thin suspension of resin. This will immediately slow the dripping, and you can keep the column full with water while you slowly add more resin to the 2 ml mark. Tapping the column can help to get the dripping started. Be very careful not to trap air bubbles.*

STRIPPING & CONDITIONING RESIN:

- Strip the resin by filling each column headspace with 3 M HCl (This is 9 ml, equal to 4-5 resin-bed volumes.) Allow it to drain completely.

- Condition first with 9 ml 1.2 M HCl. Drain completely.

- Make up a beaker of 0.2 M H_2SO_4 containing a few drops of 30% peroxide (or trace of 2% H_2O_2.)
  This is 4 parts 0.5 M H_2SO_4 to 6 parts MQ water
  (**75 ml MQ-water + 50 ml 0.5M H_2SO_4 + 3 drops H_2O_2** works well)
  John says: Can use roughly 50-50 solution. *Accurate volumes are not important; the aim is to match roughly the acid strength of the sample solution.*

- Condition the columns by filling the headspace (9 ml) with above solution. Allow it to drain through.

- Discard any leftover conditioning acid in the waste container, and replace it with **0.5 M H_2SO_4 containing a dash of 2% H_2O_2.** (about 0.5 ml peroxide to 50 ml acid). Remove waste containers and discard waste in acid-waste container.

Cation Exchange Columns

ELUTE Ti:

- Place labeled 60 ml Nalgene ("Ti/Al Fraction") bottles under columns.

- Load each sample onto its column using a clean disposable pipette. Ti will form a narrow brown band at the top of each resin bed, and then begin to move down the columns. Allow the sample to run into the resin completely.

- Add 1 ml of **0.5 M H_2SO_4 w/ trace 2% H_2O_2** to each beaker as a rinse. Swirl the beakers to pick up any droplets of the original solution left over from the first load. Add the rinse solutions to the columns after they have drained. Allow this to run in completely.

You will add 10 ml (5 bed volumes) of **0.5 M H_2SO_4 w/ trace 2% H_2O_2** to each column in three additions (4 ml + 4 ml + 2 ml). If Ti is present, you can see the Ti band move down the resin and elute from the columns. For samples containing Ti but very little Al, the Ti will elute slower and it may be necessary to add another 1 – 4 ml to completely remove Ti.

- Add 4 ml **0.5 M H_2SO_4 w/ trace 2% H_2O_2**.
- Add 4 ml **0.5 M H_2SO_4 w/ trace 2% H_2O_2**. Allow first 8 ml to drain through completely.
- Add 2 ml **0.5 M H_2SO_4 w/ trace 2% H_2O_2**. Drain.
- Add additional **0.5 M H_2SO_4 w/ trace 2% H_2O_2** in <u>1 ml</u> increments to completely remove Ti.
- Repeat above step until columns are no longer dripping yellow and eluate is clear

Roseanne says: You can safely elute until the eluate is clear. If the drips are immediately yellow, the column is probably overloaded with Al. Take note of this, but continue on. You will probably have to do a second column to clean up the sample. If you suspect an overload, still add 10 ml of 0.5 M H_2SO_4 w/ trace 2% H_2O_2 to the columns.
John says: 12 ml of the sulfuric acid eluent can be run through the columns without risk of losing Be. Yellow drips start with the first Ti - this shouldn't be immediate upon adding the acid. Drip will go clear when Ti is gone. Do not add >14 ml.

Make a note in your notebook how many mls is took to elute the Ti, how dark or light, narrow or broad the Ti band is, and when it started dripping yellow.

- Remove Ti/Al Fraction bottles

Cation Exchange Columns

ELUTE Be:

- Place 30 ml labeled Savillex teflon vials under each column. Reuse from before.
- Add 10 ml (5 bed volumes) of 1.2 M HCl ("10%" HCl). This will have to be added in 2 lots. There is no need to allow the first to drain completely before adding the second. Allow it to drain through completely.
- Elute Blanks with 12 ml 1.2 M HCl (2 additional mls). With no other ions "pushing" the Be through the column, it takes a little more to get the Be out.

ELUTE Al:

- Replace 60 ml Nalgene ("Ti/Al Fraction") bottles under columns.
- Elute Al from the columns with 6 ml (~3 bed volumes) of 3M HCl.

Clean Columns:

- Flush columns with MQ-water
- Fill columns with MQ-water, cap, and store.

Tip: make sure there are clean centrifuge tubes for the next step. Tubes should be washed in dilute nitric - sit about a week, rinsed twice with water and dried in oven.

Beryllium Recovery

Dry down

- Add ~5 drops of 7.5 M HNO_3 to each Be sample and dry on a hotplate at 275 °F (will take ~8 hrs. If drying overnight, you can put temp slightly lower)

- Label cleaned 15-ml screw cap centrifuge tubes for each sample.

- Once the Be fractions have dried, cool and remove them from the hotplate. The Be fraction should have contracted to a tiny, clear droplet of concentrated H_2SO_4. *Occasionally they will form a small white cake. This usually indicates the presence of either Ti or Al.*

John says: If the Be sample is troublesome to dissolve, even with heat, additional acid can be added as an aid. A lot of precipitate that won't dissolve implies a problem, likely calcium sulfate. Intractable samples usually can be dissolved with the addition of a lot of extra acid and heat. Such samples almost certainly will need to go back through cation columns again. Check the Ca ppm in the original ICP check. If the original Ca was low, this problem should never materialize.

Transfer to Centrifuge Tubes

- Pipette 2 ml of 1% HNO_3 (TM-grade) into each vial. If pure, the Be fractions will dissolve freely. If they don't, you can warm the vials for a few minutes on the edge of the hotplate with the lid on, or just wait a few hours.

- Carefully pour the solution into a labeled centrifuge tube. Don't worry if a last drop clings to the floor of the Be beaker, but if its large, you can pick it up w/ a disposable pipette.

- Immediately add another 2 ml of 1% HNO_3 into the vial as a rinse, and transfer to the c-tube.

Brenda says: Precipitate, ignite, and pack Al and Be samples shortly before the accelerator run in which they will be measured. Superstition among practitioners hold that Al-and Be-oxides slowly rehydrate if left for weeks or months after baking and will produce lower beam currents. Cathodes packed in advance of a run (or cathodes which have to be stored after a cancelled run) should be stored in the desiccator cabinet in the Al-Be lab.

Beryllium Hydroxide $Be(OH)_2$ Precipitations & Washes

You will precipitate the samples two times, and do 3 washes with a pH adjusted water. This step cleans up your sample and gets rid of Boron contamination. You will see your samples get more clear and translucent with each step.

- Add ~ 250 µl NH_4OH to the centrifuge tube, cap it, and mix well on the vortex mixer. You should see the white $Be(OH)_2$ precipitate swirling around. Using a clean pipette tip for each sample, remove ~ 1 µl to check the pH. It should be close to 9. If the pH is below 8.5, add more NH_4OH (add ~30 µl at a time until you reach the correct pH).
  Roseanne says: If you overshoot and the pH is 10, leave it. It's better a little high than low.

- Centrifuge for 10 minutes at 3500 RPM.

- LOOK AT YOUR SAMPLES CAREFULLY AT THIS POINT and compare the sample Be to the blank Be. <u>They should all be the same size</u>.
  Roseanne says: If the samples are larger than the blank, it indicates Al and you probably need to do a second cation column. If the sample is smaller than the blank, you may have lost Be. But, before you make this assumption, check the pH of the supernatant. If it is just pH 8, try adding more NH_4OH and bring the pH to 9. Centrifuge again. If it is still small, just proceed to the 2nd precipitation. This always improves the clarity and often the size of the precipitate. If the precipitate is still too big (indicating that there is probably Al in the Be fraction) go to the section on preparing a sample for a second column (Appendix).

- Pour supernatants back into labeled 22-ml Savillex Teflon. Be careful not to pour out any precipitate.

- Do a 2nd precipitation: Add 100µl of 7.5M HNO_3 to all your samples. Swirl on the vortex mixer until precipitate has dissolved completely. Bring the volume up to 5-ml with MQ-water. Swirl again on vortex mixer. Re-precipitate $Be(OH)_2$ by adding ~100µl TM NH_4OH. Mix well on the vortex mixer.

- Centrifuge for 10 minutes again at 3500 RPM. Decant supernatant into same rinse bottle.

Roseanne says: After precipitating the $Be(OH)_2$, do not let the samples sit around. Always centrifuge and pour off the supernatant immediately. Impurities in the supernatant may precipitate out of the solution over time defeating the purpose of precipitation and wash steps.

pH 8 RINSES:

Roseanne says: This step presumably gets rid of any Boron-10 contamination, an isobar of ^{10}Be.

- Bring solution volume up to 5 ml with the pH 8 adjusted water (pH8 water is MQ-water w/ few drops NH_4OH). Swirl on the vortex mixer, centrifuge, LOOK!, and decant the supernatant into the rinse bottles. Do three pH 8 rinses in total.

$Be(OH)_2$ Combustion

Transfer Samples to Quartz crucibles

- Set up clean crucibles in the Quartz sled, and on the sled, write the sample ID next to the crucible. If possible, do not fill all 10 positions on the sled, and make a diagram in your notebook with the position of each sample in the sled. *Samples located over sled legs may take slightly longer to dry-down on hotplate.*

- Dissolve the $Be(OH)_2$ in the C-tubes with 25 µl 7.5M HNO_3.
  Good place to pause overnight or longer.

- Swirl on the vortex mixer.

- Bring up to speed in centrifuge (3500 RPM @ 0 seconds) to ensure all liquid is collected.

- Transfer to the crucible using the 200 µl pipette.
  Reach all the way into crucible with pipette tip, try not to get liquid on sides of crucible

- With another pipette, add another 25 µl 7.5M HNO_3 as a rinse. Pick this up w/ the same pipette you used for the sample transfer, and add this to the crucible. Use a new pipette tip for each sample. Cover all crucibles with lids except the one into which sample is being transferred.

Hotplate Dry-Down

After all samples have been transferred to the crucibles, place the sled on ceramic hotplate in the fume hood with crucible and sled covers off. Begin with a low temperature. You want the sample to dry on the bottom of the crucible and heating it too fast can result in it drying around the sides making it more difficult to get the sample out of the crucible after its been combusted. Suggested times:

- 200 °C for 15 minutes
- 250 °C for 75 minutes
- 300 °C for 150 minutes
- 350 °C for ~30+ minutes (until dry)
- 400 °C for 15 minutes (once dry)

Samples will likely form small white cakes at the bottom of crucible. Samples may dry-down without forming white cakes, in which case the sample is very difficult to see. Don't worry, it is not lost! Assuming all transfers went well, the $Be(OH)_2$ will appear after combustion.

Cobust Samples

- Fetch a propane torch from the flammable cabinet,
- Set up torch, ring stand, and crucible tongs in the fume hood
- Light the torch.
- After removing the crucible covers from the vial, grasp the vial with the tongs about halfway up. Wave the crucible through the flame cautiously at first (if not completely dry, sample may sputter and bubble up if heated too fast). Once the sample begins to glow orange, hold it in the flame for 30 to 40 seconds more. Some samples never glow, in which case 2 minutes is be more than sufficient. Remove it from the heat and place it back in the same spot in the quartz sled in the hood to cool.
- Once cool enough to handle, cover with labeled crucible covers, and store in the recirculating bench for loading. Samples should be loaded as soon as possible after combusting.

Tip: make sure your cathode loading tools are clean for the next step. The cleaning procedures are on the following page.

Loading Cathodes for LLNL

Equipment List

- Cathodes
- Drill Rods, #55
- Stainless Spatulas (scrapers)
- Quartz rods
- Niobium powder
- Scooper
- Cathode holder/stand
- Hammer
- Dust Mask
- Ionizer

Be extremely careful when working with beryllium metal (oxide form). Beryllium is a known health risk and all precautions must be followed when working with it. Always work in the glovebox, and wear a dust mask.

- **Label Cathodes**
  - Make sure you are using cathodes that have been cleaned, and check each cathode to make sure the hole is centered, and is the correct size. We occasionally get cathodes with holes that are too small. Check this with the drill rod.
  - Label the cathode with the sample number, full sample name and LLNL BE#.

- **Clean Drill Rods**
  - If you are starting with new drill rods, you only need to wipe them down with methanol. If you are reusing your drill rods, first wipe them off with methanol. You can rinse them with some water, but dry them off immediately, because they rust easily. Then, clean the ends off with some fine sandpaper (400 or 600 grit). Finally, rinse them off again and wipe them down with methanol.

- **Stainless Spatula's (Scrapers)**
  - These should be cleaned in a 10% nitric solution overnight. They should also get at least 1 hour in the ultrasonic bath. Pour off the cleaning acid into the 2nd spatula cleaning acid bottle, and then rinse the spatulas thoroughly. Wrap them well with KimWipes and dry them in the oven.

- **Quartz Rods**
  - These are cleaned in a 20% nitric solution. Follow the spatula instructions. They have their own teflon bottle labelled "glass cleaning".

SET UP IN THE GLOVEBOX

- Wipe down the glovebox with MQ-water thoroughly.
- Place ionizer in the glovebox
- Set up your tools on a clean KimWipe.
- Set up the cathode holder on a KimWipe.
- Set up the following waste containers:
  - Be-waste plastic bag for used crucibles, KimWipes, and gloves.
  - A waste cup with isopropanol for the used drill rods
  - A waste cup with MQ-water for the used spatulas, quartz rods
  - A waste cup with MQ-water for the used crucible covers
- You will need the tiny scoop and niobium powder and a hammer. Wipe off the hammer with some isopropanol first.
- Put on clean gloves and sleeves, and close the sample door from the inside. You'll be here for a while, so you might want to grab a stool.

LOADING THE CATHODE

- Place the cathode on the holder
- Fetch the next crucible and take the lid off.
- Add 2 level scoops niobium. You can adjust this up or down for larger and smaller samples.
- Using the quartz rod first, gently mix the niobium into the sample. Once the Niobium is mixed in, static is usually not a problem, but before that, the Beryllium can be rather flaky.
- Grind the Niobium and Beryllium together, as you would grind something up with a mortar and pestle.
- Using the stainless steel scraper, scrape together the mixture into the bottom.
- Repeat the quartz rod grinding and scraping a few times.
- When the sample is fully homogenized, use the scraper to collect it into the bottom. You can also tap the crucible on your work surface to get it to collect.
- Carefully tilt the crucible on the edge of the cathode, at a 45 deg. angle or so, and gently tap the crucible, and the cathode with the scraper. This will cause it to pour down onto the cathode. If it doesn't slide right into the hole, simply tap the sides of the cathode. It will.
- Using the drill rod, hammer the sample into the hole. Hammer hard for about 20 taps, then remove the drill rod, take the sample off the holder and tap it a few times on the holder. Then hammer another 20 pretty hard taps. Repeats the hammer followed by tapping a total 3 times, and finish off with about 10 more gentle taps. ~70 total hammer taps!
- You can gently turn the cathode upside down on the clean KimWipe to check that it isn't going to spill out.
- Store the cathode in a labeled storage vial, and double check that all your labels are correct.
- Wipe down your work area before loading the next cathode.
- Store samples in desiccator until they are shipped to LLNL.

Notes:

Preparing Resin and Packing Columns

Resin Preparation

- Soak the resin in 6M HCl in the designated bottle. After a few hours, decant the HCl into a waste container. Fill the bottle w/ MQ-water, shake and decant after the resin has settled. This will take a couple of hours. Do this 2-3 more times so that it is no longer strong acid.

Packing columns with resin

- Before filling the columns with resin, fill the column with water and make sure it drips. Usually tapping the column up and down a few times breaks the surface tension and it'll begin to drip. Or, squirt in a few drops of methanol before adding water.

- Then, fill the column with MQ-water and using a disposable pipette immediately add some resin from the batch soaking in MQ-water. The initial resin will settle onto the frit and immediately slow the water dripping through. Keep the water volume full while you add the resin. The resin should settle out gradually and evenly as it is added thus avoiding air bubbles getting trapped in the resin bed. Continue to add resin to the column until the proper volume is reached. If you do get air bubbles, fill the column with some water and suck up the resin with the pipette to re-suspend it and usually it will resettle without bubbles.

You've overloaded a column! Preparing samples for a 2nd Cation Column

- You still have to precipitate the sample. This is the only way to remove the sulfuric acid. So, do that, and note the volume of precipitate.
- Dissolve the BeOH precipitate in 2ml of 3M HCl and transfer it back to a Teflon beaker.
- Then follow the normal procedure for Sulfate Conversions.

Table A.1. Acid strengths.

Chemical	Molecular Formula	Approx. Strength of Concd. Reagent	Molarity of Concd. Reagent
Hydrofluoric Acid	HF	49.0 %	28.9
Hydrochloric Acid	HCl	37.2 %	12.1
Nitric Acid	HNO_3	70.4 %	15.9
Sulfuric Acid	H_2SO_4	96.0 %	18.0
Ammonium Hydroxide	NH_4OH	56.6 %	14.8

DOUBLE CATION COLUMN – (4ml resin)

- Use the larger columns.
- Fill w/ 4 ml resin. *Note, that these columns are marked w/ height in cm., and not volume. 4 ml is just under the 6 cm. mark.*

STRIPPING & CONDITIONING RESIN:

- ~ 18 ml 3 M HCl (Fill to the top twice.) Allow it to drain completely.
- ~ 18 ml 1.2 M HCl. Drain completely.
- ~ 18 ml 0.2 M H_2SO_4 containing a trace of 2% H_2O_2. Drain.

Remove waste trays and discard acid into waste containers.

ELUTE Ti:

- Place 60 ml rinsed and labeled ("Ti/Al Fraction") bottles under columns.
- Load each sample onto its column using a clean disposable pipette. YOU STILL LOAD in 4 ml. Allow to soak into the resin completely.
- Add 1 ml 0.5 M H_2SO_4 containing a trace of 2% $H_2O_2$to each beaker as a rinse and add to the column.
- Add 18 ml of 0.5 M H_2SO_4 w/ trace 2% $H_2O_2$to each column. It may be necessary to add a further 4-5 ml of 0.5 M H_2SO_4 to completely remove Ti. Note how much you use.

ELUTE Be:

- Place 22 ml labeled Teflon vials under each column.
- Add exactly 20 ml of 1.2 M HCl ("10%" HCl).

ELUTE Al:

- Place 15-ml bottles under each column to collect the Al fraction. Add 12 ml of 3M HCl.

APPENDIX B

ICP-OES RESULTS

Table B.1. ICP-OES results for quartz used in surface-exposure dating.

ID	Al (ppm)	Be (ppm)	Ca (ppm)	Fe(ppm)	Ti (ppm)
TGP-16-01	238	0.046	165	108	75
TGP-16-02	230	0.125	173	207	72
TGP-16-03	270	0.050	100	178	123
TGP-16-07	243	0.140	126	292	86
TGP-16-08	227	0.077	101	114	54
TGP-16-09	224	0.125	165	105	81
TGP-16-10	270	0.099	136	60	75
TGP-16-12	209	0.000	162	41	65
TGP-16-13	199	0.050	269	245	83
TGP-16-14	243	0.075	152	94	101
TGP-16-16	262	0.043	122	89	95
TGP-16-18	211	0.026	40	33	65
TGP-16-19	220	0.036	63	41	70
TGP-16-30	222	0.038	52	33	75
TGP-16-31	202	-0.006	104	33	68
TGP-16-32	230	-0.011	89	38	69
TGP-16-35	205	0.037	178	52	66
TGP-16-36	211	0.061	117	32	66
TGP-16-37	225	0.044	128	82	71
TGP-16-38	269	0.118	88	69	74
TGP-16-39	210	0.049	115	34	69
TGP-16-40	178	0.041	165	55	48
TGP-16-51	225	0.060	150	72	74
TGP-16-52	191	0.063	218	23	63
TGP-16-53	217	0.113	225	147	92
TGP-16-56	306	0.086	112	61	60
TGP-16-57	239	0.076	121	32	60
TGP-16-59	278	0.110	119	149	193
TGP-16-60	269	0.000	23	139	19
TGP-16-61	298	0.132	117	52	65
TGP-16-62	365	0.132	157	69	78
TGP-16-65	223	0.127	104	50	78
TGP-16-66	273	0.151	97	107	70
TGP-16-67	258	0.099	99	91	84
TGP-16-68	255	0.043	167	44	67
TGP-16-69	247	0.107	227	80	81

Table B.1. Continued.

TGP-16-70	233	0.071	100	49	76
TGP-16-71	192	0.071	46	66	40
TGP-16-73	182	0.133	4	5	45
TGP-16-74	223	0.119	122	50	69
TGP-16-75	248	0.118	95	98	80

APPENDIX C

SAMPLE CATALOG

Appendix C is catalog of all boulders sampled from the Tsagaan Gol-Potanin Glacier valley (TGP). Of the 76 samples collected, 41 were processed for surface-exposure dating. The form includes latitude, longitude, elevation, boulder dimensions, shielding values, dip, and dip direction of the sample site. Also included are photographs of each sampled boulder and a description of boulder and geomorphic setting. For pages describing processed samples, the form includes the ^{10}Be age and shielding values.

Mongolia Exposure Sample Descriptions

TGP-16-01

Boulder Dimensions (cm):

Length:	750
Width:	605
Height N:	180
Height E:	150
Height S:	170
Height W:	150
Height Avg.:	162.5

Latitude (°):	49.09520
Longitude (°):	88.14508
Elevation (m a.s.l.):	2404.615
Ridge Location:	West of Holy Mountain

Exposure Age (ka):

22.67 ± 0.43

Date: 7/6/2016

Personel: MJR & team

Shielding:

Dip (°):	16
Dip Dir. (°):	294
Correction:	0.99245

Azimuth (°):	Inclination (°):
0	17
21	10
45	4
65	3
76	10
102	7
129	11
164	16
181	12
215	7
221	4
234	5
259	5
278	4
311	17
333	19
341	15
346	17

Sample Views:

Very large granite boulder embedded in flat recessional ground moraine; boulder polished on several sides; sample taken from lower dipping surface, slightly pitted; some evidence of sheet water on top of boulder below sample.

Mongolia Exposure Sample Descriptions

TGP-16-02

Boulder Dimensions (cm):

Length:	290
Width:	290
Height N:	100
Height E:	70
Height S:	60
Height W:	110
Height Avg.:	85

Latitude (°):	49.09529
Longitude (°):	88.14750
Elevation (m a.s.l.):	2420.374
Ridge Location:	West of Holy Mountain

Exposure Age (ka):

15.69 ± 0.30

Date: 7/6/2016

Personel: MJR & team

Shielding:

Dip (°):	12
Dip Dir. (°):	90
Correction:	0.99335

Azimuth (°):	Inclination (°):
0	5
15	8
45	4
68	0
72	12
102	10
139	15
175	18
215	6
240	9
250	4
260	5
265	3
273	6
281	5
316	15
333	19
343	16
350	17

Sample Views:

Medium granite boulder embedded in ground moraine in hummocky terrain; many cobbles surrounding boulder; south side varnished and some flaking on top of boulder; sample surface polished and quartz vein flush with rock near sample.

Mongolia Exposure Sample Descriptions

TGP-16-03

Boulder Dimensions (cm):

Length:	100
Width:	95
Height N:	30
Height E:	40
Height S:	40
Height W:	50
Height Avg.:	40

Latitude (°):	49.08736
Longitude (°):	88.15555
Elevation (m a.s.l.):	2673.023
Ridge Location:	West of Holy Mountain

Exposure Age (ka):

18.23 ± 0.34

Date: 7/6/2016

Personel: MJR & team

Shielding:

Dip (°):	22
Dip Dir. (°):	240
Correction:	0.98701

Azimuth (°):	Inclination (°):
0	2
20	6
50	4
60	6
90	4
170	20
193	19
209	16
225	6
235	6
240	3
265	5
291	3
315	6
356	6

Sample Views:

Small granite boulder on till-mantled greywacke bedrock shallowly embedded in the till; located next to bedrock ridge above valley floor; sample is polished with lots of lichen.

Mongolia Exposure Sample Descriptions

TGP-16-04

Boulder Dimensions (cm):

Length:	230
Width:	110
Height N:	135
Height E:	90
Height S:	60
Height W:	65
Height Avg.:	87.5

Latitude (°):	49.08513
Longitude (°):	88.15744
Elevation (m a.s.l.):	2763.48
Ridge Location:	West of Holy Mountain

Exposure Age (ka):

Date: 7/6/2016

Personel: MJR & team

Shielding:

Dip (°):	19
Dip Dir. (°):	239
Correction:	

Azimuth (°):	Inclination (°):
0	6
7	7
27	5
31	6
36	3
48	3
50	4
60	12
71	11
84	9
88	2
119	14
133	25
175	19
226	11
259	11
275	5
291	4
294	2
308	5
334	6
354	5

Sample Views:

Large granite boulder shallowly embedded in till-mantled bedrock ridge, higher elevation than TGP-16-03; boulder located off the top of the ridge; top of boulder pitted so sampled lower dipping surface; sample polished and varnished.

Mongolia Exposure Sample Descriptions

TGP-16-05

Boulder Dimensions (cm):

Length:	135
Width:	102
Height N:	28
Height E:	22
Height S:	19
Height W:	27
Height Avg.:	24

Latitude (°):	49.08552
Longitude (°):	88.15350
Elevation (m a.s.l.):	2718.437
Ridge Location:	West of Holy Mountain

Exposure Age (ka):

Date: 7/6/2016

Personel: MJR & team

Shielding:

Dip (°):	25
Dip Dir. (°):	283
Correction:	

Azimuth (°)		Inclination (°)	
0	27	7	4
31	43	4	1
48	55	2	4
58	61	6	6
69	70	5	6
76	82	4	3
103	129	14	20
137	151	22	21
163	175	23	24
184	197	21	20
224	226	6	7
231	237	6	3
243	244	2	4
249	254	3	4
256	276	4	3
292	305	3	5
312	329	5	6
354		6	

Sample Views:

Small granite boulder well embedded in moraine on top of hill; boulder low to the ground; sample polished and varnished.

Mongolia Exposure Sample Descriptions

TGP-16-06

Boulder Dimensions (cm):

Length:	250
Width:	218
Height N:	115
Height E:	98
Height S:	117
Height W:	98
Height Avg.:	107

Latitude (°):	49.09391
Longitude (°):	88.17165
Elevation (m a.s.l.):	2582.759
Ridge Location:	Holy Mountain

Exposure Age (ka):

Date: 7/7/2016

Personel: MR NN PS AP KS

Shielding:

Dip (°):	40
Dip Dir. (°):	279
Correction:	

Azimuth (°):	Inclination (°):
0	10
14	9
23	6
39	10
48	8
64	19
69	18
91	19
101	15
110	14
111	13
117	10
125	5
156	4
169	7
197	6
208	11
215	10
225	8
230	6
234	7
237	3
260	4
280	4
291	7
321	9

Sample Views:

Medium, angular granite boulder well embedded in moraine; off of ridge that divides flow around Holy Mountain; boulder next to animal hole; lots of lichen on boulder and some exfoliation and pitting at top of boulder; sample taken from dipping slope with polished grains.

Mongolia Exposure Sample Descriptions

TGP-16-07

Boulder Dimensions (cm):

Length:	280
Width:	200
Height N:	75
Height E:	80
Height S:	100
Height W:	80
Height Avg.:	83.75

Latitude (°):	49.09411
Longitude (°):	88.17302
Elevation (m a.s.l.):	2591.422
Ridge Location:	Holy Mountain

Exposure Age (ka):

15.95 ± 0.34

Date:	7/7/2016
Personel:	PS MR NN AP KS

Shielding:

Dip (°):	20
Dip Dir. (°):	131
Correction:	0.98783

Azimuth (°)		Inclination (°)	
0	29	9	11
36	44	14	16
57	64	19	21
68	73	24	23
80	87	22	22
99	105	15	15
107	115	14	12
119	123	9	5
157	163	3	4
167	190	7	8
196	202	12	7
213	224	9	6
227	236	5	3
243	253	4	5
260	261	3	2
283	302	5	7
305	339	9	9
356		8	

Sample Views:

Medium, well-rounded granite boulder well embedded in moraine on west ridge of Holy Mountain; animal hole near base of boulder; sample has polished grains.

Mongolia Exposure Sample Descriptions

TGP-16-08

Boulder Dimensions (cm):

Length:	270
Width:	260
Height N:	90
Height E:	110
Height S:	140
Height W:	110
Height Avg.:	112.5

Latitude (°):	49.09488
Longitude (°):	88.17347
Elevation (m a.s.l.):	2608.136
Ridge Location:	Holy Mountain

Exposure Age (ka):

17.06 ± 0.31

Date:	7/7/2016
Personel:	MR NN PS AP KS

Shielding:

Dip (°):	5
Dip Dir. (°):	0
Correction:	0.99392

Azimuth (°):		Inclination (°):	
0	12	9	8
13	15	10	7
16	23	7	11
26	34	9	12
41	84	11	25
90	94	22	19
109	123	15	9
130	155	5	4
160	171	7	7
202	209	6	8
217	219	8	10
225	233	6	5
240	265	3	5
282	291	4	7
320		10	

Sample Views:

Large quartzite boulder on till-mantled bedrock ridge of Holy Mountain; bedrock composed of greywacke; on flat, stable ground; side of boulder exfoliating and top is polished; boulder has a water filled depression below where the sample was taken; sample is polished and varnished.

Mongolia Exposure Sample Descriptions

TGP-16-09

Boulder Dimensions (cm):

Length:	170
Width:	130
Height N:	120
Height E:	92
Height S:	113
Height W:	130
Height Avg.:	113.75

Latitude (°):	49.09494
Longitude (°):	88.17373
Elevation (m a.s.l.):	2613.000
Ridge Location:	Holy Mountain

Exposure Age (ka):

16.08 ± 0.26

Date:	7/7/2016
Personel:	MR NN PS AP KS

Shielding:

Dip (°):	16
Dip Dir. (°):	72
Correction:	0.99214

Azimuth (°)		Inclination (°)	
0	17	10	5
26	30	7	4
53	76	10	22
84	94	25	21
100	109	19	15
115	122	11	9
127	151	4	2
156	161	4	3
167	200	5	5
209	222	8	4
236	252	3	4
258	273	3	3
278	292	2	7
300	337	5	8

Sample Views:

Medium granite boulder on ice-molded bedrock with many striations; uphill from TGP-16-08; stable position; lichen covering boulder; exfoliation on top of boulder; sample polished and varnished.

Mongolia Exposure Sample Descriptions

TGP-16-10

Boulder Dimensions (cm):

Length:	190
Width:	180
Height N:	80
Height E:	70
Height S:	80
Height W:	80
Height Avg.:	77.5

Latitude (°):	49.09385
Longitude (°):	88.18276
Elevation (m a.s.l.):	2797.074
Ridge Location:	Holy Mountain

Exposure Age (ka):

37.78 ± 0.62

Date: 7/7/2016

Personel: NN MR PS AP KS

Shielding:

Dip (°):	10
Dip Dir. (°):	195
Correction:	0.99880

Azimuth (°):	Inclination (°):
0	6
14	4
39	7
51	8
59	11
84	10
89	9
126	8
136	4
159	4
162	5
180	3
195	4
200	5
225	3
234	5
240	2
264	3
289	3
317	6
329	5
350	7

Sample Views:

Medium granite boulder on till mantled bedrock on low-angle ramp of Holy Mountain; no bedrock exposures near sample; boulder polished on multiple sides and top pitted; sample has polished grains and is mildly pitted.

Mongolia Exposure Sample Descriptions

TGP-16-11

Boulder Dimensions (cm):

Length:	350
Width:	310
Height N:	140
Height E:	130
Height S:	155
Height W:	135
Height Avg.:	140

Latitude (°):	49.13919
Longitude (°):	87.96282
Elevation (m a.s.l.):	3007.476
Ridge Location:	Outboard of Potanin moraines

Exposure Age (ka):

Date: 7/9/2016

Personel: NRN PDS MJR AEP KCS

Shielding:

Dip (°): 12

Dip Dir. (°): 222

Correction:

Azimuth (°):	Inclination (°):
0	11
121	1
134	3
140	2
164	3
200	8
221	11
241	11
249	5
267	9
288	5
295	8
311	6
321	9
350	11

Sample Views:

Large granite boulder embedded in till on grassy terrace north of Potanin Glacier; standing water near sample; some exfoliation on boulder and multiple polished surfaces; sample taken from flat, well-polished surface.

Mongolia Exposure Sample Descriptions

TGP-16-12

Boulder Dimensions (cm):

Length:	240
Width:	225
Height N:	55
Height E:	65
Height S:	90
Height W:	100
Height Avg.:	77.5

Latitude (°):	49.13869
Longitude (°):	87.96374
Elevation (m a.s.l.):	3008.439
Ridge Location:	Outboard of Potanin moraines

Exposure Age (ka):

15.73 ± 0.29

Date: 7/9/2016

Personel: MJR PDS NRN AEP KCS

Shielding:

Dip (°):	21
Dip Dir. (°):	221
Correction:	0.99193

Azimuth (°):	Inclination (°):
0	12
86	7
118	0
131	4
138	2
162	4
178	5
202	9
222	12
241	11
254	6
266	8
281	5
293	8
305	5
320	8
347	11

Sample Views:

Medium granite boulder well embedded in till located on grassy terrace outboard of Potanin Glacier; one terrace level above TGP-16 -11; boulder covered with lichen, polished, and varnished; top of boulder has pitting; sample taken from lower polished surface.

Mongolia Exposure Sample Descriptions

TGP-16-13

Boulder Dimensions (cm):

Length:	370
Width:	240
Height N:	90
Height E:	110
Height S:	100
Height W:	100
Height Avg.:	100

Latitude (°):	49.13788
Longitude (°):	87.96466
Elevation (m a.s.l.):	3002.784
Ridge Location:	Outboard of Potanin moraines

Exposure Age (ka):

11.18 ± 0.20

Date:	7/9/2016
Personel:	MJR PDS NRN AEP KCS

Shielding:

Dip (°):	20
Dip Dir. (°):	326
Correction:	0.99215

Azimuth (°):	Inclination (°):
0	11
63	10
119	1
133	3
139	2
165	3
178	5
201	8
223	12
236	10
251	6
265	9
276	5
287	5
293	7
299	4
315	9
345	12

Sample Views:

Large granite boulder well embedded in till, located on grassy terrace outboard of Potanin Glacier; on same terrace level as TGP-16-12; some animal erosion near boulder; boulder has lichen, polish, and varnish; top of boulder pitted; sample taken from polished dipping surface.

Mongolia Exposure Sample Descriptions

TGP-16-14

Boulder Dimensions (cm):

Length:	190
Width:	160
Height N:	70
Height E:	70
Height S:	90
Height W:	100
Height Avg.:	82.5

Latitude (°):	49.13658
Longitude (°):	87.96981
Elevation (m a.s.l.):	3013.46
Ridge Location:	Outboard of Potanin moraines

Exposure Age (ka):

16.26 ± 0.37

Date: 7/9/2016

Personel: NRN MJR PDS AEP KCS

Shielding:

Dip (°): 12

Dip Dir. (°): 164

Correction: 0.99817

Azimuth (°):	Inclination (°):
0	10
20	8
93	5
121	1
135	3
144	1
166	5
181	6
204	9
230	11
247	10
253	5
268	8
278	4
289	5
291	6
302	3
319	7
343	10

Sample Views:

Small granite boulder shallowly embedded in grassy terrace outboard of Potanin Glacier and moraines; embedded in northeast side; boulder has polish and varnish; sample taken from polished surface on top of boulder.

Mongolia Exposure Sample Descriptions

TGP-16-15

Boulder Dimensions (cm):

Length:	290
Width:	200
Height N:	100
Height E:	90
Height S:	90
Height W:	100
Height Avg.:	95

Latitude (°):	49.13639
Longitude (°):	87.96998
Elevation (m a.s.l.):	3012.029
Ridge Location:	Outboard of Potanin moraines

Exposure Age (ka):

Date: 7/9/2016

Personel: NRN KCS MJR PDS AEP

Shielding:

Dip (°): 25

Dip Dir. (°): 210

Correction:

Azimuth (°):	Inclination (°):
0	10
77	5
123	0
135	2
144	1
166	2
206	7
228	10
240	8
254	6
269	7
276	4
286	4
290	7
301	4
315	9
351	10

Sample Views:

Large granite boulder resting on top of till on terrace outboard of Potanin Glacier and moraines; boulder on moderate slope with water movement below; boulder has lichen, polish and varnish; boulder resting on cobbles on west side; sample surface polished.

Mongolia Exposure Sample Descriptions

TGP-16-16

Boulder Dimensions (cm):

Length:	540
Width:	410
Height N:	110
Height E:	130
Height S:	120
Height W:	140
Height Avg.:	125

Latitude (°):	49.13736
Longitude (°):	87.97159
Elevation (m a.s.l.):	3034.757
Ridge Location:	Outboard of Potanin moraines

Exposure Age (ka):

18.27 ± 0.28

Date:	7/9/2016
Personel:	NRN AED PDS MJR

Shielding:

Dip (°):	20
Dip Dir. (°):	173
Correction:	0.99338

Azimuth (°):	Inclination (°):
0	12
24	12
35	8
113	1
128	2
138	4
144	2
170	4
182	5
206	8
229	10
244	9
253	5
269	8
278	4
289	4
294	6
300	4
315	9
353	11

Sample Views:

Very large granite boulder embedded in till, located on grassy terrace outboard of Potanin Glacier; terrace flat and boulder stable; boulder has shining polish and varnish; sample take from polished, varnished surface.

Mongolia Exposure Sample Descriptions

TGP-16-17

Boulder Dimensions (cm):

Length:	310
Width:	270
Height N:	85
Height E:	70
Height S:	90
Height W:	70
Height Avg.:	78.75

Latitude (°):	49.13726
Longitude (°):	87.97182
Elevation (m a.s.l.):	3033.819
Ridge Location:	Outboard of Potanin moraines

Exposure Age (ka):

Date:	7/9/2016
Personel:	NRN MJR PDS AEP

Shielding:

Dip (°):	6
Dip Dir. (°):	169
Correction:	

Azimuth (°)		Inclination (°)	
0	20	11	8
50	82	8	4
116	125	0	0
138	144	3	1
167	168	2	3
173	181	1	4
201	206	5	8
208	228	6	10
237	240	7	10
245	248	8	9
254	265	4	6
270	278	8	4
289	292	5	7
295	299	6	6
302	310	5	7
319	350	8	10

Sample Views:

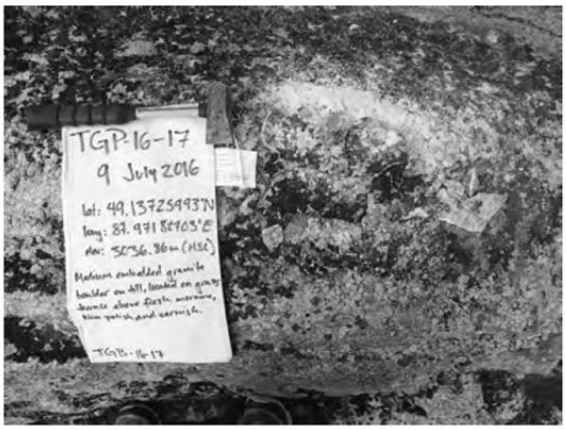

Medium granite boulder embedded in till, located on grass terrace outboard of Potanin Glacier and moraines; boulder on flat stable ground and low-lying; sampled polished and varnished surface from top of boulder.

Mongolia Exposure Sample Descriptions

TGP-16-18

Boulder Dimensions (cm):

Length:	275
Width:	270
Height N:	60
Height E:	70
Height S:	90
Height W:	110
Height Avg.:	82.5

Latitude (°):	49.13710
Longitude (°):	87.97178
Elevation (m a.s.l.):	3031.861
Ridge Location:	Outboard of Potanin moraines

Exposure Age (ka):

16.14 ± 0.21

Date:	7/9/2016
Personel:	NRN MJR PDS AEP

Shielding:

Dip (°):	15
Dip Dir. (°):	131
Correction:	0.99722

Azimuth (°):		Inclination (°):	
0	20	9	7
46	80	7	5
115	127	0	0
137	144	4	1
167	170	2	3
172	176	1	2
180	200	5	5
205	209	8	7
214	227	8	10
237	240	5	9
248	254	9	4
267	279	7	4
290	292	4	7
296	300	7	4
307	309	5	7
317	340	8	9

Sample Views:

Large granite boulder embedded in till, located on grassy terrace outboard Potanin Glacier and moraines; boulder on gentle slope; striations, polish and varnish; sample has polish and varnish.

Mongolia Exposure Sample Descriptions

TGP-16-19

Boulder Dimensions (cm):

Length:	235
Width:	225
Height N:	95
Height E:	90
Height S:	125
Height W:	125
Height Avg.:	108.75

Latitude (°):	49.13722
Longitude (°):	87.97223
Elevation (m a.s.l.):	3034.703
Ridge Location:	Outboard of Potanin moraines

Exposure Age (ka):

17.81 ± 0.27

Date:	7/9/2016
Personel:	NRN MJR PDS AEP

Shielding:

Dip (°):	13
Dip Dir. (°):	122
Correction:	0.99802

Azimuth (°):	Inclination (°):
0	9
17	7
84	3
124	0
128	1
135	3
142	1
168	3
181	5
205	8
221	10
240	9
247	4
268	7
277	4
286	4
293	7
300	4
303	4
327	10
353	10

Sample Views:

Large granite boulder embedded in till on grassy terrace outboard of Potanin Glacier and moraines; boulder on shallowly dipping slope; lichen, polish, and varnish present; sample taken from polished surface on top of boulder.

Mongolia Exposure Sample Descriptions

TGP-16-20

Boulder Dimensions (cm):

Length:	310
Width:	290
Height N:	130
Height E:	125
Height S:	95
Height W:	120
Height Avg.:	117.5

Latitude (°):	49.13674
Longitude (°):	87.97251
Elevation (m a.s.l.):	3030.514
Ridge Location:	Outboard of Potanin moraines

Exposure Age (ka):

Date: 7/9/2016

Personel: MJR PDS NMN AEP

Shielding:

Dip (°): 17

Dip Dir. (°): 238

Correction:

Azimuth (°):	Inclination (°):
0	10
17	7
71	6
122	0
134	2
142	5
149	3
158	1
185	5
195	5
209	9
218	8
231	11
237	9
245	11
250	10
257	6
270	8
276	5
290	5
294	8
298	5
310	6
317	9
344	10

Sample Views:

Large granite boulder embedded in till, located on grassy terrace outboard of Potanin Glacier and moraines; boulder near margin of the terrace; some erosion on southwest side of boulder; pitting and exfoliation on boulder; sample taken from lower, polished surface.

Mongolia Exposure Sample Descriptions

TGP-16-21

Boulder Dimensions (cm):

Length:	180
Width:	100
Height N:	70
Height E:	70
Height S:	70
Height W:	50
Height Avg.:	65

Latitude (°):	49.14341
Longitude (°):	87.95324
Elevation (m a.s.l.):	3035.039
Ridge Location:	Potanin-I

Exposure Age (ka):

Date: 7/10/2016

Personel: MJR & team

Shielding:

Dip (°): 2

Dip Dir. (°): 133

Correction:

Azimuth (°):	Inclination (°):
0	14
25	12
96	2
113	1
126	0
131	3
137	0
160	4
164	2
170	3
174	5
180	4
210	12
222	8
229	12
240	7
294	10
304	4
318	6
343	12

Sample Views:

Small, rounded granite boulder resting on left-lateral Potanin-I moraine ridge; 10 m away from the top of the moraine ridge; boulder low to the ground; boulder polished and no lichen present; sample has polish and quartz vein.

Mongolia Exposure Sample Descriptions

TGP-16-22

Boulder Dimensions (cm):

Length:	144
Width:	94
Height N:	78
Height E:	91
Height S:	63
Height W:	74
Height Avg.:	76.5

Latitude (°):	49.14417
Longitude (°):	87.95175
Elevation (m a.s.l.):	3046.31
Ridge Location:	Potanin-I

Exposure Age (ka):

Date: 7/10/2016

Personel: MJR & team

Shielding:

Dip (°):	4
Dip Dir. (°):	145
Correction:	

Azimuth (°):	Inclination (°):
0	13
28	10
91	1
110	0
130	1
137	2
159	3
173	5
182	7
205	11
216	8
224	12
235	6
256	6
262	9
274	4
289	6
293	9
302	6
317	8
330	12
344	13

Sample Views:

Small, rounded granite boulder resting on left-lateral Potanin-I moraine ridge; on top of ridge and shallowly embedded in till; orange lichen growing on north side of boulder; sample taken from polished surface.

Mongolia Exposure Sample Descriptions

TGP-16-23

Boulder Dimensions (cm):

Length:	231
Width:	105
Height N:	75
Height E:	64
Height S:	52
Height W:	67
Height Avg.:	64.5

Latitude (°):	49.14421
Longitude (°):	87.95169
Elevation (m a.s.l.):	3046.495
Ridge Location:	Potanin-I

Exposure Age (ka):

Date: 7/10/2016

Personel: MJR & team

Shielding:

Dip (°):	8
Dip Dir. (°):	164
Correction:	

Azimuth (°):	Inclination (°):
0	13
24	10
91	0
109	0
125	1
130	2
133	1
138	2
147	1
158	3
171	4
183	7
206	10
216	7
225	12
237	5
238	7
255	6
261	10
269	6
286	5
293	8
303	5
319	7
356	14

Sample Views:

Small, shallowly-embedded granite boulder on left-lateral Potanin-I moraine ridge located on top of ridge; boulder has orange spots of rust, no lichen; boulder rough on top but roughness seems to be original; sample is polished.

Mongolia Exposure Sample Descriptions

TGP-16-24

Boulder Dimensions (cm):

Length:	230
Width:	150
Height N:	83
Height E:	80
Height S:	120
Height W:	120
Height Avg.:	100.75

Latitude (°):	49.14466
Longitude (°):	87.95044
Elevation (m a.s.l.):	3052.079
Ridge Location:	Potanin-I

Exposure Age (ka):

Date: 7/10/2016

Personel: MJR & team

Shielding:

Dip (°):	8
Dip Dir. (°):	253
Correction:	

Azimuth (°):	Inclination (°):
0	14
29	11
92	1
107	0
125	2
128	3
134	1
137	3
164	2
175	4
180	6
203	9
223	12
232	5
238	7
255	6
259	8
274	4
285	5
291	8
300	3
316	7
325	12
341	13

Sample Views:

Medium, rounded granite boulder embedded in left-lateral Potanin-I moraine ridge; 2 meters off of ridge; boulder has polish and small orange lichen; boulder prominent on moraine ridge; sample is polished.

Mongolia Exposure Sample Descriptions

TGP-16-25

Boulder Dimensions (cm):

Length:	206
Width:	120
Height N:	120
Height E:	100
Height S:	120
Height W:	126
Height Avg.:	116.5

Latitude (°):	49.14659
Longitude (°):	87.94726
Elevation (m a.s.l.):	3074.231
Ridge Location:	Potanin-I

Exposure Age (ka):

Date: 7/10/2016

Personel: MJR & team

Shielding:

Dip (°):	17
Dip Dir. (°):	149
Correction:	

Azimuth (°):	Inclination (°):
0	14
31	11
91	2
108	1
127	3
135	3
154	4
175	6
199	11
217	12
230	5
233	7
251	7
256	11
271	5
282	6
289	10
300	6
317	9
351	15

Sample Views:

Medium granite boulder resting on left-lateral Potanin-I moraine ridge; 1 m away from crest of ridge; orange lichen and polish present; sample taken from top polished surface and was hard to retrieve.

Mongolia Exposure Sample Descriptions

TGP-16-26

Boulder Dimensions (cm):

Length:	165
Width:	119
Height N:	115
Height E:	137
Height S:	129
Height W:	119
Height Avg.:	125

Latitude (°):	49.14823
Longitude (°):	87.94423
Elevation (m a.s.l.):	3081.655
Ridge Location:	Potanin-I

Exposure Age (ka):

Date: 7/11/2016

Personel: MR NN PS DW JS KS

Shielding:

Dip (°): 8

Dip Dir. (°): 276

Correction:

Azimuth (°):	Inclination (°):
0	17
20	12
100	2
116	0
120	0
132	2
168	2
176	6
197	9
205	8
218	12
229	5
235	7
239	5
250	8
257	11
262	9
268	8
276	5
289	6
293	10
302	6
321	10
345	16

Sample Views:

Medium, rounded granite boulder resting on left-lateral Potanin-I moraine ridge on crest of ridge, close to steep slope but looks stable; boulder has orange rust spots and small lichen on north side; sample taken from polished surface.

Mongolia Exposure Sample Descriptions

TGP-16-27

Boulder Dimensions (cm):

Length:	390
Width:	300
Height N:	62
Height E:	91
Height S:	141
Height W:	136
Height Avg.:	107.5

Latitude (°):	49.14818
Longitude (°):	87.94376
Elevation (m a.s.l.):	3082.416
Ridge Location:	Potanin-I

Exposure Age (ka):

Date: 7/11/2016

Personel: MR NN PS AP DW JS KS

Shielding:

Dip (°):	10
Dip Dir. (°):	165
Correction:	

Azimuth (°):	Inclination (°):
0	11
34	11
103	1
126	1
130	2
134	1
165	3
199	10
204	8
213	12
227	7
231	6
235	8
237	6
250	7
256	11
271	5
286	6
295	10
301	6
323	9
336	14

Sample Views:

Large granite boulder embedded in left-lateral Potanin-I moraine ridge; 30 m away from ridge crest; north side of boulder lodged into till; has a "bullet" shape; boulder has striations, polish, and chatter marks; sample is polished.

Mongolia Exposure Sample Descriptions

TGP-16-28

Boulder Dimensions (cm):

Length:	189
Width:	131
Height N:	138
Height E:	130
Height S:	155
Height W:	143
Height Avg.:	141.5

Latitude (°):	49.14871
Longitude (°):	87.94230
Elevation (m a.s.l.):	3086.285
Ridge Location:	Potanin-I

Exposure Age (ka):

Date: 7/11/2016

Personel: MR NN PS DW JS

Shielding:

Dip (°):	20
Dip Dir. (°):	332
Correction:	

Azimuth (°):	Inclination (°):
0	12
38	11
111	0
132	2
166	2
198	10
202	8
213	12
215	10
217	11
226	7
230	6
235	8
239	6
249	7
255	11
262	8
274	5
286	5
294	10
302	6
325	9
346	15

Sample Views:

Large, sub-rounded granite boulder embedded in left-lateral Potanin-I moraine ridge; on flat stable surface 20 m away from ridge crest; boulder has small orange lichen and polish; top of boulder has exfoliation so sampled lower polished surface.

Mongolia Exposure Sample Descriptions

TGP-16-29

Boulder Dimensions (cm):

Length:	287	Latitude (°):	49.15052	Exposure Age (ka):	
Width:	200	Longitude (°):	87.93996		
Height N:	111	Elevation (m a.s.l.):	3103.086	Date:	7/11/2016
Height E:	97	Ridge Location:	Potanin-I	Personel:	MJR & team
Height S:	130				
Height W:	96				
Height Avg.:	108.5				

Shielding:

Dip (°):	0
Dip Dir. (°):	359
Correction:	

Azimuth (°):	Inclination (°):
0	18
42	13
111	0
131	2
164	2
195	10
199	6
212	11
224	7
227	4
232	7
243	6
252	12
260	6
265	8
272	6
284	6
292	10
300	5
324	9
341	16

Sample Views:

Large granite boulder resting on left-lateral Potanin-I moraine ridge, 10 m away from crest of moraine ridge; sample on shallowly dipping slope; boulder is well rounded and has polish; sample has polish.

Mongolia Exposure Sample Descriptions

TGP-16-30

Boulder Dimensions (cm):

Length:	485
Width:	358
Height N:	156
Height E:	171
Height S:	172
Height W:	186
Height Avg.:	171.25

Latitude (°):	49.13651
Longitude (°):	87.97297
Elevation (m a.s.l.):	3028.112
Ridge Location:	Outboard of Potanin moraines

Exposure Age (ka):

17.25 ± 0.21

Date:	7/12/2016
Personel:	MR NN PS AP DW JS ST

Shielding:

Dip (°):	10
Dip Dir. (°):	217
Correction:	0.99880

Azimuth (°):	Inclination (°):
0	8
13	7
24	8
116	1
129	1
140	3
148	2
171	3
180	4
184	5
201	5
208	8
215	7
235	10
238	8
245	10
250	9
255	5
269	8
276	4
288	5
293	7
299	3
311	7
353	10

Sample Views:

Very large, rounded granite boulder embedded in grassy terrace outboard of Potanin Glacier and moraines, resting on flat surface; next to well-sorted cobbles and permafrost cracking; boulder has lichen, polish, and varnish; sample taken from polished surface on top of boulder.

Mongolia Exposure Sample Descriptions

TGP-16-31

Boulder Dimensions (cm):

Length:	200
Width:	199
Height N:	73
Height E:	83
Height S:	74
Height W:	75
Height Avg.:	76

Latitude (°):	49.13576
Longitude (°):	87.97454
Elevation (m a.s.l.):	3026.129
Ridge Location:	Outboard of Potanin moraines

Exposure Age (ka):

19.28 ± 0.26

Date:	7/12/2016
Personel:	MR NN PS AP DW JS

Shielding:

Dip (°):	7
Dip Dir. (°):	286
Correction:	0.99897

Azimuth (°):	Inclination (°):
0	8
10	7
49	8
121	0
131	1
140	4
149	1
171	3
182	5
201	5
206	8
215	6
235	10
240	7
245	10
252	9
259	5
272	7
276	4
287	5
292	6
300	4
314	8
357	10

Sample Views:

Medium, low-lying, sub-angular granite boulder embedded in grassy terrace outboard of Potanin Glacier, located on shallowly dipping slope; boulder polished, varnished, with lichen present; sample taken from polished surface on top of boulder.

Mongolia Exposure Sample Descriptions

TGP-16-32

Boulder Dimensions (cm):

Length:	354
Width:	262
Height N:	83
Height E:	115
Height S:	108
Height W:	117
Height Avg.:	105.75

Latitude (°):	49.13518
Longitude (°):	87.97523
Elevation (m a.s.l.):	3022.67
Ridge Location:	Outboard of Potanin moraines

Exposure Age (ka):

17.90 ± 0.29

Date:	7/12/2016
Personel:	MR NN PS AP DW JS

Shielding:

Dip (°):	8
Dip Dir. (°):	338
Correction:	0.99888

Azimuth (°):	Inclination (°):
0	9
6	8
35	9
115	1
132	2
140	4
147	2
170	4
184	6
203	5
206	8
215	5
236	9
241	8
247	9
256	8
260	5
275	7
279	4
297	7
302	4
316	8
351	9

Sample Views:

Large granite boulder on grassy terrace outboard of Potanin Glacier and moraines, located on shallowly dipping slope; signs of water movement on west side of boulder; boulder has lichen, polish, and varnish; sample taken from polished and striated surface on top of boulder.

Mongolia Exposure Sample Descriptions

TGP-16-33

Boulder Dimensions (cm):

Length:	191
Width:	180
Height N:	84
Height E:	91
Height S:	91
Height W:	89
Height Avg.:	88.75

Latitude (°):	49.13496
Longitude (°):	87.97550
Elevation (m a.s.l.):	3020.9
Ridge Location:	Outboard of Potanin moraines

Exposure Age (ka):

Date: 7/12/2016

Personel: MR NN PS AP DW JS

Shielding:

Dip (°):	23
Dip Dir. (°):	248
Correction:	

Azimuth (°):	Inclination (°):
0	9
6	8
128	2
134	4
138	2
141	5
150	2
171	5
177	3
186	6
206	7
212	10
216	6
236	10
243	8
245	10
255	9
260	6
274	8
280	5
290	6
296	7
303	5
325	7

Sample Views:

Small, rounded granite boulder shallowly embedded in grassy terrace outboard of Potanin Glacier and moraines, located on shallowly dipping slope; boulder has grass on the north side and cobbles on south side; lichen, polish, and varnish present; top of boulder pitted so sampled dipping, polished, varnished surface.

Mongolia Exposure Sample Descriptions

TGP-16-34

Boulder Dimensions (cm):

Length:	205
Width:	115
Height N:	65
Height E:	65
Height S:	65
Height W:	70
Height Avg.:	66.25

Latitude (°):	49.13469
Longitude (°):	87.97581
Elevation (m a.s.l.):	3018.767
Ridge Location:	Outboard of Potanin moraines

Exposure Age (ka):

Date: 7/12/2016

Personel: MR NN PS AP

Shielding:

Dip (°):	18
Dip Dir. (°):	222
Correction:	

Azimuth (°):	Inclination (°):
0	9
8	8
131	1
140	4
146	2
173	4
180	4
186	6
205	7
211	10
216	6
238	10
242	7
245	10
254	9
259	5
273	8
281	4
291	5
295	7
301	5
309	6
330	9

Sample Views:

Medium, rounded granite boulder shallowly embedded on grassy terrace outboard of Potanin Glacier and moraines; many boulders surrounding sample; lichen, polish, and varnish present; sample taken from polished surface on top of boulder.

Mongolia Exposure Sample Descriptions

TGP-16-35

Boulder Dimensions (cm):

Length:	275
Width:	275
Height N:	60
Height E:	85
Height S:	80
Height W:	90
Height Avg.:	78.75

Latitude (°):	49.13352
Longitude (°):	87.97780
Elevation (m a.s.l.):	3014.424
Ridge Location:	Outboard of Potanin moraines

Exposure Age (ka):

17.31 ± 0.33

Date: 7/12/2016

Personel: MR NN PS AP

Shielding:

Dip (°):	5
Dip Dir. (°):	130
Correction:	0.99939

Azimuth (°):	Inclination (°):
0	8
125	2
132	2
136	3
140	5
151	1
174	5
179	3
187	6
207	6
215	9
218	6
239	9
243	6
249	8
255	7
260	5
272	8
280	5
291	5
296	7
301	5
327	7

Sample Views:

Medium, rounded granite boulder shallowly embedded on grassy terrace outboard of Potanin Glacier and moraines; boulder more embedded on north side than south side; lichen, polish, and varnish present; sample taken from polished surface on top of boulder.

Mongolia Exposure Sample Descriptions

TGP-16-36

Boulder Dimensions (cm):

Length:	210
Width:	195
Height N:	80
Height E:	70
Height S:	75
Height W:	80
Height Avg.:	76.25

Latitude (°):	49.13351
Longitude (°):	87.98372
Elevation (m a.s.l.):	3047.17
Ridge Location:	Bedrock knob

Exposure Age (ka):

84.04 ± 1.74

Date:	7/12/2016
Personel:	MR NN PS AP KS

Shielding:

Dip (°):	13
Dip Dir. (°):	280
Correction:	0.99798

Azimuth (°):	Inclination (°):
0	8
73	3
87	5
99	1
124	1
135	2
140	3
152	5
159	3
186	4
191	6
210	5
217	8
224	5
241	8
246	6
249	9
256	8
262	6
274	6
280	4
290	4
294	7
301	5
322	8

Sample Views:

Medium, well-rounded granite boulder resting on frost-shattered bedrock on upper molded bedrock slope outboard of Potanin Glacier and moraines near bedrock knob; sample has varnish, lichen, and some polished grains; sample take from lower surface because top of boulder was pitted.

Mongolia Exposure Sample Descriptions

TGP-16-37

Boulder Dimensions (cm):

Length:	385
Width:	275
Height N:	70
Height E:	80
Height S:	95
Height W:	80
Height Avg.:	81.25

Latitude (°):	49.13263
Longitude (°):	87.98461
Elevation (m a.s.l.):	3043.825
Ridge Location:	Bedrock kob

Exposure Age (ka):

98.82 ± 1.23

Date:	7/12/2016
Personel:	MR NN PS AP KS

Shielding:

Dip (°):	8
Dip Dir. (°):	141
Correction:	0.99940

Azimuth (°):	Inclination (°):
0	7
26	5
62	7
122	0
135	0
150	6
162	2
188	3
190	5
212	5
216	7
225	5
242	9
248	6
251	9
258	7
262	5
289	5
293	7
300	4
329	7

Sample Views:

Large granite boulder embedded in thin till layer mantling frost shattered bedrock; boulder has lichen, varnish, and some polished grains; sample has polished grains.

Mongolia Exposure Sample Descriptions

TGP-16-38

Boulder Dimensions (cm):

Length:	220
Width:	125
Height N:	80
Height E:	90
Height S:	55
Height W:	60
Height Avg.:	71.25

Latitude (°):	49.13369
Longitude (°):	87.98587
Elevation (m a.s.l.):	3046.815
Ridge Location:	Bedrock knob

Exposure Age (ka):

38.17 ± 0.52

Date: 7/12/2016

Personel: MR NN PS AP

Shielding:

Dip (°):	18
Dip Dir. (°):	157
Correction:	0.99538

Azimuth (°):	Inclination (°):
0	9
68	4
90	5
104	1
136	2
141	3
154	5
159	4
162	2
188	3
191	6
212	5
217	8
224	4
241	9
246	7
251	9
257	8
261	4
274	6
280	3
290	4
295	6
300	4
329	9

Sample Views:

Medium granite boulder embedded in till on shallow slope near the bedrock knob; near frost shattered bedrock; on ridge that divides flow around the knob; small hole on north side of boulder; sample has shallow cracks showing minor material removed and polished grains.

Mongolia Exposure Sample Descriptions

TGP-16-39

Boulder Dimensions (cm):

Length:	150
Width:	95
Height N:	75
Height E:	70
Height S:	70
Height W:	70
Height Avg.:	71.25

Latitude (°):	49.13069
Longitude (°):	87.98518
Elevation (m a.s.l.):	3039.511
Ridge Location:	Outboard of Potanin moraines

Exposure Age (ka):

24.04 ± 0.44

Date: 7/12/2016

Personel: MR NN PS AP

Shielding:

Dip (°):	14
Dip Dir. (°):	250
Correction:	0.99765

Azimuth (°):	Inclination (°):
0	6
13	7
19	3
62	5
66	4
82	5
100	1
124	0
139	3
151	5
160	2
187	4
192	6
215	6
219	9
226	4
245	9
250	8
251	10
260	8
265	5
271	5
276	7
281	5
292	5
295	7

Sample Views:

Medium, angular granite boulder resting on frost shattered bedrock on upper molded bedrock outboard of the Potanin Glacier and moraines; boulder has lichen and polish; sampled polished surface from top.

Mongolia Exposure Sample Descriptions

TGP-16-40

Boulder Dimensions (cm):

Length:	280
Width:	195
Height N:	90
Height E:	80
Height S:	85
Height W:	95
Height Avg.:	87.5

Latitude (°):	49.13059
Longitude (°):	87.98475
Elevation (m a.s.l.):	3035.775
Ridge Location:	Bedrock knob

Exposure Age (ka):

17.98 ± 0.34

Date: 7/12/2016

Personel: MR NN PS AP

Shielding:

Dip (°):	12
Dip Dir. (°):	113
Correction:	0.99865

Azimuth (°):	Inclination (°):
0	6
15	6
62	5
82	4
90	1
109	0
121	2
139	2
148	6
156	2
187	4
190	5
214	6
218	9
225	5
244	8
249	6
252	10
260	8
264	5
274	6
280	5
291	5
295	7
303	4
351	7

Sample Views:

Large, well-rooted granite boulder on upper molded bedrock terrace outboard of Potanin Glacier; boulder has lichen, polish, varnish, and striations; sampled polished quartz vein on top of boulder.

Mongolia Exposure Sample Descriptions

TGP-16-41

Boulder Dimensions (cm):

Length:	388
Width:	355
Height N:	200
Height E:	170
Height S:	160
Height W:	185
Height Avg.:	178.75

Latitude (°):	49.14989
Longitude (°):	87.93735
Elevation (m a.s.l.):	3072.31
Ridge Location:	Potanin-II

Exposure Age (ka):

Date: 7/13/2016

Personel: MR NN PS DW JS N O

Sample Views:

Shielding:

Dip (°): 3

Dip Dir. (°): 312

Correction:

Azimuth (°):	Inclination (°):
0	18
35	13
101	6
118	1
161	3
192	10
195	9
206	12
215	12
220	7
229	6
244	7
253	12
260	9
266	10
272	6
286	7
293	10
302	7
331	9

Large granite boulder resting on Potanin-II moraine ridge; on stable bench next to small turquoise pond; boulder angular to south end and rounded and polished on top and north side; minor orange lichen growth and chatter marks on the top; sample taken from polished top of boulder.

Mongolia Exposure Sample Descriptions

TGP-16-42

Boulder Dimensions (cm):

Length:	253
Width:	238
Height N:	151
Height E:	154
Height S:	210
Height W:	205
Height Avg.:	180

Latitude (°):	49.14867
Longitude (°):	87.93945
Elevation (m a.s.l.):	3067.945
Ridge Location:	Potanin-II

Exposure Age (ka):

Date: 7/13/2016

Personel: MR NN PS DW JS N O

Shielding:

Dip (°): 15

Dip Dir. (°): 217

Correction:

Azimuth (°):	Inclination (°):
0	18
24	15
114	1
130	2
134	1
162	3
194	11
199	9
210	13
218	12
224	7
231	6
232	8
245	8
254	12
262	9
268	10
273	5
286	6
296	10
305	7
330	10

Sample Views:

Large granite boulder shallowly embedded in Potanin-II; on moderately dipping slope; boulder rounded on N side; has chatter marks and striations; west side has minor lichen growth; sampled top polished surface.

Mongolia Exposure Sample Descriptions

TGP-16-43

Boulder Dimensions (cm):

Length:	245
Width:	245
Height N:	100
Height E:	120
Height S:	110
Height W:	90
Height Avg.:	105

Latitude (°):	49.14736
Longitude (°):	87.94123
Elevation (m a.s.l.):	3049.624
Ridge Location:	Potanin-II

Exposure Age (ka):

Date: 7/13/2016

Personel: MR NN PS DW JS N O

Shielding:

Dip (°): 0

Dip Dir. (°): 236

Correction:

Azimuth (°):	Inclination (°):
0	17
27	15
109	0
125	0
129	3
133	1
164	3
196	11
202	9
214	13
220	12
226	7
233	8
238	7
251	8
257	11
266	8
274	4
286	7
295	10
305	6
328	10

Sample Views:

Large, rounded granite boulder resting on Potanin-II; at sample location, ridge is not well defined; sand and gravel on top of boulder; no lichen; sample taken from polished surface on top of boulder.

Mongolia Exposure Sample Descriptions

TGP-16-44

Boulder Dimensions (cm):

Length:	230
Width:	120
Height N:	85
Height E:	124
Height S:	130
Height W:	130
Height Avg.:	117.25

Latitude (°):	49.14632
Longitude (°):	87.94312
Elevation (m a.s.l.):	3037.569
Ridge Location:	Potanin-II

Exposure Age (ka):

Date: 7/13/2016

Personel: MR NN PS DW JS N O

Shielding:

Dip (°):	11
Dip Dir. (°):	196
Correction:	

Azimuth (°):	Inclination (°):
0	16
28	12
125	0
130	3
134	1
163	2
200	10
203	8
219	13
228	5
235	8
239	6
252	7
258	12
267	9
275	5
286	6
296	10
305	6
326	10

Sample Views:

Large, angular granite boulder embedded in Potanin-II; on moderately dipping ice-contact slope; sample located in area with hummocks; sample taken from polished surface.

Mongolia Exposure Sample Descriptions

TGP-16-45

Boulder Dimensions (cm):

Length:	362
Width:	231
Height N:	115
Height E:	110
Height S:	145
Height W:	120
Height Avg.:	122.5

Latitude (°):	49.14248
Longitude (°):	87.94862
Elevation (m a.s.l.):	2984.593
Ridge Location:	Potanin-II

Exposure Age (ka):

Date: 7/13/2016

Personel: MR NN PS DW JS O N

Shielding:

Dip (°):	1
Dip Dir. (°):	17
Correction:	

Azimuth (°):	Inclination (°):
0	15
116	1
130	4
134	2
169	3
209	12
212	10
216	10
230	15
239	6
241	8
244	6
257	7
265	11
276	7
291	7
298	10
306	6
323	9

Sample Views:

Large, rounded granite boulder embedded in Potanin-II, located on flat surface on crest of moraine ridge; sample has orange tinge and may have more iron-bearing minerals; samples taken from highly polished surface on top of boulder.

Mongolia Exposure Sample Descriptions

TGP-16-46

Boulder Dimensions (cm):

Length:	242
Width:	149
Height N:	114
Height E:	130
Height S:	150
Height W:	120
Height Avg.:	128.5

Latitude (°):	49.14051
Longitude (°):	87.95212
Elevation (m a.s.l.):	2973.71
Ridge Location:	Potanin-II

Exposure Age (ka):

Date: 7/13/2016

Personel: MR NN PS DW JS

Shielding:

Dip (°): 5

Dip Dir. (°): 119

Correction:

Azimuth (°):	Inclination (°):
0	14
36	10
123	2
129	3
134	2
170	3
214	12
224	9
235	15
246	6
261	6
269	10
278	6
292	6
298	10
307	5
322	8

Sample Views:

Large granite boulder resting on Potanin-II on edge of moraine ridge; some anthropogenic forcer placed debris on top of boulder; boulder has some rough and polished surface; sample taken from polished surface on top.

Mongolia Exposure Sample Descriptions

TGP-16-47

Boulder Dimensions (cm):

Length:	370
Width:	237
Height N:	124
Height E:	132
Height S:	103
Height W:	105
Height Avg.:	116

Latitude (°):	49.14045
Longitude (°):	87.95223
Elevation (m a.s.l.):	2972.914
Ridge Location:	Potanin-II

Exposure Age (ka):

Date: 7/13/2016

Personel: MR NN PS DW JS N O T

Shielding:

Dip (°):	19
Dip Dir. (°):	322
Correction:	

Azimuth (°):	Inclination (°):
0	12
31	10
122	2
130	4
136	2
169	4
174	6
211	13
224	9
233	15
245	6
261	7
268	10
279	5
290	6
300	9
306	6
324	9

Sample Views:

Large, angular granite boulder resting on Potanin-II; 10 m away from TGP-16-46; sand and gravel on top of boulder; poppies and fireweed growing in surrounding till; sample taken from polished top of the boulder.

Mongolia Exposure Sample Descriptions

TGP-16-48

Boulder Dimensions (cm):

Length:	305
Width:	260
Height N:	105
Height E:	135
Height S:	98
Height W:	99
Height Avg.:	109.25

Latitude (°):	49.14038
Longitude (°):	87.95236
Elevation (m a.s.l.):	2971.554
Ridge Location:	Potanin-II

Exposure Age (ka):

Date: 7/13/2016

Personel: MR NN PS DW JS N O T

Shielding:

Dip (°):	19
Dip Dir. (°):	322
Correction:	

Azimuth (°):	Inclination (°):
0	12
29	10
124	1
128	4
134	2
169	4
174	5
213	14
225	10
238	14
246	7
261	8
268	9
278	6
290	7
299	10
308	5
323	9

Sample Views:

Large, angular granite boulder embedded in Potanin-II; located 15 m away from TGP-16-47; on stable surface; boulder has polish and is exfoliation on the top; sample taken from polished surface on top.

Mongolia Exposure Sample Descriptions

TGP-16-49

Boulder Dimensions (cm):

Length:	170
Width:	77
Height N:	87
Height E:	84
Height S:	89
Height W:	65
Height Avg.:	81.25

Latitude (°):	49.06146
Longitude (°):	88.64297
Elevation (m a.s.l):	2209.156
Ridge Location:	Bayan-I

Exposure Age (ka):

Date: 7/25/2016

Personel: MR NN PS AP N O TKS

Shielding:

Dip (°): 19

Dip Dir. (°): 148

Correction:

Azimuth (°):	Inclination (°):
0	5
52	7
61	4
64	5
86	2
90	0
141	2
170	8
183	4
232	3
249	5
263	2
276	1
282	3
316	5
322	2
340	6

Sample Views:

Medium granite boulder embedded in Bayan-I moraine ridge; 2 m away from crest of moraine ridge; east side embedded and west side undercut by erosion; boulder orange colored and had some lichen; polish and varnish present; top of boulder pitted so sample taken from polished surface on east side.

Mongolia Exposure Sample Descriptions

TGP-16-50

Boulder Dimensions (cm):

Length:	180
Width:	144
Height N:	134
Height E:	84
Height S:	110
Height W:	144
Height Avg.:	118

Latitude (°):	49.06057
Longitude (°):	88.63646
Elevation (m a.s.l):	2213.184
Ridge Location:	Bayan-I

Exposure Age (ka):

Date: 7/25/2016

Personel: MR NN AP JS N O TKS

Shielding:

Dip (°): 26

Dip Dir. (°): 254

Correction:

Azimuth (°):	Inclination (°):
0	5
35	6
56	3
63	5
91	3
132	1
145	5
155	6
176	5
206	2
235	4
259	3
294	2
309	4
324	1
334	4
340	2

Sample Views:

Large granite boulder well-embedded in till, located next to a paleo-meltwater channel on Bayan-I moraine ridge; boulder has lichen, varnish, and polished grains; top of boulder was a rough and pointed surface so sample taken from lower surface with polished grains.

Mongolia Exposure Sample Descriptions

TGP-16-51

Boulder Dimensions (cm):

Length:	145
Width:	95
Height N:	63
Height E:	75
Height S:	68
Height W:	67
Height Avg.:	68.25

Latitude (°):	49.05964
Longitude (°):	88.63541
Elevation (m a.s.l):	2210.047
Ridge Location:	Bayan-I

Exposure Age (ka):

16.05 ± 0.37

Date:	7/25/2016
Personel:	MR NN AP JS N O TKS

Shielding:

Dip (°):	17
Dip Dir. (°):	324
Correction:	0.99629

Azimuth (°):	Inclination (°):
0	5
36	6
56	3
61	5
85	0
99	0
141	5
154	6
174	5
202	2
234	4
245	4
261	1
266	3
278	0
285	2
308	1
312	3
325	2
334	4

Sample Views:

Medium granite boulder resting on crest of Bayan-I moraine ridge; moraine ridge has steep slopes on both sides of ridge; till look eroded underneath boulder; boulder "bullet" shaped and polished with light varnish; sample taken from polished surface on top of boulder.

Mongolia Exposure Sample Descriptions

TGP-16-52

Boulder Dimensions (cm):

Length:	250
Width:	190
Height N:	185
Height E:	150
Height S:	135
Height W:	135
Height Avg.:	151.25

Latitude (°):	49.05721
Longitude (°):	88.63370
Elevation (m a.s.l):	2201.84
Ridge Location:	Bayan-I

Exposure Age (ka):

24.57 ± 0.57

Date:	7/25/2016
Personel:	MR NN AP JS N O TKS

Shielding:

Dip (°):	21
Dip Dir. (°):	349
Correction:	0.99265

Azimuth (°):	Inclination (°):
0	5
44	6
52	3
64	4
83	0
108	1
135	5
146	7
161	3
186	9
230	4
252	4
265	3
273	4
297	3
311	3
318	5
326	7

Sample Views:

Large granite boulder shallowly embedded in ice-contact slope off of Bayan-I moraine ridge, 3 m away from crest of moraine ridge; on moderate slope that shows no sign of sluffing; animal hole underneath the downhill side of the boulder; boulder has varnish and polish; sample taken from polished surface on top of boulder.

Mongolia Exposure Sample Descriptions

TGP-16-53

Boulder Dimensions (cm):

Length:	130
Width:	105
Height N:	95
Height E:	100
Height S:	98
Height W:	85
Height Avg.:	94.5

Latitude (°):	49.05466
Longitude (°):	88.62732
Elevation (m a.s.l.):	2208.052
Ridge Location:	Bayan-I

Exposure Age (ka):

24.47 ± 0.38

Date:	7/25/2016
Personel:	MR NN AP JS N O TKS

Shielding:

Dip (°):	17
Dip Dir. (°):	110
Correction:	0.99616

Azimuth (°):	Inclination (°):
0	5
23	3
49	5
55	3
60	4
78	2
95	0
133	8
185	6
198	3
215	5
252	6
270	4
282	3
285	5
315	2
330	3
344	4

Sample Views:

Medium granite boulder well embedded in Bayan-I, on crest of slope; smaller moraine ridge is located outboard of Bayan-I at boulder location; sample is well polished and varnished; top of boulder pitted so sampled a lower polished knob.

Mongolia Exposure Sample Descriptions

TGP-16-54

Boulder Dimensions (cm):

Length:	172
Width:	126
Height N:	70
Height E:	78
Height S:	77
Height W:	71
Height Avg.:	74

Latitude (°):	49.05360
Longitude (°):	88.62293
Elevation (m a.s.l):	2206.334
Ridge Location:	Bayan-I

Exposure Age (ka):

Date: 7/25/2016

Personel: MR NN AP JS N O TKS

Shielding:

Dip (°):	10
Dip Dir. (°):	193
Correction:	

Azimuth (°):	Inclination (°):
0	3
27	3
50	5
55	3
67	4
86	0
126	3
178	5
212	2
240	6
262	5
268	7
280	5
290	2
301	5
333	6

Sample Views:

Medium granite boulder resting on Bayan-I moraine ridge on crest of ridge; boulder perched on cobbles and possible that underneath eroded away; boulder is well polished on top and has striations; sample taken from polished surface on top of boulder.

Mongolia Exposure Sample Descriptions

TGP-16-55

Boulder Dimensions (cm):

Length:	91
Width:	83
Height N:	55
Height E:	60
Height S:	56
Height W:	58
Height Avg.:	57.25

Latitude (°):	49.05151
Longitude (°):	88.61917
Elevation (m a.s.l):	2198.644
Ridge Location:	Bayan-I

Exposure Age (ka):

Date: 7/25/2016

Personel: MR NN AP JS N O TKS

Shielding:

Dip (°): 19

Dip Dir. (°): 293

Correction:

Azimuth (°):	Inclination (°):
0	4
30	3
49	4
55	2
61	4
86	0
117	7
164	8
210	3
240	5
273	6
285	3
289	5
302	6
317	7
330	3

Sample Views:

Small granite boulder resting on crest of Bayan-I; lack of vegetation around boulder indicates animal erosion; boulder is polished and varnished; sample taken from polished surface of the boulder.

Mongolia Exposure Sample Descriptions

TGP-16-56

Boulder Dimensions (cm):

Length:	235
Width:	150
Height N:	74
Height E:	92
Height S:	104
Height W:	86
Height Avg.:	89

Latitude (°):	49.06277
Longitude (°):	88.65214
Elevation (m a.s.l.):	2180.085
Ridge Location:	Bayan-I

Exposure Age (ka):

9.28 ± 0.19

Date: 7/26/2016

Personel: MR NN DW JS AP KS T

Shielding:

Dip (°):	9
Dip Dir. (°):	95
Correction:	0.99935

Azimuth (°):	Inclination (°):
0	5
47	7
59	4
63	5
91	0
140	1
151	3
159	2
184	8
215	3
230	5
236	2
240	4
262	2
265	3
275	3
276	2
285	3
311	5
317	3
335	5

Sample Views:

Large, angular granite boulder resting on crest of Bayan-I; sample resting on cobbles with low vegetation around boulder; sample taken from flat polished and varnished surface of boulder.

Mongolia Exposure Sample Descriptions

TGP-16-57

Boulder Dimensions (cm):

Length:	146
Width:	112
Height N:	56
Height E:	58
Height S:	67
Height W:	71
Height Avg.:	63

Latitude (°):	49.06442
Longitude (°):	88.65321
Elevation (m a.s.l.):	2172.179
Ridge Location:	Bayan-I

Exposure Age (ka):

13.13 ± 0.26

Date: 7/26/2016

Personel: MR NN AP JS DW KS

Shielding:

Dip (°):	16
Dip Dir. (°):	181
Correction:	0.99696

Azimuth (°):	Inclination (°):
0	6
27	9
55	4
70	7
90	0
113	1
147	2
160	3
183	5
194	3
211	2
223	2
230	1
244	3
253	1
269	2
271	0
280	4
338	6

Sample Views:

Medium granite boulder shallowly embedded in Bayan-I in saddle between two defined moraine ridges; boulder is angular, polished, and varnished; setting looks similar to TGP-15-56; boulder is polished and varnished, with some pitting; sample is polished.

Mongolia Exposure Sample Descriptions

TGP-16-58

Boulder Dimensions (cm):

Length:	333
Width:	214
Height N:	95
Height E:	87
Height S:	90
Height W:	80
Height Avg.:	88

Latitude (°):	49.06457
Longitude (°):	88.65285
Elevation (m a.s.l.):	2173.997
Ridge Location:	Bayan-I

Exposure Age (ka):

Date: 7/26/2016

Personel: MR NN DW JS AP T

Shielding:

Dip (°): 28

Dip Dir. (°): 257

Correction:

Azimuth (°):	Inclination (°):
0	6
33	8
59	5
70	7
91	0
110	1
120	3
140	2
143	1
150	2
159	1
182	7
210	2
221	3
228	2
242	3
253	1
264	2
271	1
280	2
297	2
307	4
315	2
340	6

Sample Views:

Large angular granite boulder embedded in Bayan-I moraine ridge; boulder is polished, varnished, and striated; minor erosion at base of boulder; sample taken from lower dipping polished slope.

Mongolia Exposure Sample Descriptions

TGP-16-59

Boulder Dimensions (cm):

Length:	165
Width:	130
Height N:	73
Height E:	47
Height S:	77
Height W:	88
Height Avg.:	71.25

Latitude (°):	49.06566
Longitude (°):	88.65267
Elevation (m a.s.l.):	2175.32
Ridge Location:	Bayan-I

Exposure Age (ka):

56.83 ± 0.71

Date: 7/26/2016

Personel: MR NN AP JS DW T

Shielding:

Dip (°):	13
Dip Dir. (°):	196
Correction:	0.99843

Azimuth (°):	Inclination (°):
0	8
35	9
62	7
67	6
91	1
110	1
134	1
143	0
156	3
180	6
208	2
229	1
243	4
254	2
267	3
273	1
290	4
297	2
306	4
315	1
335	7

Sample Views:

Large, sub-rounded granite boulder resting on Bayan-I moraine ridge; signs of animal erosion near boulder; boulder varnished and polished; sample is polished.

Mongolia Exposure Sample Descriptions

TGP-16-60

Boulder Dimensions (cm):

Length:	176
Width:	137
Height N:	104
Height E:	105
Height S:	140
Height W:	111
Height Avg.:	115

Latitude (°):	49.07239
Longitude (°):	88.65612
Elevation (m a.s.l.):	2161.743
Ridge Location:	Bayan-I

Exposure Age (ka):

51.27 ± 0.65

Date: 7/26/2016

Personel: MR NN AP JS DW T

Shielding:

Dip (°):	6
Dip Dir. (°):	100
Correction:	0.99901

Azimuth (°):	Inclination (°):
0	7
29	12
38	9
50	12
77	9
112	0
115	1
142	2
164	3
170	2
185	6
205	2
223	3
226	1
238	5
250	3
254	1
256	3
269	1
279	2
290	4
302	4
308	1
320	6
337	7
353	5

Sample Views:

Large, rounded dark fine-grain lithology on ice contact slope of Bayan-I moraine ridge, close to Tsagaan Gol River; boulder cut by many quartz veins and varnished; sampled polished quartz vein from top of boulder.

Mongolia Exposure Sample Descriptions

TGP-16-61

Boulder Dimensions (cm):

Length:	172
Width:	151
Height N:	70
Height E:	65
Height S:	67
Height W:	62
Height Avg.:	66

Latitude (°):	49.06000
Longitude (°):	88.65350
Elevation (m a.s.l.):	2142.671
Ridge Location:	Outboard Bayan-I

Exposure Age (ka):

196.1 ± 1.7

Date: 7/26/2016

Personel: MR NN AP PS DW JS

Shielding:

Dip (°):	0
Dip Dir. (°):	309
Correction:	0.99968

Azimuth (°):	Inclination (°):
0	6
26	7
40	8
51	5
62	6
86	0
103	1
137	2
146	3
155	2
183	8
207	5
212	3
218	4
233	1
244	3
256	2
275	4
338	5

Sample Views:

Medium granite boulder embedded in ground moraine outboard of Bayan-I moraine; boulder has bathtub ring of varnish; rough fresh surface on top of boulder; sample taken from rough surface on top of boulder.

Mongolia Exposure Sample Descriptions

TGP-16-62

Boulder Dimensions (cm):

Length:	180
Width:	115
Height N:	70
Height E:	66
Height S:	70
Height W:	70
Height Avg.:	69

Latitude (°):	49.05852
Longitude (°):	88.65526
Elevation (m a.s.l.):	2143.427
Ridge Location:	Outboard Bayan-I

Exposure Age (ka):

132.9 ± 1.2

Date: 7/26/2016

Personel: MR NN AP PS DW JS

Shielding:

Dip (°):	6
Dip Dir. (°):	23
Correction:	0.99964

Azimuth (°):	Inclination (°):
0	3
5	5
22	7
41	7
53	4
61	5
83	0
113	2
144	3
184	9
220	3
243	4
260	2
270	3
321	4
338	6

Sample Views:

Medium, rounded granite boulder embedded in ground moraine outboard of Bayan-I moraine ridge; boulder has bathtub ring of varnish 15 cm up from base; rough fresh surface on top of boulder covered in bird droppings; sample taken from rough surface on top of boulder.

Mongolia Exposure Sample Descriptions

TGP-16-63

Boulder Dimensions (cm):

Length:	243
Width:	188
Height N:	78
Height E:	77
Height S:	70
Height W:	63
Height Avg.:	72

Latitude (°):	49.05823
Longitude (°):	88.65660
Elevation (m a.s.l.):	2140.537
Ridge Location:	Outboard Bayan-I

Exposure Age (ka):

Date: 7/26/2016

Personel: MR NN AP PS DW JS

Shielding:

Dip (°):	17
Dip Dir. (°):	311
Correction:	

Azimuth (°):	Inclination (°):
0	4
19	6
39	8
51	6
62	7
85	1
112	2
145	3
157	2
193	9
211	3
220	4
234	2
255	5
262	2
267	4
320	3
330	6

Sample Views:

Large, rounded granite boulder embedded in ground moraine outboard of Bayan-I moraine; next to margin of ground moraine; boulder has bathtub ring of varnish; lichen present and no polished surfaces; sample taken from rough surface on top of boulder.

Mongolia Exposure Sample Descriptions

TGP-16-64

Boulder Dimensions (cm):

Length:	221
Width:	216
Height N:	141
Height E:	147
Height S:	143
Height W:	140
Height Avg.:	142.75

Latitude (°):	49.05803
Longitude (°):	88.65658
Elevation (m a.s.l.):	2140.596
Ridge Location:	Outboard Bayan-I

Exposure Age (ka):

Date: 7/26/2016

Personel: MR NN AP PS DW JS

Shielding:

Dip (°):	1
Dip Dir. (°):	260
Correction:	

Azimuth (°):	Inclination (°):
0	5
16	6
36	8
50	5
60	6
85	0
109	2
145	4
156	2
190	10
222	5
244	6
262	4
267	5
276	3
325	4
338	6

Sample Views:

Large, rounded granite boulder embedded in ground moraine outboard of Bayan-I moraine; boulder has bathtub ring of varnish; rough fresh surface on top of boulder and minor exfoliation around boulder; sample taken from rough surface on top of boulder.

Mongolia Exposure Sample Descriptions

TGP-16-65

Boulder Dimensions (cm):

Length:	206
Width:	157
Height N:	67
Height E:	80
Height S:	98
Height W:	92
Height Avg.:	84.25

Latitude (°):	49.05836
Longitude (°):	88.65848
Elevation (m a.s.l.):	2134.494
Ridge Location:	Outboard Bayan-I

Exposure Age (ka):

162.5 ± 1.5

Date: 7/26/2016

Personel: MR NN AP PS DW JS

Shielding:

Dip (°):	6
Dip Dir. (°):	28
Correction:	0.99960

Azimuth (°):	Inclination (°):
0	6
40	7
51	5
66	6
87	0
116	1
144	0
169	2
192	9
231	5
244	5
263	3
267	4
314	3
330	6

Sample Views:

Medium, rounded granite boulder embedded in ground moraine outboard of Bayan-I moraine complex; boulder has bathtub ring of varnish; boulder surface is rough and exfoliated; sample taken from rough surface.

Mongolia Exposure Sample Descriptions

TGP-16-66

Boulder Dimensions (cm):

Length:	152
Width:	104
Height N:	76
Height E:	77
Height S:	77
Height W:	80
Height Avg.:	77.5

Latitude (°):	49.06439
Longitude (°):	88.61502
Elevation (m a.s.l.):	2227.728
Ridge Location:	Bayan-II

Exposure Age (ka):

23.24 ± 0.47

Date: 7/27/2016

Personel: MR NN DW

Shielding:

Dip (°): 1

Dip Dir. (°): 198

Correction:

Azimuth (°):	Inclination (°):
0	6
62	5
66	3
69	5
85	2
87	0
118	1
136	4
149	3
174	3
198	1
210	7
222	5
225	6
255	2
274	3
278	0
281	2
320	2
329	4
336	2

Sample Views:

Small granite boulder shallowly embedded in Bayan-II moraine ridge; some erosion under boulder; polished and no varnish; sampled polished granite next to feldspathic vein.

Mongolia Exposure Sample Descriptions

TGP-16-67

Boulder Dimensions (cm):

Length:	120
Width:	91
Height N:	82
Height E:	80
Height S:	55
Height W:	76
Height Avg.:	73.25

Latitude (°):	49.06767
Longitude (°):	88.62363
Elevation (m a.s.l.):	2218.111
Ridge Location:	Bayan-II

Exposure Age (ka):

62.55 ± 0.71

Date: 7/27/2016

Personel: MR NN DW

Shielding:

Dip (°):	23
Dip Dir. (°):	107
Correction:	0.99024

Azimuth (°):	Inclination (°):
0	6
61	5
66	3
70	5
86	3
92	0
148	5
159	3
170	5
195	3
223	4
234	4
250	2
272	3
274	2
281	2
287	3
311	2
323	5
332	3
340	5

Sample Views:

Small granite boulder resting on Bayan-II moraine ridge; boulder exposed on north side and embedded on south side; boulder has rough surface on top and orange lichen; sampled polished surface on edge of boulder.

Mongolia Exposure Sample Descriptions

TGP-16-68

Boulder Dimensions (cm):

Length:	115
Width:	78
Height N:	66
Height E:	60
Height S:	67
Height W:	64
Height Avg.:	64.25

Latitude (°):	49.07405
Longitude (°):	88.62976
Elevation (m a.s.l.):	2193.778
Ridge Location:	Bayan-II

Exposure Age (ka):

23.79 ± 0.48

Date: 7/27/2016

Personel: MR NN DW KS

Shielding:

Dip (°): 4

Dip Dir. (°): 264

Correction:

Azimuth (°):	Inclination (°):
0	8
64	6
71	5
77	5
100	0
158	5
166	4
174	5
196	3
222	5
225	4
231	5
240	3
253	4
261	4
265	3
273	3
305	5
315	5
323	3

Sample Views:

Small, rounded granite boulder embedded in Bayan-II moraine ridge; boulder in location where Bayan-II is discontinuous; sample is polished and varnished.

Mongolia Exposure Sample Descriptions

TGP-16-69

Boulder Dimensions (cm):

Length:	328
Width:	135
Height N:	93
Height E:	132
Height S:	162
Height W:	136
Height Avg.:	130.75

Latitude (°):	49.07570
Longitude (°):	88.62942
Elevation (m a.s.l.):	2194.303
Ridge Location:	Bayan-II

Exposure Age (ka):

22.27 ± 0.42

Date: 7/27/2016

Personel: NN MR DW KS

Shielding:

Dip (°):	18
Dip Dir. (°):	347
Correction:	0.99523

Azimuth (°):	Inclination (°):
0	9
65	6
73	5
79	6
102	0
160	5
169	14
215	9
220	4
245	7
261	4
269	5
277	2
284	3
300	4
304	6
313	6
323	3

Sample Views:

Very large, angular granite boulder well embedded into Bayan-II moraine ridge, 10 m west of moraine ridge; close to where Tsagaan Gol River cuts the moraine complex but no sign of fluvial erosion near sample; sample taken from polished top surface of boulder; no varnish.

Mongolia Exposure Sample Descriptions

TGP-16-70

Boulder Dimensions (cm):

Length:	184
Width:	170
Height N:	75
Height E:	84
Height S:	66
Height W:	72
Height Avg.:	74.25

Latitude (°):	49.06738
Longitude (°):	88.62217
Elevation (m a.s.l.):	2222.319
Ridge Location:	Bayan-II

Exposure Age (ka):

28.49 ± 0.40

Date: 7/27/2016

Personel: MR NN AP PS DW KS

Shielding:

Dip (°):	14
Dip Dir. (°):	292
Correction:	0.99788

Azimuth (°):	Inclination (°):
0	7
62	7
68	4
72	6
88	3
92	0
146	5
167	4
181	4
189	2
212	3
234	5
246	3
258	2
270	5
274	3
283	3
289	4
313	3
325	5
331	3

Sample Views:

Large, rounded granite boulder embedded in Bayan-II moraine ridge; 3 m west of moraine ridge; small animal hole on S side; on stable slope; boulder and sample are polished and varnished.

Mongolia Exposure Sample Descriptions

TGP-16-71

Boulder Dimensions (cm):

Length:	157
Width:	143
Height N:	65
Height E:	76
Height S:	83
Height W:	69
Height Avg.:	73.25

Latitude (°):	49.06602
Longitude (°):	88.62004
Elevation (m a.s.l.):	2219.999
Ridge Location:	Bayan-II

Exposure Age (ka):

27.67 ± 0.52

Date: 7/27/2016

Personel: MR NN AP PS DW KS

Shielding:

Dip (°):	23
Dip Dir. (°):	80
Correction:	0.99015

Azimuth (°):	Inclination (°):
0	8
63	5
66	3
70	4
86	1
90	0
143	4
154	3
166	5
190	1
210	3
235	6
255	2
259	5
273	5
275	2
284	2
287	3
317	3
328	5
333	3

Sample Views:

Medium quartzite boulder embedded in Bayan-II moraine ridge; 2 m to the southeast of ridge crest; ridge well defined in this location; on shallowly dipping slope; boulder and sample are polished and varnished.

Mongolia Exposure Sample Descriptions

TGP-16-72

Boulder Dimensions (cm):

Length:	162
Width:	150
Height N:	87
Height E:	88
Height S:	95
Height W:	95
Height Avg.:	91.25

Latitude (°):	49.06797
Longitude (°):	88.61470
Elevation (m a.s.l.):	2212.909
Ridge Location:	Inboard Bayan-II

Exposure Age (ka):

Date: 7/27/2016

Personel: NN KS MR PS DW

Shielding:

Dip (°): 22

Dip Dir. (°): 44

Correction:

Azimuth (°):	Inclination (°):
0	8
63	6
69	3
72	5
91	0
139	5
150	4
190	4
197	6
205	4
218	7
241	5
251	4
270	5
274	2
296	4
319	3
324	5
338	4

Sample Views:

Medium granite boulder embedded in ground moraine inboard of Bayan-II; boulder is polished, varnished and pitted at top; sampled from lower polished surface.

Mongolia Exposure Sample Descriptions

TGP-16-73

Boulder Dimensions (cm):

Length:	322
Width:	202
Height N:	86
Height E:	90
Height S:	69
Height W:	78
Height Avg.:	80.75

Latitude (°):	49.06723
Longitude (°):	88.60464
Elevation (m a.s.l.):	2227.867
Ridge Location:	Inboard Bayan-II

Exposure Age (ka):

21.10 ± 0.40

Date:	7/27/2016
Personel:	MR NN PS DW KS

Shielding:

Dip (°):	8
Dip Dir. (°):	351
Correction:	0.99944

Azimuth (°):	Inclination (°):
0	5
12	7
65	5
69	3
74	5
91	0
131	4
149	4
151	6
158	5
160	4
180	4
187	8
192	6
198	9
222	7
240	2
257	5
328	4
336	5
349	4

Sample Views:

Very large, sub-rounded granite boulder embedded in ground moraine inboard of Bayan-II; boulder is on shallowly dipping slope and there is a ring of cobbles around the boulder; boulder is polished, varnished, and striated; sample taken from polished surface on top of boulder.

Mongolia Exposure Sample Descriptions

TGP-16-74

Boulder Dimensions (cm):

Length:	248
Width:	186
Height N:	114
Height E:	115
Height S:	114
Height W:	117
Height Avg.:	115

Latitude (°):	49.06795
Longitude (°):	88.59813
Elevation (m a.s.l.):	2252.947
Ridge Location:	Inboard Bayan-II

Exposure Age (ka):

19.54 ± 0.36

Date:	7/27/2016
Personel:	NN MR PS JW KS

Shielding:

Dip (°):	12
Dip Dir. (°):	122
Correction:	0.99858

Azimuth (°):	Inclination (°):
0	5
14	7
66	5
68	3
74	4
92	0
129	4
152	4
156	2
159	5
167	2
181	7
210	8
231	3
256	6
272	6
275	2
284	3
290	4
330	3
341	5
350	3

Sample Views:

Large, sub-rounded granite boulder embedded in ground moraine inboard of Bayan-II; on crest of hummock; boulder is polished and varnished with minor exfoliation at top; sample is polished.

Mongolia Exposure Sample Descriptions

TGP-16-75

Boulder Dimensions (cm):

Length:	325
Width:	195
Height N:	160
Height E:	130
Height S:	120
Height W:	140
Height Avg.:	137.5

Latitude (°):	49.06294
Longitude (°):	88.61145
Elevation (m a.s.l.):	2219.519
Ridge Location:	Inboard Bayan-II

Exposure Age (ka):

22.11 ± 0.41

Date: 7/28/2016

Personel: MR NN PS JS

Shielding:

Dip (°): 29

Dip Dir. (°): 84

Correction: 0.97948

Azimuth (°):	Inclination (°):
0	6
6	6
61	5
65	3
69	4
89	0
115	1
132	5
173	4
192	13
218	7
224	9
251	2
265	4
276	5
280	1
284	2
290	3
326	3
332	5
341	4

Sample Views:

Large, sub-rounded granite boulder embedded in ground moraine inboard of Bayan-II; on shallowly dipping slope; boulder is polished, varnished, and striated; sample taken from lower polished surface because top of boulder is weathered; small lichens present.

Mongolia Exposure Sample Descriptions

TGP-16-76

Boulder Dimensions (cm):

Length:	155
Width:	130
Height N:	85
Height E:	85
Height S:	85
Height W:	90
Height Avg.:	86.25

Latitude (°):	49.06354
Longitude (°):	88.60708
Elevation (m a.s.l.):	2222.385
Ridge Location:	Inboard Bayan-II

Exposure Age (ka):

Date: 7/28/2016

Personel: NN MR JS PS

Shielding:

Dip (°): 30

Dip Dir. (°): 352

Correction:

Azimuth (°):	Inclination (°):
0	5
9	6
62	5
66	4
71	5
90	1
130	5
141	5
152	11
161	10
169	6
174	7
187	2
199	7
215	11
235	8
250	2
256	1
264	5
277	4
279	1
286	1
289	3
328	3
335	5
342	3

Sample Views:

Large granite boulder well embedded in ground moraine inboard of Bayan-II; boulder is on shallowly dipping slope and there is a ring of cobbles around the boulder; boulder is polished and varnished; top of boulder pitted so sampled lower dipping polished surface.

BIOGRAPHY OF THE AUTHOR

Mariah Radue was born in Washington, D.C. and grew up in Maryland. She graduated from Sandy Spring Friends School in 2010. Mariah attended Carleton College, where she received a degree in geology in 2014. After Carleton, Mariah was a student on the Juneau Icefield Research Program, a ski instructor at Grand Targhee Resort, and a Geological Society of American GeoCorp intern at Mount Rainier National Park. As a part of geology field work, Mariah has traveled to South Dakota, Minnesota, Missouri, Washington, California, New Zealand, West Virginia, southeast Alaska, northern Maine, Mongolia, and China. She entered the University of Maine in June 2014. Mariah is a candidate for the Master of Science degree in Quaternary and Climate Studies from the University of Maine in May 2018.